Functional Studies of Selected Extracellular Carbohydrate-Active Hydrolases in Wood Formation

Junko Takahashi Schmidt
Faculty of Forest Sciences
Department of Forest Genetics and Plant Physiology
Umeå

Acta Universitatis Agriculturae Sueciae
2008:76

Cover: cellulase and exo-glucosidase activity in fiber cell walls of mature Arabidopsis stem, see section 3.2 (photo: Junko Takahashi Schmidt)

ISSN 1652-6880
ISBN 978-91-86195-09-0

Tryck: Arkitektkopia, Umeå, Sweden, 2008

Abstract

Takahashi Schmidt, J. 2008. Functional Studies of Selected Extracellular Carbohydrate-Active Hydrolases in Wood Formation. Doctoral thesis, ISSN 1652-6880, ISBN 978-91-86195-09-0

Wood is an essential natural and renewable resource for human activities; e.g. paper and pulp industries, house construction and energy production. Wood cells such as fibers are fundamentally important cells whose morphology and chemical components influence the wood quality. They are formed in the vascular cambium and differentiate to maturity through cell elongation/expansion and deposition of secondary cell wall during the highly organized process of wood formation. Final cell morphology is largely determined by plasticity of its primary cell walls, while cell wall chemical composition is mainly determined during the secondary cell wall formation. These features are directly regulated by cell-wall residing enzymes, which modulate the cell wall components. Here I describe the functions of selected carbohydrate-active extracellular hydrolases including cellulases, a xylanase and a xyloglucan endotransglycosylase (XET), which are identified to be highly expressed at specific phases of wood formation in hybrid aspen (*Populus tremula* L. x *Populus tremuloides* Michx.).

The XET *Ptt*XET16-34 is expressed during the primary cell wall stage and regulates cell growth by strengthening or weakening xyloglucan-cellulose microfibril networks. A putative xylanase, *Ptt*Xyn10A, and a membrane anchored cellulase, *Ptt*Cel9A1, are highly expressed during the secondary wall stage of xylem cell development. *Ptt*Xyn10A may assist with the remaining fiber elongation at the early stage of secondary cell wall deposition by softening the walls by degrading xylans cross-linking to lignins. *Ptt*Cel9A1 facilitates cellulose biosynthesis in a way that decreases cellulose crystallinity in cell walls, which is of great importance for the properties of cell wall structural framework.

Thus, the elaboration of wood cells is performed through the well-coordinated biosynthesis and modification of chemical components, and through the diverse and dynamic actions of specific carbohydrate-active hydrolases. The understanding of these enzyme actions will lead to the improvement of wood characteristics to create biomaterials more applicable for different aspects of the forest industry.

Keywords: cell wall, cellulase, cellulose, cellulose crystallinity, hybrid aspen, *Populus*, wood formation, XET, xylanase

Author's address: Junko Takahashi Schmidt, Department of Forest Genetics and Plant Physiology, SLU, SE-901 83, Umeå, Sweden
E-mail: Junko.Takahashi@genfys.slu.se

To my family in Sweden, Japan and Austria

Ph.D.
P…Patience
h…Humiliation
D…Depression

Dr. Renuka Jain

Contents

List of Publications

This thesis is based on the work contained in the following papers, referred to by Roman numerals in the text:

I **Poplar carbohydrate-active enzymes. Gene identification and expression analyses.**
Jane Geisler-Lee, Matt Geisler, Pedro M. Coutinho, Bo Segerman, Nobuyuki Nishikubo, Junko Takahashi, Henrik Aspeborg, Soraya Djerbi, Emma Master, Sara Andersson-Gunnerås, Björn Sundberg, Stanislaw Karpinski, Tuula T. Teeri, Leszek A. Kleczkowski, Bernard Henrissat and Ewa J. Mellerowicz. (2006) *Plant Physiology*, 140: 946-962.

II ***KORRIGAN1*** **and its aspen homologue** ***PttCel9A1*** **regulate cellulose crystallinity in Arabidopsis stem.**
Junko Takahashi, Ulla J. Rudsander, Mattias Hedenström, Alicja Banasiak, Jesper Harholt, Nicolas Amelot, Peter Ryden, Satoshi Endo, Farid M. Ibatulllin, Harry Brumer, Elena del Campillo, Emma R. Master, Henrik Vibe Scheller, Björn Sundberg, Tuula T. Teeri and Ewa J. Mellerowicz.
Submitted.

III **Suppression of wood expressed xylanase affects cell expansion and secondary wall composition.**
Junko Takahashi*, Tatsuya Awano*, Åsa Kallas, Christine Ratke, Anders Winzéll, András Gorzsás, Joanna Lesniewska, Anne Gouget, Fredrik Berthold, Tuula T. Teeri, Björn Sundberg and Ewa J. Mellerowicz.
Manuscript.

IV **Dual role of XET activity in cell expansion in the developing wood of hybrid aspen (*Populus tremula x tremuloides*).**
Nobuyuki Nishikubo, Junko Takahashi, Alexandra Andersson Roos, Kathleen Piens, Harry Brumer, Tuula T Teeri, Henrik Stålbrand, Björn Sundberg and Ewa J. Mellerowicz.
Submitted.

* To be considered joint first authors.
Paper I is reproduced with the permission of the publisher.

Related publication not presented in this thesis.

i **Liquid-phase fluorescence *in situ* RT-PCR analysis for gene expression analysis in woody stems.** Madoka Gray-Mitsumune, Hisashi Abe, Junko Takahashi, Björn Sundberg and Ewa J. Mellerowicz. (2004) *Plant Biology*, Special issue on poplar genomics, 6: 47-54.

1. Introduction

Wood formation (xylogenesis) is an important process with both biological and economical aspects. Wood has been a natural and renewable resource for timber, paper and pulp industries and production of energy. During the last decades, in order to meet the demand by a growing human population, production of wood has been constantly increasing. Hence, better use and management of existing forest plantations in order to protect the world's scarce natural forests have to be sought.

The quality of wood is evaluated by many criteria such as solidity, cellulose and lignin content, and fiber length. Improvement of these parameters requires a better understanding of the basic mechanisms of wood formation in trees and the mechanisms for biosynthesis and modification of the plant cell wall *in vivo* during wood formation, which determine fiber chemistry and morphology.

Cellulose is primarily found as the major structural component of both primary and secondary cell walls of plants. Cellulose biosynthesis has been a focus of research for more than 40 years (Somerville, 2006). During the last decade, great progress has been made on several fronts by applying cellulose deficient mutant lines of Arabidopsis (*Arabidopsis thaliana*) – the model species for which the necessary genetic and genomic tools are well developed. Cellulose is massively produced in the secondary cell walls during wood formation. However, the molecular tools for woody perennial species were only developed more recently, first with expressed sequence tags (ESTs) from wood forming tissues of hybrid aspen (*Populus tremula* L. x *Populus tremuloides* Michx.) (Sterky et al., 1998) and pine (*Pinus taeda* L.) (Sederoff et al., 2002). This progress was followed by the first transcriptome analysis across the wood forming tissues in *Populus,* performed using a microarray with nearly 3 000 ESTs (Hertzberg et al., 2001). These pioneering studies in *Populus* were the basis for selecting putative cell wall related hydrolases discussed in this thesis. Some of them were specifically expressed during secondary wall formation. For example, a membrane-anchored cellulase, *Ptt*Cel9A1, homologuous to Arabidopsis KORRIGAN1 known to be essential for cellulose synthesis, or a putative endoxylanase *Ptt*Xyn10A whose expression coincides with the xylan biosynthesis. Other selected enzymes were highly expressed during the primary-wall phase of xylem cell development (Mellerowicz et al., 2001). These include a putative cellulase *Ptt*GH9B3, and a xyloglucan endotransglycosylase/hydrolase (XTH), *Ptt*XET16-34, previously called *Ptt*XET16A.

The functions of these four *Populus* hydrolases were investigated using the reverse genetics approach in hybrid aspen and Arabidopsis. A special focus was given to the membrane-anchored cellulase *Ptt*Cel9A1, employing Arabidopsis mutants deficient in the orthologous enzyme. The new insights presented here give a deeper understanding of wood cell wall biosynthesis and modification, which might eventually improve the properties of wood for industrial applications.

1.1 Wood formation

1.1.1 Wood cell differentiation

Many monocot plants cease growth with maturation of primary tissues. In contrast, most dicot plants as well as gymnosperms continue to increase the diameter in the regions of roots and stems that are no longer elongating. This increase in thickness of the plant body is termed secondary growth. It results from the activities of two lateral meristems: the vascular cambium and the cork cambium. Wood (secondary xylem), is initiated on the inner side of the vascular cambium and formed towards the middle of the stem. The secondary phloem is formed towards the outer side of the vascular cambium (bark side) and is responsible for the transport of photosynthate from source to sink tissues.

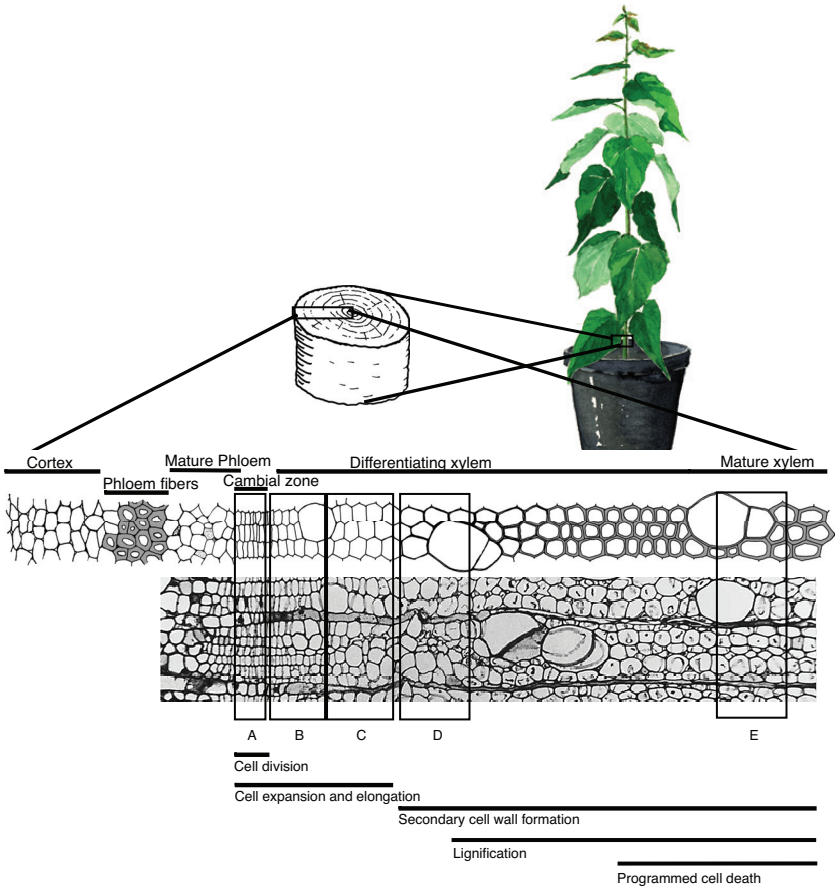

Figure 1. Schematic overview of different stages of the wood formation in *Populus* together with a cross section of *Populus tremula* L. x *tremuloides* Michx. wood forming tissues. Bars indicate the timing and approximate relative duration of the developmental stages. Tissues marked with A-E are the sample locations of the microarray analysis referred to in section 1.4.5. Figure modified from Schrader (2003), micrograph courtesy of Dr. E.J. Mellerowicz and artwork by G. Lövdahl.

The developing xylem cells pass through four distinct developmental stages: cell division of xylem mother cells, radial expansion and elongation, secondary cell wall thickening followed by subsequent lignification and programmed cell death (PCD) (Figure 1). These processes are tightly interlinked, hence, modulation of any one aspect of wood formation may affect many other aspects. In most trees, xylem cells enter a process called heartwood formation, where the wood becomes non-functional in conduction and storage of water and nutrients, and accumulates extractives as a consequence of aging (Mellerowicz et al., 2001; Plomion et al., 2001).

In hardwoods (angiosperm trees such as poplar), wood consists of vertically elongated cells, typically fibers, vessel elements, axial parenchyma cells, and in some species also tracheids, and horizontally oriented ray cells, which typically are sclerified parenchyma. In softwoods (conifer trees such as pine), the vertically elongated cells are predominantly tracheids, although a small amount of axial parenchyma might be associated with resin canals in some species, while the ray cells are usually sclerifying parenchyma as in hardwoods. Vertically elongated cells are formed from the fusiform initials that are meristematic stem cells in the vascular cambium, whereas ray cells arise from ray initials (Barnett, 1981; Larson, 1994).

In the cambium, fusiform initials increase in number by undergoing multiplicative anticlinal divisions that divide cells obliquely in half (Figure 2).

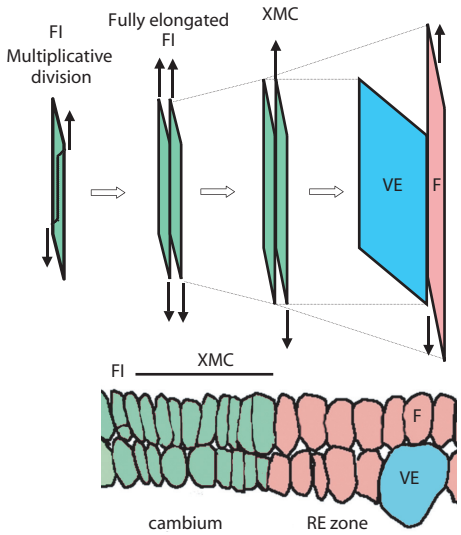

Figure 2. A schematic diagram of cell elongation by intrusive growth during three secondary xylem cell developmental stages (I, II, III). The radial longitudinal view (top) and the corresponding transverse view (bottom) are presented. Stage I; multiplicative anticlinal division of fusiform initial (FI) is followed by daughter cell elongation by intrusive tip growth in the cambium. Stage II; intrusive growth between periclinal division results in elongation of xylem mother cells (XMC) in the cambial zone. Stage III; Intrusive growth is responsible for elongation of fibers (F), while vessel elements (VE) do not elongate in the radial expansion (RE) zone. Figure reprinted with permission from Siedlecka et al. (2008).

This division shortens the length of fusiform initials. A unique elongation mechanism called intrusive tip growth restores the initial's length, leading also to an overall increase in initial length as the cambium ages (Larson, 1994; Siedlecka et al., 2008). Fusiform initials give rise to xylem and phloem mother cells by periclinal divisions. The mother cells continue to divide periclinaly accompanied by intrusive tip growth in the cambial meristem (Figure 2). The length of xylem mother cells within the cambium results in a slight increase after these processes.

During the subsequent expansion phase, intrusive tip growth occurs only in fibers. While the tips of fibers elongate, the middle part of the fibers remains fixed. This intrusive tip growth might proceed even after the deposition of the secondary wall starts in the middle part of the fibers (Mellerowicz, 2006). In hardwoods, fibers may elongate several folds during this phase, whereas in softwoods the tracheids elongate only slightly (Wenham and Cusick, 1975; Barnett, 1981; Larson, 1994). Thus, the extent of intrusive elongation determines wood fiber length, which is one of the most critical parameters for industrial use. In contrast, vessel elements greatly expand radially by symplastic and lateral intrusive growth but maintain the length of the xylem mother cells (Barnett, 1981; Larson, 1994; Mellerowicz et al., 2001; Mellerowicz, 2006) (Figure 2). Ray parenchyma cells elongate in the radial direction by symplastic growth, where cells remain attached to the expanding radial walls of adjacent vessel elements or fibers (Mellerowicz, 2006). These cells transport nutrients and water between secondary phloem and xylem and store reserves during the dormant season.

At the end of the cell expansion phase, secondary cell walls start depositing inside the primary cell wall (Abe et al., 1997) and consequently form a three-layered structure (S1, S2 and S3 for the outer, middle and inner layer, respectively) (Figure 3). The rigidity increases simultaneously with the development of secondary cell walls. Secondary walls are especially important in fiber cells for strengthening and in vessel elements for conducting water.

The final phase of development for secondary xylem cells is PCD. At this stage, the living cell contents are autodigested by the release of proteases and nucleases into the cytoplasm, accompanying a range of morphological and nuclear changes in a strictly coordinated manner in vessel elements (Barnett, 1981; Fukuda, 1996; Fukuda, 2000) and fibers (Courtois-Moreau, 2008). Ray cells that also form a secondary cell wall typically remain alive for an extended period, even after fibers and vessel elements lose their functional cytosol by PCD (Larson, 1994).

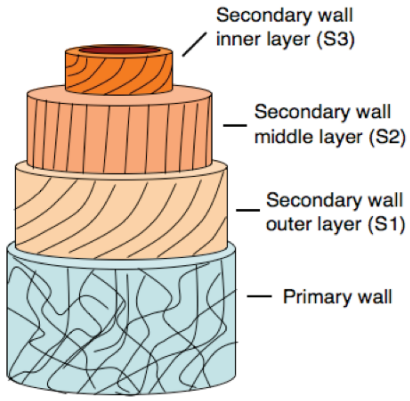

Figure 3. A diagrammatic representation of the cell wall layers in a wood fiber showing cellulose microfibril orientation. The secondary cell wall consists of three distinct layers denoted as S1, S2 and S3. Figure courtesy of Dr. E.J. Mellerowicz.

1.1.2 Variability of wood

Wood structure and composition vary within each individual stem. For example, juvenile wood is characterized by thin secondary cell walls, low density, short cell length and low crystallinity of fibers compared to mature wood, and is produced during the first 5 to 10 years of cambial growth in poplar (Mellerowicz et al., 2001). Earlywood/latewood is an example of variability seen within the annual growth ring, where earlywood, formed at the beginning of a growth period, has more and larger vessel elements, but shorter xylem cell length with thinner cell walls in contrast to latewood. Lignin composition is also altered in earlywood/latewood (Liese and Ammer, 1958; Takabe et al., 1992).

Variability is also influenced by environmental factors. For example, wind and physical load or gravity induces tension wood (TW) in hardwoods, which keeps thick stems and branches in the right position. It is formed on the upper side of a leaning stem associated with increased growth and higher crystalline cellulose content (Timell, 1986, Pilate et al., 2004; Mellerowicz et al., 2008). TW fibres form a specialized cell wall layer called gelatinous (G-) layer in some species, which is composed of highly crystalline cellulose, xyloglucan, rhamnogalacturonan1 (RG1) and arabinogalactan-proteins (AGPs) (Nishikubo et al., 2007; Mellerowicz et al., 2008). In *Populus*, the G-layer is produced over the partially formed S2 layer (reviewed by Mellerowicz et al., 2001). Wood variability is currently being intensively studied to elucidate the molecular mechanisms governing it.

1.2 Model system for studying wood formation

Various plant model systems including whole plant-models such as *Populus* sp. (Mellerowicz et al., 2001), Arabidopsis (Ye et al., 2002; Demura and Fukuda, 2007; Turner et al., 2007) and xylogenic cell culture models such as *Zinnia* (*Zinnia elegans*) (Fukuda, 2004), have been widely used to reveal the molecular mechanisms of wood formation. In this thesis, *Populus* sp. and Arabidopsis were extensively used.

1.2.1 *Populus*

The genus *Populus* contains approx. 30 species, for example, European aspen (*P. tremula*) and black cottonwood (*P. trichocarpa* Torr. & Gray), which are found in the northern hemisphere and exhibit some of the fastest growth rates observed in temperate trees. *Populus* has been suggested as a good model system for xylogenesis due to its ease of genetic transformation and vegetative propagation, and short generation time (Bradshaw et al., 2000; Taylor, 2002; Bhalerao et al., 2003; Brunner et al., 2004; Jansson and Douglas, 2007). The relatively small genome size (approx. 480 Mbp, containing 45 000 putative genes) is also a great advantage for sequencing (Tuskan et al., 2006). By comparison, pines have a diploid genome on average of 31 000 Mbp and much longer generation times than poplar (Leitch et al., 2001; Whetten et al., 2001). Well-established *Populus* molecular resources include ESTs, full genome sequences, chloroplast sequence, bacterial artificial chromosome (BAC) physical maps and simple sequence repeats (SSR) markers (Wullschleger et al., 2002).

The EST collection in *Populus* is largely based on hybrid aspen (*P. tremula* L. x *P. tremuloides* Michx.) and has over 120 000 ESTs (Sterky et al., 2004; http://www.populus.db.umu.se/) from 19 cDNA libraries, each originating from different *Populus* tree tissues. From this collection, cDNA microarrays have been produced and used extensively for the analyses of genes expressed during wood formation (Hertzberg et al., 2001; Schrader et al., 2004; Aspeborg et al., 2005; Moreau et al., 2005; Andersson-Gunneråas et al., 2006; Goué et al., 2008).

Populus trichocarpa is the first sequenced woody plant species by the Joint Genome Institute US Department of Energy (Tuskan et al., 2006; http://www.jgi.doe.gov/). The fully sequenced poplar genome offers the best tool to study tree functional genomics.

1.2.2 Arabidopsis

Arabidopsis (*Arabidopsis thaliana*) is a small annual plant from the mustard family. It has a small genome size (125 Mbp, approx. 25 500 putative genes), rapid life cycle, prolific seed production and an efficient transformation system. These advantages promoted the growth of a scientific community studying fundamental questions of plant biology using this model. Since its genome has been published in 2000 (The Arabidopsis initiative, 2000), Arabidopsis has become the most standard model plant for functional genomic studies. Transferred

DNA (T-DNA) tagged Arabidopsis lines were produced in various research institutes, which are available for reverse genetic approaches.

Although Arabidopsis is an annual plant species, it forms wood in the mature root (Dolan et al., 1993; Dolan and Roberts, 1995; Lev-Yadun, 1994), hypocotyl (Gendreau et al., 1997; Chaffey et al., 2002) and stem (Altamura et al., 2001; Baima et al., 2001). The developed secondary xylem in Arabidopsis hypocotyls resembles that in hardwoods, except for the lack of ray cells (Chaffey et al., 2002; Nieminen et al., 2004). Therefore, genes involved in secondary growth in Arabidopsis hypocotyls can be correlated to wood development in trees (Zhao et al., 2000; Oh et al., 2003; Ko and Han, 2004; Ko et al., 2004; Zhao et al., 2005).

1.3 Poplar wood cell wall

The distinguishable feature of plant cells from animal cells is the presence of the cell wall. Plant cells are surrounded by cell walls that are complex and dynamic structures. Besides its fundamental role in giving a plant body tensile strength against turgor pressure, plant cell walls have several important physiological functions during the life of the plant. Thick walled cells provide protection from insects and pathogens, both mechanically and physiologically. Defensive responses are actively triggered by cell wall polysaccharides as latent signal molecules that are released during the cell wall degradation by pathogenesis (Vorwerk et al., 2004). In addition, polysaccharide fragments and proteoglycans in the walls contribute to cell-to-cell communication in developmental processes (Motose et al., 2004). Thus, the diverse structure of the cell wall represents key determinants of overall plant growth and the responses to environmental stresses.

Wood cells consist of three chemically distinct layers, namely, middle lamella, primary cell wall and secondary cell wall (Figure 3; Figure 4). The morphology of wood cells is determined during the primary cell wall period, whereas the mechanical and chemical properties of wood are largely governed by the secondary cell wall. An understanding of the mechanisms that regulate the properties of cell walls could provide new insight in improving woody raw materials (Mellerowicz and Sundberg, 2008).

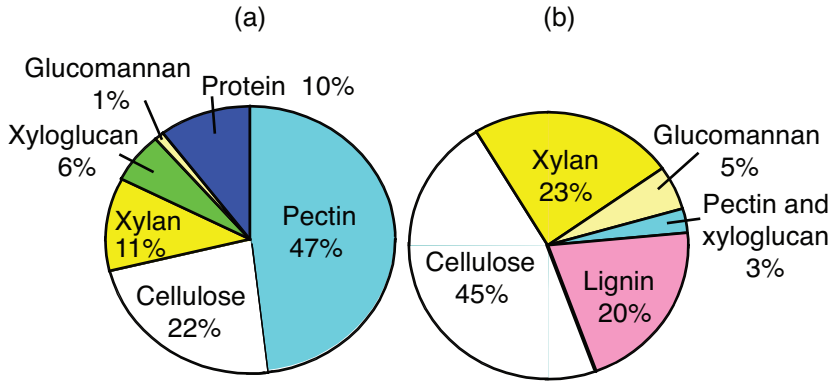

Figure 4. Poplar wood cell wall composition in primary cell walled (a) and secondary cell walled (b) stages. Figure was constructed after Mellerowicz et al. (2001) based on the original data from Simson and Timell (1978 a-d).

1.3.1 Poplar xylem cell primary cell wall

The primary wall is secreted through the plasma membrane and deposited against the outermost layer, the middle lamella, which is composed of pectic compounds and proteins (O'Neill and York, 2003). The primary cell wall consists of randomly arranged layers of cellulose microfibrils as a rigid skeleton, cross-linked by hemicelluloses (Figure 5). The hemicelluloses, especially xyloglucans, are known to contribute to strength with extensibility of the primary cell walls, by acting as tethers between cells to enable cells to expand in a well-coordinated manner during growth (Pauly et al., 1999). They are embedded in a gel-like matrix composed of

pectins, structural glycoproteins such as extensin and numerous enzymes (Carpita and Gibeaut, 1993).

In *Populus tremuloides*, xylan and xyloglucan are the most abundant hemicelluloses in the primary cell walled stage of xylem and they constitute up to 11% and 6% of the total component of the wall, respectively (Figure 4; Simson and Timell, 1978 a-d). However, a recent report indicates that the primary cell wall of suspension-cultured cells of *P. alba* contains little xylan and it is mainly composed of pectin, arabinan, arabinogalactan I, glucomannan and xyloglucan (Edashige and Ishii, 1999).

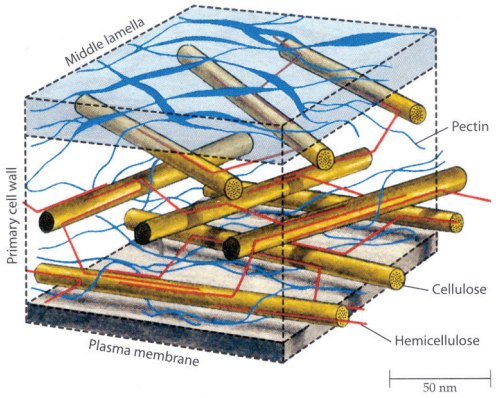

Figure 5. Present model of the primary cell wall. Cellulose microfibrils are cross-linked by hemicelluloses such as xyloglucan that bind to the microfibrils by hydrogen bonds. The space surrounding the cellulose-hemicellulose network is filled with pectins. Structural glycoproteins such as extensin and enzymes are also situated (not shown) in the primary cell wall. The middle lamella is a pectin-rich layer that cements the primary cell walls of adjacent cells. Later in development, lignin is deposited starting from the middle lamella. Figure reprinted with permission from Raven et al. (1999).

1.3.2 Poplar xylem cell secondary cell wall

The secondary cell wall has a strengthening function that is important in both fibers and the water conducting cells. It is extremely rigid and provides compression strength. The strength is attributed to more abundant cellulose than in primary walls and a lack of pectin. For example, in poplar xylem, cellulose constitutes 43 - 48 % of all components in the secondary walls, compared to 22% in the primary walls (Figure 4, Simson and Timell, 1978 a-d). The matrix of the secondary wall is composed of hemicelluloses and lignin. The major hemicellulose in the secondary cell wall is glucuronoxylan, which may constitute 18 - 28% in poplar (Simson and Timell, 1978 a-d; Willför et al., 2005; Davis et al., 2006). The second most abundant hemicellulose is mannan (Willför et al., 2005). Structural proteins, which are relatively rich in primary cell walls, are apparently absent in secondary cell walls. A model of the arrangement of different secondary wall components is depicted in Figure 6.

Secondary walls differ from primary walls not only in chemical constituents but also in the organization of their cellulose microfibrils (Timell, 1986). In the primary cell wall, cellulose microfibrils are randomly oriented tending to align

parallel to the longitudinal axis, whereas microfibrils in the secondary wall are highly organized, lying parallel to each other in a helicoidal pattern (Figure 3). The microfibril angle differs among the three secondary cell wall layers (S1 - S3). In the outermost S1 layer the microfibrils are almost perpendicular to the cell axis (about 50 to 90°) in most cases, whereas the middle and the thickest S2 layer has more longitudinally arranged microfibrils (5 - 30°), which has a major impact on the elasticity of wood (Timell, 1967). In the innermost S3 layer, the microfibrils have again a more perpendicular angle. The S1 layer is suggested to have a crossed microfibrillar texture (Figure 3) with its lamellae exhibiting both S (spiral upward to the left) and Z (spiral upward to the right) helical orientations (Harada and Côté, 1985).

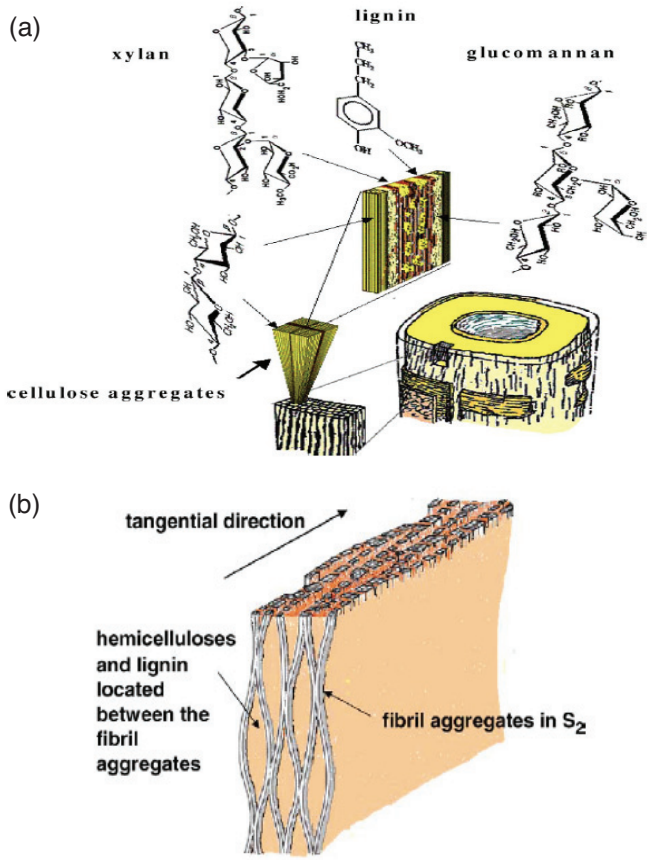

Figure 6. Present model of the secondary cell wall of a softwood fiber indicating arrangement of cellulose aggregates, major hemicelluloses (xylan and glucomannan) and lignin. Detailed drawing of the cellulose aggregate structure is shown (b). Figure reprinted with permission from Salmén (2004).

During secondary wall development, a high amount of syringal (S) and guaiacyl (G) lignin monomers are deposited in the cell wall, where they polymerize to form lignin. The lignin distribution is non-uniform across cell wall layers and is the most concentrated in the middle lamella and primary wall layers (Donaldson et al., 2001; Boerjan et al., 2003).

Table 1. Chemistry of the main components of the primary and secondary cell walls of *Populus*[1].

Polysaccharides or lignins	Occurrence	Major monomers	Backbone	Substituents
Cellulose	Primary and secondary cell wall	β-Glc	β-1,4-Glc	Unbranched.
Xyloglucan	Mainly primary cell wall	β-Glc, α-Xyl, β-Gal, α-Fuc	β-1,4-Glc	α-Xyl-1,6-β-Glc, β-Gal-1,2-α-Xyl-1,6-β-Glc, α-Fuc-1,2-β-Gal-1,2-α-Xyl-1,6-β-Glc. β-Gal is partially acetylated.
Glucuronoxylan	Mainly secondary cell wall	β-Xyl, α-GlcUA	β-1,4-Xyl	α-GlcUA-1,2-b-Xyl. Some α-GlcUA are as 4-O-metyl ether. Some β-Xyl are acetylated.
Glucomannan	Mainly secondary cell wall	β-Glc, β-Man	β-1,4-Glc/β-1,4-Man (ratio 1:2)	Unbranched.
Pectin Homogalacturonan	Primary cell wall	α-GalUA	α-1,4-GalUA	Unbranced. Some α-GalUA are as methyl ester.
Pectin RG-I	Primary cell wall	α-GalUA, α-Rha, β-Gal, α-Ara, α-Fuc	α-1,4-GalUA-α-1,2-Rha	Rich in α-Ara and/or β-Gal, attached to O-4 of α-Rha.
Pectin RG-II	Primary cell wall	Eleven different glycosyl residues including unusual sugars. Usual sugars are α-GalUA, β-Rha, α-Gal, α-Fuc, α-Rha, β-GalUA, α-Ara, β-GlcUA.	At least eight α-1,4-GalUA	Two structurally distinct disaccharides attached to C3 and two structurally distinct oligosaccharides attached to C2 of the backbone.
Lignins	Middle lamella, primary cell wall (higher concentration) and secondary cell wall (lower concentration) during secondary cell wall stage.	Guaiacyl (G) and syringyl (S) units and traces of *p*-hydroxyphenyl (H) phenylpropanoid units.		

[1] Based on Fry (1988); Donaldson et al. (2001); Mellerowicz et al. (2001); O'Neill and York (2003).

1.3.3 Major wood cell wall polysaccharides

1.3.3.1 Cellulose

Cellulose is the most abundant biopolymer on earth and accounts for more than 50% of the carbon in the biosphere. Most of the cellulose is produced by vascular plants, but there are a few other organisms that can also produce cellulose, for example, most groups of algae, slime molds, a number of bacterial species, fungi, protists and some marine invertebrates (Nakashima et al., 2004; Saxena and Brown, 2005).

1.3.3.1.1 Cellulose structure

The basic chemical structure of cellulose is simple. It is a linear polymer of covalently linked β-1,4-D-glucan residues (Table 1). The degree of polymerization (DP) (number of glucose residues in a chain) in the secondary cell wall is high, in the region of 10 000 and can be up to 25 000, whereas 2 000 to 6 000 is typically found in the primary cell wall (Reid, 1997). These chains are tightly linked by intra-molecular hydrogen bonds between O5 and O3, as well as between O2 and O6, and 30 to 200 β-1,4-glucan chains are held together to form microfibrils. In higher plants, one microfibril has been proposed to consist of 36-glucan chains on average, with a core crystalline arrangement, and a paracrystalline (amorphous) surface cellulose. The measured cellulose fibril diameter is usually about 3 nm, but ranges from about 2 to 70 nm depending on species, cell and cell wall types (Ha et al., 1998; Salmén, 2004; Müller et al., 2006; Donaldson, 2007; Kennedy et al., 2007). Therefore it has been proposed that cellulose microfibrils aggregate further into larger entities called macrofibrils, especially in the secondary cell walls (Figure 6). For example, macrofibril diameter of about 14 nm for G-layer and 16 nm and for S2 layer were reported in poplar (Donaldson, 2007).

Cellulose crystallinity within macrofibrils is not perfect. Amorphous regions exist in particular near the crystal surfaces in microfibrils, and some of them become buried after macrofibril formation. It is proposed that hidden chain ends contributing to structural disorder are buried even in the highly crystalline regions of cellulose. (Teeri, 1997).

Crystalline cellulose is synthesized naturally in two different forms, designated cellulose I (prevalent) and II (found only rarely in some algae and bacteria) (Delmer, 1999). Their difference is visualized by X-ray crystallography. Cellulose I consists of microfibrils in which all the chains are organized in parallel (Koyama et al., 1997), whereas cellulose II is composed of antiparallel chains. Through regeneration (dissolution in specific solvents) and mercerization (swelling in strong alkali solutions) followed by recrystallization, cellulose II can be artificially and irreversibly produced from cellulose I (Franz and Blaschek, 1990).

1.3.3.1.2 Cellulose biosynthesis

Gluconoacetobacter xylinus (formerly called *Acetobacter xylinum*), cotton and Arabidopsis have been used as model systems to understand the mechanism of

cellulose biosynthesis. During recent years, significant insight into the molecular details of cellulose biosynthesis has been achieved using forward and reverse genetics coupled with advances in plant genomics (Somerville, 2006). The progress of revealing the mechanism of cellulose biosynthesis is well described by numerous researchers (e.g. Doblin et al., 2002; Mølhøj et al., 2002; Reiter 2002; Williamson et al., 2002; Somerville et al., 2004; Scheible and Pauly, 2004; Joshi et al., 2004; Hayashi et al., 2005; Saxena and Brown, 2005; Lerouxel et al., 2006; Somerville, 2006; Joshi and Mansfield, 2007; Taylor, 2008 and Mutwil et al., 2008).

In higher plants, cellulose synthase (CESA) catalytic subunit proteins form a symmetrical "rosette" complex (also called cellulose synthase complex (CSC) or terminal complex (TC)) in the plasma membrane (Kimura et al., 1999) (Figure 7). The complex is one of the largest protein complexes known with a diameter of approx. 25-30 nm. Each rosette comprises six rosette subunits and each of the subunits is thought to contain six CESA proteins. Each CESA is proposed to synthesize a single β-1,4-glucan molecule from UDP-D-glucose and therefore a rosette terminally produces 36 β-1,4-glucan chains to the apoplastic side of the plasma membrane (Figure 7). These rosette complexes migrate in the plasma membrane along microtubules, propelled by the polymerization of the β-1,4-glucan chains (Paredez et al., 2006).

Plant *CESA* genes are members of multigene families. The presence of ten *CESAs* in Arabidopsis, at least nine in rice (Keegstra and Walton, 2006), and 18 in poplar (Djerbi et al., 2005) is reported. In Arabidopsis, three CESA proteins (CESA1, CESA3 and CESA6-related) are required for primary wall synthesis and physically interact in rosette subunits. CESA6-related CESA5 and CESA2 compete with CESA6 for the same position in the rosette complex (Desprez et al., 2007; Persson et al., 2007b). For secondary cell wall synthesis, at least three CESA proteins (CESA4, CESA7 and CESA8) are essential (Taylor et al., 2003). All members of CESA family are glycosyltransferases (GTs) belonging to GT family 2 (GT2). They are integral membrane proteins that have eight predicted transmembrane domains and a large hydrophilic domain that faces the cytosol.

However, cellulose synthesis cannot be completed without the actions of other proteins. For example, the involvement of cellulase in β-glucan synthesis was already discussed more than 30 years ago (Wong et al., 1977a). During the last years, the membrane-anchored cellulase, KORRIGAN1, is suggested to be one of the most important proteins involved in cellulose synthesis in addition to CESA and is described in section 1.4.2.2.

1.3.3.2 Xylan

1.3.3.2.1 Xylan structure

Xylans including arabinoxylans, glucuronoxylans and glucuronoarabinoxylans possess a backbone composed of approx. 200 β-1,4-D-linked xylose (Xyl) residues (Table 1). Many of them are branched bearing substitute residues, for example, arabinoxylans with α-L-arabinose residues at O2 or O3, glucuronoxylans with α-D-glucuronic acid (GlcUA) at O2. In *O*-acetyl-4-*O*-methyl-glucuronoxylans, simply called glucuronoxylans, approx. 1 out of 10 xylose units in the backbone is

substituted with a α-1,2-linked 4-*O*-methyl-D-glucuronic acid (Me-GlcUA) residue. It is often the case that approx. 7 out of 10 xylose units are acetylated at C2 or C3 (Reid, 1997). Glucuronoarabinoxylans comprise both α-D-glucuronic acid and α-L-arabinose residues (Carpita, 1996; Reid, 1997). In addition, a complex oligosaccharide containing rhamnose (Rha) and galacturonic acid (GalUA), β-D-Xyl-(1,4)-β-D-Xyl-(1,3)-α-L-Rha-(1,2)-α-D-GalUA-(1,4)-D-Xyl has been found at the reducing ends of xylan backbones, which appears to be highly conserved in a number of divergent plant species (Johansson and Samuelson, 1977; Andersson and Samuelson, 1983; Peña et al., 2007).

Xylans are major components of the secondary cell walls of woody species (Ebringerová and Heinze, 2000), especially glucuronoxylans are the most abundant in dicotyledon species and are thought to interact with lignin through ester bonds to GlcUA and Me-GlcUA (Imamura et al., 1994; Spániková. and Biely 2006; Spániková et al., 2007; Li et al., 2007). In contrast, the primary cell walls of poplar contain less xylan (Simson and Timell, 1978 a-d; Edashige and Ishii, 1999).

1.3.3.2.2 Xylan biosynthesis and modification

Recently, the genes responsible for xylan biosynthesis have begun to be revealed by the characterization of several T-DNA insertion mutants named *fra8* (which is allelic to *irx7*), *irx8* (referred also as *gaut12)*, *irx9*, *irx14* and *parvus* (Brown et al., 2005; Persson et al., 2005; Zhong et al., 2005; Brown et al., 2007; Persson et al., 2007a). The orthologous poplar proteins to FRA8, IRX8 and IRX9 were localized in the Golgi, the predicted location of xylan biosynthesis (Zhou et al., 2006; Zhou et al., 2007). *FRA8* encodes a GT family 47, while *IRX8* and *PARVUS* encode GTs family 8 (Zhong et al., 2005; Persson et al., 2007a; Brown et al., 2007). The mutants of these GT genes exhibit dramatic reductions in xylan and lack the complex oligosaccharide sequences described above. In contrast, IRX9 and IRX14 are members of GT family 43, which may be required for elongation of the xylan backbone (Bauer et al., 2006; Brown et al., 2007). There are two models proposed for glucuronoxylan biosynthesis in the Golgi (York and O'Neill, 2008). The first model is that glucronoxylan backbone is elongated by addition of xylosyl residues to the reducing end, which is mediated by IRX9/IRX14. Termination of elongation occurs when the complex oligosaccharide sequence produced by FRA8/IRX8/PARVUS is introduced to the reducing end. The alternative model is that the complex oligosaccharide sequence acts as a primer and xylosyl residues are sequentially added to the nonreducing end by the activity of IRX9/IRX14.

Xylan-hydrolytic enzymes secreted to the walls may be the candidate proteins that could modify xylans after deposition. A putative xylanase gene in hybrid aspen, *PttXyn10A* has been found to be co-expressed with xylan biosynthetic genes (Mellerowicz and Sundberg, 2008).

1.3.3.3 Xyloglucan

1.3.3.3.1 Xyloglucan structure

Xyloglucan (XG) is the most abundant hemicellulosic polysaccharide in the primary cell wall of dicotyledonous plants, often comprising about 20% of the dry mass of the wall (Hayashi, 1989). Xyloglucan consists of a cellulosic backbone of 1,4-linked β-D-glucose (Glc) residues (Table 1). The chain length of the backbone varies from about 300 to 3 000 glucose units (Fry, 1989). Although the type of side chains and the degree of substitution depend on plant species, tissues and even cell-types (Freshour et al., 1996; Vincken et al., 1997; Vierhuis et al., 2001), in most dicotyledonous plants up to 75% of the backbone residues are substituted with α-D-Xyl residues at O6 (O'Neill and York, 2003). Many of the Xyl residues extend the side chain bearing β-D-Gal, and α-L-Fuc-1,2-β-D-Gal substituents at O2. Most of these substituents are arranged in a very regular fashion along the backbone. Three consecutive glucosyl residues commonly carry substituents while the forth does not in most plants. This is represented as X-X-X-Glc structure where X is substituted with α-D-1,6-Xyl residues. Side chains are considered to be important for the interaction of xyloglucan with cellulose by determining the three-dimentional conformation of the xyloglucan (Levy et al., 1997).

1.3.3.3.2 Xyloglucan biosynthesis and modification

Similar to xylan, xyloglucan biosynthesis occurs in the Golgi, involving many actions of GTs. The backbone of xyloglucan, the β-1,4 glucan structure, is made by a member of the cellulose synthase like C (CslC) gene family (Richmond and Somerville, 2001). Each of the enzymes that bring sugars to side chains has been identified, except for the arabinosyltransferase that synthesizes arabinosyl side chain of xyloglucan in the Solanaceae (Lerouxel et al., 2006). For example, MUR2 encodes a fucosyltransferase from GT34. MUR3 encodes a galactosyltransferase from family GT47 that specifically adds galactose (Gal) onto the third Xyl of the X-X-X-Glc backbone. A different GT47 member adds Gal to the second Xyl. Furthermore, XT1 transfers Xyl to the Glc of the backbone.

After synthesis is completed, xyloglucans are secreted to cell walls and attach to cellulose microfibrils by hydrogen bonds and may cross-link adjacent microfibrils (Hayashi, 1989; McCann et al., 1990). Therefore, they are considered to be the main regulator of primary cell wall plasticity (Cosgrove, 2005) and need to be modulated during cell growth. XTHs – xyloglucan endotransglycosylases and hydrolases (XETs and XEHs) are suggested as the key enzymes.

1.4 Carbohydrate-active enzymes (CAZymes) involved in wood cell wall formation and modification

1.4.1 CAZymes classification and carbohydrate-binding modules (CBMs)

Carbohydrates such as cellulose, hemicelluloses, starch and sugars build up the plant body as the main component of plant cell walls and provide the energy for cell functions. Carbohydrate-active enzymes (CAZymes) are the key enzymes in synthesis, degradation and modification of carbohydrates. On the basis of amino acid sequence similarity, CAZymes have been divided into glycoside hydrolases (GHs), GTs, polysaccharide lyases (PLs) and various carbohydrate esterases (CEs). They have been further classified into families sharing the same catalytic reaction mechanism and a similar three-dimensional structure (Henrissat and Davies, 1997). They are listed in the database (DB) (http://www.cazy.org/; Coutinho and Henrissat, 1999). In addition, this DB also includes accessory modules engaged in carbohydrate-binding, the so called CBMs. The recent genome-sequencing projects in various organisms ranging from prokaryotes to higher eukaryotes augmented the number of CAZymes. At present, DB includes 753 species identified by their completely sequenced genomes.

The GH group is the largest with 112 families at present. GHs degrade carbohydrates by hydrolyzing glycosidic bonds via two major mechanisms giving rise to either an overall retention or an inversion of anomeric configuration (Henrissat, 1991; Davies and Henrissat, 1995). GH enzymes can be further divided into endo- and exo-acting, depending on the substrate site of hydrolysis. The endo-hydrolase type cleaves bonds anywhere along the substrate chain, while the exo-hydrolase type the substrate polymer successively at the chain ends (Teeri, 1997). However, it is also possible that some enzymes have both endo- and exo-action.

According to Coutinho and Henrissat (1999), many glycoside hydrolases have a modular structure, consisting of two or more functional modules, such as a catalytic module and a CBM. The initial discovery of several modules that have a binding affinity to cellulose classified CBMs as cellulose-binding domains (CBDs) (Tomme et al., 1988; Gilkes et al., 1988). However, additional modules in carbohydrate-active enzymes are continually being discovered that bind carbohydrates other than cellulose, therefore they were reclassified using more inclusive terminology (http://www.cazy.org/). CBMs constitute important functional domains in CAZymes, with 51 families identified so far. A CBM is defined as a consecutive amino acid sequence within a carbohydrate-active enzyme with a discreet fold having carbohydrate-binding activity (http://www.cazy.org/). A CBM itself is a non-catalytic component and usually targets enzymes to polysaccharide substrates, and may exhibit a wide range of binding specificities (Boraston et al., 2004). In principle, CBMs increase the efficiency of their catalytic modules through prolonged contact between the enzyme and the substrate (Bolam et al., 1998) or by targeting the catalytic module to a specific region of the substrate (Carrard et al., 2000). The CBMs so far characterized are primarily from microorganisms and information on CBMs from plant enzymes concerns mainly two GH families, GH10 and GH9.

GH10 xylanases from microorganisms commonly contain one or more family 22 CBMs linked to the catalytic module. Members of the CBM family 22 have been shown to have an affinity for soluble polysaccharides such as to xylan or mixed β-

1,3-1,4-glucans (Charnock et al., 2000; Meissner et al., 2000; Shin et al., 2002) or for insoluble polysaccharides (Devillard et al., 2003). They can even alter the substrate preferences of the catalytic module (Araki et al., 2004). It has been shown that plant GH10 xylanases can also contain one or several family 22 CBMs (Suzuki et al., 2002). However, it seems that some enzymes contain CBMs that are non-functional and need to go through proteolysis to cleave off the CBMs before the catalytic module can exhibit full xylanase activity (Caspers et al., 2001, Wu et al., 2002; Chen and Paull, 2003).

CBMs are also common modules in cellulases (Wilson and Irwin, 1999). It is reported that most cellulases from microorganisms showing activity against crystalline cellulose have a CBM. Cellulases lose much of their enzymatic capacity on insoluble substrates by removal of the CBM (Tomme et al., 1995). Recently, some plant cellulases were discovered that comprise a CBM (family 49). The CBM family 49 is shown to have a binding ability to crystalline cellulose (Urbanowicz et al., 2007a).

1.4.2 Cellulases and their roles in plants

Cellulases (also termed as endo-β-1,4-glucanases or EGases; EC 3.2.1.4) are the enzymes hydrolyzing internal β-1,4-glucosidic bonds, such as those found in cellulose and hemicelluloses, and have been identified and characterized in bacteria, fungi, plants, insects and marine animals (Lynd et al., 2002; Hildén and Johansson, 2004; Libertini et al., 2004). Cellulolytic activities are also found in cellobiohydrolases (also termed as exo-β-1,4-glucosidases; EC 3.2.1.91). Cellulases hydrolyze 1,4-β-glucan linkages in the middle of the glucan chain by endo-acting, whereas cellobiohydrolases catalyze the hydrolysis from the non-reducing end of the glucan chain processively.

1.4.2.1 *In vitro* substrates and proposed functions of plant cellulases

Cellulases are classified into 10 families (5, 6, 7, 8, 9, 12, 44, 45, 51 and 61) in the CAZymes DB but the plant cellulases characterized so far belong to family 9 (GH9) (Henrissat et al., 2001). Possibly more plant cellulases can be identified in family GH5 that includes mannanases. GH9 enzymes operate via an inverting mechanism to cleave the β-1,4-glucosidic bonds between two unsubstituted glucose units (Gebler et al., 1992). The presence of a large number of cellulase families in microbes presumably results from the abundance of cellulose and the complexity and variability of plant cell wall constituents, which are the actual substrates of most cellulases (Wilson and Irwin, 1999).

Cellulolytic enzymes from microbes act synergistically to catalyze efficient hydrolysis of crystalline cellulose to glucose (Henrissat, 1991; Teeri, 1997; Henrissat and Davies, 2000). In contrast, plant cellulases catalyze limited hydrolysis. To date, it has been shown that most of the plant GH9 cellulases studied have negligible activity on crystalline cellulose, but clearly detectable activity on soluble cellulose derivatives, such as carboxymethyl cellulose (CMC), noncrystalline phosphoric acid swollen cellulose (PASC), and/or a range of other plant polysaccharide substrates, including xyloglucan, xylans, 1,3-1,4-β-glucans,

and glucomannans (Hatfield and Nevins, 1986; Nakamura and Hayashi, 1993; Ohmiya et al., 1995; Mølhøj et al., 2001; Woolley et al., 2001; Master et al., 2004; Yoshida and Komae, 2006; Urbanowicz et al., 2007a). An exception to this is the ability of cellulases isolated from pea epicotyls (Wong et al., 1977b) and periwinkle (Smriti and Sanwal, 1999) to hydrolyze insoluble crystalline and swollen forms of cellulose, although with lower activities than towards CMC (Table 2).

Plant GH9 cellulases form a multigene family (Mølhøj et al., 2002). They are classified into three subclasses, designated by the letters A-C, corresponding to the domain structure, or subclass of the corresponding protein (Urbanowicz et al., 2007b). Subclass A contains the enzymes with a predicted N-terminal membrane-spanning domain, likely to be targeted to the plasma membrane, which would act at the innermost layers of the cell wall. Subclass B is the secreted enzymes with a predicted signal peptide, which may interact in all cell wall layers. Subclass C enzymes consist of secreted enzymes containing a C-terminal CBM family 49. This standardized nomenclature provides information about potential function of the GH9 enzymes.

Plant cellulases characterized so far, most of which belong to the subclass B, are considered to be involved in both cell wall loosening during cell elongation and expansion as well as in the wall disassembly that accompanies processes such as organ abscission and fruit ripening (reviewed by del Campillo, 1999; Rose and Bennett, 1999; Mølhøj et al., 2002).

For example, an Arabidopsis type B cellulase, Cel5, is expressed exclusively in root cap cells and appears to be associated with sloughing them from the root tip (del Campillo et al., 2004). Another Arabidopsis cellulase in the subclass B, Cel1, is strongly expressed in the elongation zone of stems (Shani et al., 1997), involved in enhancement of leaf enlargement and height growth (Shani et al., 2004). In *Populus*, type B cellulases, *Pa*PopCel1 and its paralogue, *Pa*PopCel2, were isolated from the suspension-cultured poplar (*P. alba*) (Nakamura and Hayashi, 1993; Ohmiya et al., 1995; Ohmiya et al., 2000) and they are thought to function in cell enlargement by hydrolysis of amorphous cellulose cross-linking with xyloglucan (Park et al., 2003).

In contrast, the involvement of the type A cellulase, KORRIGAN1 (KOR1) in cellulose biosynthesis has been implied during the last decade (Nicol et al., 1998; Lane et al., 2001; Sato et al., 2001, Peng et al., 2002; Szyjanowicz et al., 2004).

1.4.2.2 Involvement of membrane-anchored cellulase, KOR1, in cellulose biosynthesis

Characterization of an extreme dwarf mutant in Arabidopsis, *kor1-1*, demonstrated for the first time that the corresponding plasma membrane-bound cellulase was required for normal wall assembly, cell elongation and cellulose synthesis in plants (Nicol et al., 1998; His et al., 2001) (Table 3). Additional alleles of *kor1* were subsequently isolated. *kor1-2* shows more severe phenotype than *kor1-1,* including defects in cell plate formation during cytokinesis (Zuo et al., 2000). Temperature-sensitive alleles with point mutations, *radial swelling2* (*rsw2;* Lane et al., 2001) and *altered cell wall1* (*acw1;* Sato et al., 2001) were subsequently isolated and they show abnormal cell expansion as well as a specific reduction in cellulose

Table 2. *In vitro* substrates of plant cellulases.

Subclass	Species	Protein name	Enzyme purification	Substrates (relative activity within the tested substrates, %)											References
				Crystalline cellulose (Avicel, filter paper, BMCC)	CMC (4CM/10Glc or 7-9CM/10Glc)	HEC (25HE/ 10Glc)	PASC	Cello-biose	Lichenan or barley ß-1,3, ß-1,4 mixed glucan	Laminarin (ß-1,3-glucan)	Xylo-glucan	Xylan	Gluco-mannan	Starch	
A	Oilseed rape, *Brassica napus*	BnCel16	Recombinant protein of catalytic domain expressed in *Pichia pastoris*.	3	100(4CM) / 25(8M)	1	18	NT	2	NT	2	0	NT	NT	Molhoj et al. (2001)
A	Poplar, *P.tremula x tremuloides*	PttCel9A1	Recombinant protein of catalytic domain expressed in *P. Pastoris*.	0	100(4CM) / 55(7-9CM)	5	28	0	4	NT	3	4.5	5	NT	Master et al. (2004)
B	Poplar, *P.alba*	PaPopCel1/PtCel9B1	From suspension-culture medium by gel filtration chromatography.	0	100	NT	72	0	35	0	1.7	0	NT	NT	Nakamura and Hayashi (1993)
B	Poplar, *P.alba*	PaPopCel2/PtCel9B2	From suspension-cultured cells by gel filtration chromatography.	0	100	NT	40.5	0	47.6	0	6.1	5.4	NT	NT	Ohmiya et al. (1995)
B	Rice, *Oryza sativa* L.		From primary root tissues by anion exchange chromatography.	Trace	144(4CM) / 100(8CM)	NT	25	NT	81-87	0	Trace	18-38	14	NT	Yoshida and Komae (2006)
B	Strawberry, *Fragaria* x *ananassa* Duch.	FaEG1 (Cel1)	From ripe strawberry fruit by cellulose affinity chromatography.	0	100	NT	NT	NT	8	9	44	0	NT	0	Woolley et al. (2001)
B	Avocado, *Persea americana* Mill cv. Fuerte	PaCel1	From ripening avocado fruits by gel filtration chromatography.	0	100(4CM) / 46(7CM)	6.3	NT	NT	39	0	3.8	NT	NT	NT	Hatfield and Nevins (1986)
C	Tomato, *Solanum lycopersicum*	SlCel9C1	Recombinant protein of catalytic domain expressed in *P. Pastoris*.	*	20-34	NT	*	NT	100	NT	0	38	NT	NT	Urbanowicz et al. (2007a)
?	Periwinkle, *Catharanthus roseus*		From stem by anion exchange, gel filtration and affinity chromatography.	64	100	NT	75	0	NT	NT	NT	0	NT	NT	Smriti and Sanwal (1999)

NT - Not tested

* Recombinant fusion protein *T. fusca* Cel6A/SlCel9C1CBM can hydrolyze but not comparable to the other substrates listed.

Table 3. *korrigan1* (*kor1*) mutants in Arabidopsis.

Mutant alleles (ecotype background)	Mutation	Strength of allele	Phenotype	References
kor1-1 (Ws)	T-DNA insertion in the promoter, 200 bp upstream of the start codon.	Reduced level of transcript and protein.	Severe growth defect (dwarf). Cell elongation defect and radially expanded cells. Reduced cellulose and altered pectin deposition in the primary cell wall.	Nicol et al. (1998); His et al. (2001)
kor1-2 (C24)	1 kb deletion: the entire promoter and 5'-UTR by T-DNA.	No detectable level of transcript and protein.	Aberrant cell plates, incomplete cell walls and multinucleated cells leading to defects in cytokinesis.	Zuo et al. (2000)
irx2-1 (Ler), *irx2-2* (Col)	Point mutation by EMS in highly conserved amino acids. *irx2-1*, ^{250}Pro to Leu; *irx2-2*, ^{553}Pro to Leu (5 aa to the conserved GH9 active site motif 2)	Same level of transcript. Protein structure and activity may be affected.	Collapsed xylem elements. No primary growth defect. Cellulose deficiency in the secondary cell wall but not in the primary cell wall. A mature plant is slightly smaller than the WT.	Turner and Somerville (1997); Szyjanowicz et al. (2004)
acw1 (Col)	Point mutation by EMS. ^{429}Gly to Arg, which is predicted to be on surface of the protein.	Thermosensitive phenotype, non-permissive temperature at 31°C, which may be due to the reduced activity or stability.	Cell elongation defect and cell swelling. Dwarf. Reduction in cellulose content and increase in pectin at 31°C.	Sato et al. (2001)
rsw2-1,2,3,4	Point mutation by EMS, which is predicted to be on surface of the protein. *rsw2-1* & *2-2*, ^{429}Gly to Arg; *rsw2-3*, ^{183}Ser to Asn; *rsw2-4*, ^{344}Gly to Arg.	Thermosensitive phenotype, non-permissive temperature at 31°C, which may be due to the reduced activity or stability.	Cytokinesis and cell expansion abnormalities, and radial swelling. Dwarf. Decrease in cellulose but accumulation in short glucan chains.	Lane et al. (2001)
kor1-3	Point mutation by EMS. ^{343}Thr to Ile, which is within the catalytic domain.	Thermosensitive (cold sensitive) phenotype. Sensitivity to oryzalin is supressed at 29°C. Protein structure and activity may be affected.	Hypersensitive to the microtubule destabilizing drug oryzalin. Disordered cortical microtubules. Short swollen roots and hypocotyls of etiolated seedlings.	Paredez et al. (2008)

content of the primary cell wall. Accumulation of pectin in *acw1* was observed as in *kor1-1*, presumably due to reflection responses to the cellulose defect. *irregular xylem2* (*irx2*) was also identified as an allele carrying a point mutation in KOR1 (Turner and Somerville, 1997; Szyjanowicz et al., 2004). The *irx2* mutant shows collapsed xylem elements due to cellulose deficiency in the secondary cell wall. Therefore, the KOR1 enzyme is thought to play a central role in cellulose biosynthesis, which is required for proper cell expansion and formation of cell wall architecture in primary and secondary walls. However its exact function in cellulose biosynthesis is still under discussion.

Initially it was suggested that KOR1 might synthesize glycosidic bonds by way of transferase activity (Matthysse et al., 1995; Brummell et al., 1997). However, GH9 enzymes that have the inverting reaction mechanism do not allow for transglycosylation reactions (Koshland, 1953; Rudsander et al., 2008) and therefore this possibility was excluded.

One model suggests that KOR1 would cleave the sitosterol-β-glucosides (SGs) from sitosterol-cellodextrins (SCDs) possibly serving as primers for β-1,4-glucan chain elongation by CESAs (Figure 7a, Peng et al., 2002). However, as pointed out by Saxena and Brown (2005), this model requires an unknown mechanism to flip SCDs to the apoplastic side of the plasma membrane where KOR1 can act for cleavage of SCDs. The *in vitro* cellulose synthesis using solubilized proteins from plant membranes did not require any lipid intermediates (reviewed by Somerville et al., 2004; Saxena and Brown, 2005). In addition, the amounts of SGs and SCDs in extracts of wild type (WT) and *kor1-1* were found to be similar, suggesting that KOR1 is not likely involved in the recycling of SG primer (Robert et al., 2004). Furthermore, severe sitosterol deficient mutants in Arabidopsis, *fackel* (*fk*) and *hydra1* (*hyd1*) (Schrick et al., 2000; Schrick et al., 2002) still produced cellulose to more than half the WT. Furthermore, the amount of cellulose in the *dwf1* mutant that is defective in sitosterol synthesis (Klahre et al., 1998) were not affected (Schrick et al., 2004). The authors state that sitosterol may be required to maintain the environment for stability and activity of membrane-localized enzymes such as CESAs than be involved in the β-1,4-glucan chain priming (Schrick et al., 2004).

Another hypothesis is that KOR1 is required as an editor for the proper association of glucan chains in the cellulose microfibrils (Figure 7b). In this case, KOR1 would remove or partially cut-off defective chains that are incorrectly positioned or under strain due to faulty catalytic subunit function, which could eventually provoke a traffic jam and tension in the process of cellulose biosynthesis (Delmer, 1999; Mølhøj et al., 2002; Szyjanowicz et al., 2004; Somerville, 2006; Taylor, 2008). In this scenario, overexpression of *KOR1* would generate cellulose with increased crystallinity if KOR1 works in removal of defective molecules.

The third possibility is a function in cellulose chain termination to release the cellulose microfibril from the synthase complex (Figure 7c, Delmer, 1999; Szyjanowicz et al., 2004; Taylor, 2008). Nevertheless, this model requires a tight association of CESA and KOR1 in the plasma membrane, which has not been clearly experimentally demonstrated (Szyjanowicz et al., 2004; Desprez et al., 2007).

It has long been thought that 36 β-1,4-glucans spontaneously pack together to form a rigid cellulose microfibril through hydrogen bounding and Van der Waals force, directly after synthesized at rosettes. However, Ding and Himmel (2006)

recently proposed a new model for cellulose biosynthesis where each rosette forms first an elementary fibril, with crystalline cellulose in the center and amorphous cellulose surrounding the central core, which then coalesce aggregates with adjacent fibrils to form large macrofibrils. The macrofibrils are later split to form microfibrils, which are subsequently coated with hemicelluloses. As suggested by Rudsander (2007), it is possible that KOR1 may be involved in this model.

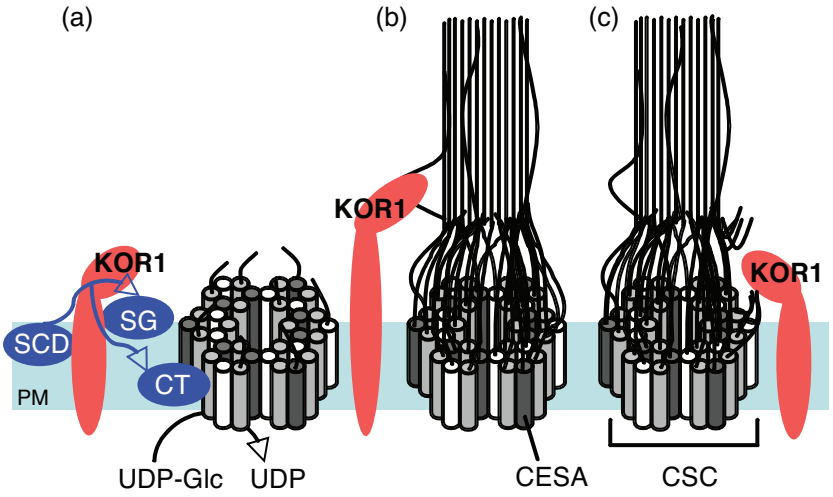

Figure 7. Current models of the involvement of KOR1 in cellulose biosynthesis. (a) KOR1 cleaving sitosterol-cellodextrin (SCD) to serve cellotriose (CT) to CESAs, which is then extended into a glucan chain by successive additions of Glc from UDP-Glc. (b) KOR1 removing or cutting off defective chains as an editor. (c) KOR1 cutting the elongating glucan chains as a terminator. Organization of CESA isoforms within cellulose synthase complex (CSC) is based on Mutwil et al. (2008).

1.4.2.3 Is KOR1 localized in the plasma membrane and associated with CESA?

An ongoing debate also concerns whether KOR1 is localized in the plasma membrane and tightly interacting with CESA proteins. If the enzyme were part of the cellulose synthesis machinery, it would be expected to associate with the rosette complex.

KOR1 homologue in tomato (*Lycopersicon esculentum*), TomCel3, was located in both the Golgi and plasma membrane by subcellular fractionation methods (Brummell et al., 1997). Zuo et al. (2000) has shown the accumulation of KOR1 in unidentified intracellular organelles in interphase cells and in the phragmoplast of dividing cells. In these experiments, a C-terminal GFP fusion to the KOR1 polar targeting sequence was expressed in tobacco BY-2 cells and localized by microscopy. Robert et al., (2005) recently reported that KOR1 localizes in endosomes and Golgi membranes but not at the plasma membrane, although some KOR1 was seen in motile compartments near the plasma membrane by introducing GFP-fused KOR1 at the N-terminus under control of the CaMV *35S* promoter. It is conceivable that KOR1 (and homologues) are shuttled to different cellular compartments depending on cell type and developmental phase. However, we

cannot exclude the possibility that intracellular endosome localization is an artifact due to overexpression by the CaMV *35S* promoter. In addition, the inability of the present microscopic techniques to detect KOR1 if only few KOR1 molecules are attached to CESA complex in the plasma membrane was pointed out by Somerville (2006). Taken together, KOR1 could be matured in the Golgi apparatus and secreted to the plasma membrane with only short lifetime (transient localization) there as is the case of CESA6 (Paredez et al., 2006).

The association of KOR1 with the secondary cell wall specific CESA protein (*At*CESA7) was analyzed by co-purification using a His-affinity resin (Szyjanowicz et al., 2004). No detectable CESA7 protein was co-purified with KOR1 protein. Furthermore, Desprez and co-workers (2007) showed that KOR1 does not coimmunoprecipitate with primary cell wall specific CESA3 or CESA6 proteins, suggesting that it is unlikely that KOR1 interacts directly with CESAs in rosette complexes. Considering the lack of co-expression with either primary or secondary cell wall *CESAs* (Brown et al., 2005; Persson et al., 2005), the KOR1 protein might rather be an independent unit of CESA rosette complex.

1.4.3 Xylanase function in plants

Xylanases (EC 3.2.1.8) cleave the β-1,4-xylosyl linkage by endo-acting (Henrissat and Bairoch, 1996). Xylosidases (EC 3.2.1.37) are other xylan backbone-degrading enzymes, but they degrade short xylan oligomers into single xylose units from the non-reducing end by exo-acting. All plant xylanases identified so far belong to GH family 10, whereas all putative plant xylosidases are classified into GH family 3 (Coutinho and Henrissat, 1999).

Many xylanases from microorganisms have been characterized in detail (Sunna and Antranikian, 1997; Beg et al., 2001; Collins et al., 2005), especially for the purpose of industrial applications, but only a few plant xylanases have been examined so far, in which mainly biochemical analysis has been performed (Benjavongkulchai and Spencer, 1986; Slade et al., 1989; Banik et al., 1996; Cleemput et al., 1997 a and b; Bih et al., 1999; Suzuki et al., 2002). Plant xylanases seem to have conserved amino acid sequences in the catalytic and substrate binding residues shown by sequence analysis with Arabidopsis, rice, maize, wheat and barley (Simpson et al., 2003).

Xylanase activity has been detected in a wide range of fruits, despite the lack of evidence for xylan degradation during ripening (Yamaki and Kakiuchi, 1979; Paull and Chen, 1983; Ronen et al., 1991; Barka et al., 2000). More precise functions of xylanases in a few species are elucidated from their expression and enzymatic activity patterns. In barley seeds during germination, a xylanase is secreted from the aleurone layer to the adjacent storage endosperm, where it hydrolyzes the cell wall, making the endosperm accessible for other hydrolytic enzymes (Slade et al., 1989; Banik et al., 1997). In maize, a xylanase expressed in the tapetum cells of the anther and, after the programmed cell death of these cells, is incorporated to the outer pollen wall, exine. It is believed to be involved in the degradation of xylan in the stigma surface for the initial penetration of pollen (Bih et al., 1999). Arabidopsis xylanase, *At*Xyn1 is predominantly expressed in vascular bundles and has been suggested to have a role in the formation of the secondary cell wall (Suzuki et al., 2002).

1.4.4 Xyloglucan endotransglycosylase/hydrolase (XTH) of plants

GH family 16 includes plant specific enzymes with two activities: xyloglucan endotransglycosylases (XETs; EC 2.4.1.207), and xyloglucan endohydrolases (XEHs; EC 3.2.1.151), jointly renamed as XTHs (Rose et al., 2002). XET activity is more prevalent in the GH16 family and it catalyzes molecular grafting between XG molecules by endolytically cleaving the XG backbone and forms a stable, covalent enzyme-substrate intermediate. This is followed by a deglycosylation step in which XET brings the newly formed reducing end of the donor molecule to the non-reducing end of the acceptor XG oligosaccharide. This leads to the formation of a new 1,4-glycosidic bond (Fry et al., 1992; Nishitani and Tominaga, 1992). XEH members use water as an acceptor, which results in hydrolysis (Fanutti et al., 1993; Tabuchi et al., 2001). In this way, XET has been considered as a key agent regulating wall expansion by cutting and rejoining XG chains, and incorporating newly synthesized XG that coats and cross-links cellulose microfibrils (Darley et al., 2001).

A large number of XTH genes have been identified in many plant species including for example, Arabidopsis (Yokoyama and Nishitani, 2001), rice (Yokoyama et al., 2004) and poplar (PaperI). Since XTH gene members within a plant species exhibit different enzymatic activities and expression patterns in different tissues (Arrowsmith and de Silva, 1995; Rose et al., 1996; Yokoyama and Nishitani, 2000; Burstin, 2000; Steele and Fry, 2000; Reidy et al., 2001; Malinowski et al., 2004; Yokoyama et al., 2004; Vissenberg et al., 2005), each gene possibly has a specific role in certain tissues or at certain developmental stages. For example, XTH members have been implicated in the wall degradation needed for cell expansion in rapidly elongation cells, in fruit ripening and in abscission (Nishitani, 1997; Nishitani, 1998; Campbell and Braam, 1999). Recently, Bourquin and co-workers (2002) revealed a new role for one of the *Populus* XTHs (*Ptt*XET16-34) during the formation of secondary cell wall of wood fibers. It was suggested that the enzyme creates and reinforces the connections between primary and secondary wall layers at the time when secondary wall layers are deposited. It has been therefore selected as one of our prime candidates for the functional genetic studies in aspen.

1.4.5 *Populus* wood-expressed CAZymes identified in previous studies

During recent years, functional genomics has been providing dynamic and high-throughput approaches for gene discovery. Several CAZymes in hybrid aspen (*Populus tremula x tremuloides*) were identified among ESTs from the cambial region tissues (Sterky et al., 1998). Although EST distribution and frequency gave a rough estimation of the expression of the corresponding genes (Mellerowicz et al., 2001), more reliable expression data were obtained with microarray analysis. High resolution transcriptome profiling studies by microarray in narrow developmental zones of developing wood tissues (Hertzberg et al., 2001; Schrader et al., 2004; Aspeborg et al., 2005) revealed that genes identified by ESTs in the cambial region, *PttGH9B3* coding for type B GH9 cellulase, and *PttXET16-34* coding for XET (Kallas et al., 2005), are highly expressed in the cambium (A) and the radial expansion zone (B) (Figure 8a & c). These genes have also abundant

transcripts in the cambial libraries (A, B and UB) (Mellerowicz et al., 2001; Sterky et al., 2004) in the EST DB. In contrast, a gene coding for a GH9 membrane-anchored cellulase, *PttCel9A1* similar to KOR1, and a gene for GH10 xylanase, *PttXyn10A*, were specifically upregulated during the secondary cell wall formation (zone D) (Figure 8a & b). The EST frequency analyses pointed to an abundant expression of *PttCel9A1*, and low expression of *PttXyn10A*, in the cambial region tissues (Mellerowicz et al., 2001; Sterky et al., 2004).

This thesis investigates functions of these four *Populus* hydrolases, *PttCel9A1*, *PttGH9B3, PttXyn10A* and *PttXET16-34* during wood formation. The reverse genetics approach was employed in both aspen and Arabidopsis. The membrane-anchored cellulase, *PttCel9A1* was studied with special emphasis using the cellulose deficient Arabidopsis mutants defective in the orthologous gene function.

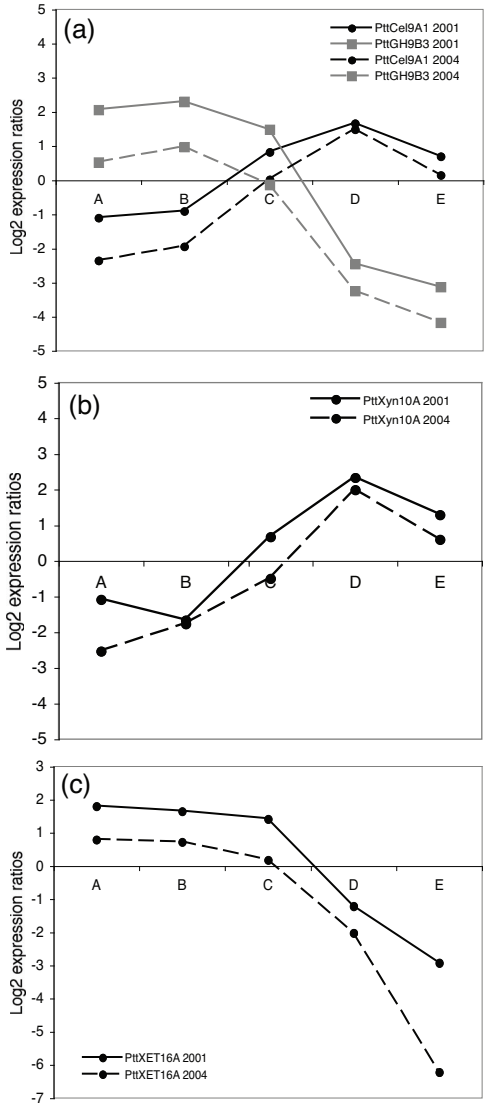

Figure 8. Expression profiling of *PttCel9A1* and *PttGH9B3* (a), *PttXyn10A* (b) and *PttXET16-34* (c) by microaarray analysis during different stages of wood formation. A, meristematic cells; B, early expansion; C, late expansion; D, early secondary wall formation; E, late maturation accompanied by PCD. Data from Hertzberg et al. (2001) (solid line) and Schrader et al. (2004) (dotted line).

2. Objectives of the investigation

The general objective of the investigation was to study the role of the selected extracellular glycoside hydrolases from families GH9, GH10 and GH16 in wood formation through:

1. Identifying all members of the selected GH families in *Populus* (Paper I)

2. Functional studies of the membrane-anchored cellulase Cel9A1/KOR1 in Arabidopsis (Paper II and section 4.2.2)

3. Gain of function studies of the wall secreted cellulase GH9B3 in Arabidopsis (section 4.2.3)

4. Loss of function studies of Xyn10A in aspen (Paper III)

5. Reverse genetics studies of XET16-34 in aspen (Paper IV)

3. Methodological overview

3.1 Reverse genetics approach

During the last decade, with accumulating information on genes and their DNA sequence, methods for conducting forward or reverse genetics in plant biology have become increasingly important. In this thesis, we adopted the reverse genetics approach in order to understand the function of the selected genes *in vivo*.

In forward genetics, a large set of randomly created mutants obtained most commonly by ethyl methanesulfonate (EMS) treatment or by insertion of T-DNA is screened for a certain phenotype. In contrast, reverse genetics is a commonly used technique to discover the function of a gene through directed strategies, in which the expression of the target gene is specifically altered by sense/antisense constructs, RNA interference (RNAi) or other techniques.

In several studies, we tried to overexpress *Populus* endogenous genes in a homologous system under control of the CaMV *35S* promoter that is frequently used for overexpression. In one of the cases, we observed a significant upregulation of the target gene (Paper IV), however, despite our expectations, in some cases transgenic plants did not show significant upregulation and/or phenotype. This could be due to the internal regulation of the endogenous gene or related similar genes within the gene family by feedback regulation or co-suppression mechanisms. A similar observation has been reported by Shani and co-workers (2004). When these authors overexpressed Arabidopsis cellulase *Cel1* using homologous systems, the transcript was not significantly increased in the stem where the gene is specifically expressed and consequently no phenotypic change in the transgenic plants was found. In contrast, it was possible to obtain poplar plants overexpressing *Cel1* at high level, exhibiting many phenotypic alterations. Introducing a gene into heterologous systems, for example from poplar into Arabidopsis, could be a way to avoid co-suppression and hence, this approach was used in Paper II.

Antisense inhibition has been long used for several different species and applications and varying degrees of success have been reported (Takayama and Inouye, 1990). In the antisense method, a plasmid encoding a sequence that is complementary to the mRNA of the gene of interest is introduced into plants and the resulting hybridization to the endogenous mRNA will lead to the duplex destruction and hence lower levels of translation. However, it is known that the antisense approach is not strong enough to completely disrupt gene expression, usually resulting only in a moderate down-regulation (Paper III) and therefore, it may not lead to strong phenotypes. This sometimes makes it difficult to elucidate the gene function.

The RNAi technique (Paper IV) is a more efficient method of gene down-regulation, discovered by Fire and co-workers (1998) through the finding by Guo and Kemphues (1995) that both sense and antisense mRNA transfection induced a remarkably precise suppression of the targeted gene. In this method, introduced sense and antisense cDNA leads to the formation of the double-stranded RNA (ds RNA) that is cleaved *in vivo* into short fragments that guide sequence-specific mRNA degradation. RNAi generally induces a stronger down-regulation than the antisense approach and might lead to a more distinct phenotype. However, an overly drastic downregulation could have serious effects on the viability of the

plant. In our study (Paper IV), the target gene, *PttXET16-34*, in most of RNAi lines was successfully reduced to approx. 50% of the level of the WT in the tissue where the transcript was abundant, without showing any critical growth defect. Transformants with stronger downregulation could be difficult to obtain if the gene function is essential for survival.

Gene knock-out lines can be very valuable for elucidation of their function. In Paper II and section 4.2.2, we employed available Arabidopsis mutants of the homologous gene to *PttCel9A1* for the comparison with Arabidopsis lines overexpressing *PttCel9A1*.

Many approaches were used to characterize phenotype caused by the altered gene expression examined during my PhD work. General plant morphology was assessed by measuring height, internode length, leaf size and hypocotyl length. Anatomical studies of secondary growth and chemical characterizations by biochemical assays, high performance liquid chromatography (HPLC), Fourier transform infrared (FT-IR) spectroscopy, nuclear magnetic resonance (NMR) and immunolocalization were also conducted. In the following part, I describe some useful methods I used intensively or developed through my projects.

3.2 Cellulase activity *in situ*[1] (Paper II)

To investigate the involvement of cellulase in the formation of secondary vascular tissues, a cellulase activity assay is needed. Traditionally, assays for extracted cellulase activity *in vitro*, in which an exogenous substrate is supplied, have been used. This approach might be of limited value for assessing the actual activity in cells because of a lack of normal protein context, for example, membrane-attachment, co-factors or protein partners might be needed for activity but are lacking in the extracts. Also, sometimes proteins cannot be efficiently extracted in their native form. In addition, a variety of factors such as inhibitory compounds, proteases or other co-extracted plant enzymes competing for the same substrates can also negatively influence the assays (Schröder et al., 2004). An *in situ* cellulase activity assay is an alternative approach that circumvents some of these problems. We developed an *in situ* cellulase assay using resorufinyl β-D-cellobioside (Glc_2-Res) with confocal laser scanning microscopy (CLSM). Previously *in situ* cellulase activity has been indirectly visualized using transmission electron microscopy (TEM) by cupric oxide precipitation as a result of hydrolysis of CMC (Krishnamurthy, 1999).

The *in situ* cellulase activity assay that we developed is based on the release of the fluorescent resorufin anion from Glc_2-Res in fresh tissue sections, which marks the location of active cellulase and the label can be observed by real-time CLSM. Since sequential exo-glucosidase hydrolysis on Glc_2-Res can also yield resorufin fluorescence, we additionally included tests with resorufinyl β-D-glucopyranoside (Glc-Res) substrate to monitor this activity. The substrates were synthesized from the commercially available acetates of glucose and cellobiose (Sigma) by Dr. Harry Brumer and Dr. Farid M. Ibatullin (KTH).

Fresh tissue sections (an approximate thickness of 200 μm) of Arabidopsis were mounted on a glass slide with either 0.1 M MES (2-(N-morpholino)ethanesulfonic acid) buffer only or the buffer containing Glc_2-Res or Glc-Res. Activity was

detected by CLSM using an excitation wavelength of 567 nm and detection wavelength of 580 nm or above.

To optimize the best condition for the resorufinyl-conjugated substrate and cellulase activity within the fresh plant, MES buffers with different pH were tested. Resorufin is a basic stable compound with a p*Ka* of approx. 6.5, meaning 50% of the maximum fluorescence intensity is displayed at pH 6.5 and approx. 90 % is displayed at pH 7.5. However, cellulases in general are thought to prefer acidic conditions from several *in vitro* studies (Mølhøj et al., 2001; Urbanowicz et al., 2007a), for example *Ptt*Cel9A1 exhibited the highest activity between 5.5 and 6.0 (Master et al., 2004). Thus, the equivalence of enzyme and substrate stability is very important and the best condition was assumed to lie at between pH 6.0 and 7.0. As a result, the strongest signal was obtained with pH 6.0, which was a more enzyme-favoured condition. As a negative control, sections heat-denatured for 30 min at 100°C were compared to non-treated sections. The level of background autofluorescence was evaluated using negative controls lacking fluorescent substrate, and the microscope detection settings were adjusted to zero detection in the developing wood. Using these settings, we did not detect any fluorescent signal on the heat-denatured sections incubated with the resorufin substrate, in contrast, the fresh sections developed a signal that increased in intensity during the 20 min incubation at which time it reached a plateau. Some autofluorescence especially in the stem cortex, coming from cytosols, which could be due to flavonoides or from chloroplasts due to chlorophyll *a* and *b*, was occasionally observed. This signal did not increase during the incubation time.

Arabidopsis plants at two different growth stages (five or eight weeks old) and two different secondary tissues (stem base or hypocotyl) were tested. The accumulation of resorufin anion was detected in a time-dependent fashion in secondary cell walls of phloem fibers and wood forming tissues of both stem and hypocotyl, regardless of different growth stages. The strong signals were observed especially in secondary cell walls of developing fibers and vessel elements close to the cambial zone (for the example of the stem section, Paper II, Figure 4). Primary cell walls exhibited fluorescence only very weakly after a long incubation.

In general, the fluorescence release from Glc-Res was equivalent or slightly higher than that from Glc_2-Res after the same incubation time in both stem and hypocotyl, indicating that the hydrolysis of Glc_2-Res is partially due to exo-glucosidase activity. In order to detect only sole cellulase activity, an improvement of a substrate compound specific for cellulase is necessary.

This method was further used to visualize the increased level of enzymatic activity of the *35S::PttCel9A1* overexpressing (OE) lines in Arabidopsis (Paper II, Figure 4). The resorufin anion was more strongly accumulated in the OE lines than in the WT. Hence, the method we developed can successfully visualize the location where cellulase activity occurs and can be used as a semi-quantitative method. Further development of the substrate compounds specific for cellulase will be the next step.

3.3 Carbohydrate analysis[2]

Although Arabidopsis is a good model plant to study wood formation, one disadvantage is that the amount of tissue, especially of secondary xylem, is small

compared to a perennial tree. Cell wall chemical composition analysis frequently requires a relatively large amount of sample. Soluble carbohydrates such as glucose, sucrose and fructose as well as insoluble starch are physiologically important compounds that can influence the carbohydrate flow leading to synthesis of cell wall materials. Here I developed a sequential quantification approach to analyze not only cell wall, but also soluble carbohydrates with a limited amount of sample.

Mature rosette leaves, inflorescence stem bases (5 cm) and hypocotyls of six-week-old plants were used for analysis (Paper II; section 4.2.3). A leaf, stem and hypocotyl sample of ten pooled plants can yield up to 40, 70 and 15 mg after lyophilization, respectively.

Soluble carbohydrates from 20 mg of lyophilized leaves and stems or 15 mg of hypocotyls were extracted a few times in ethanol with different concentrations. A part of the residual pellet containing starch and cell wall material was used to hydrolyze starch by amyloglucosidase. Digested glucose derived from starch and soluble sugars was quantified by ion chromatography.

The alcohol insoluble residue (AIR) after soluble sugar extraction was stored to analyze cell wall carbohydrates. After removing starch with amyloglucosidase or amylase, they were dried with acetone. In general, Arabidopsis leaf sample yields 3 - 6 mg, stem 8 - 10 mg and hypocotyls 7 - 9 mg. For accurate measurement of crystalline cellulose by the method of Updegraff (1969), more than 6 mg AIR is preferred.

Updegraff's method has been widely used to measure crystalline cellulose that is resistant to acetic/nitric acid hydrolysis. All non-cellulosic sugars were first hydrolyzed in acetic/nitric acid and removed, and the crystalline cellulose content was then measured as a glucose monomer by the anthrone method (Scott and Melvin, 1953) after hydrolysis in 67 - 72% sulphuric acid (Paper II; section 4.2.3).

In parallel with Updegraff's method, monosaccharide composition of non-cellulosic fraction can be analyzed with 3 mg AIR samples by trifluoroacetic acid (TFA) hydrolysis. The remaining pellet of crystalline cellulose can be also hydrolyzed in sulphuric acid. The determination of monosaccharide composition was performed by high performance anion exchange chromatography with pulsed amperometric detection (HPAEC-PAD).

Furthermore, 15mg AIR can be used for fractionation of cell wall material. Pectin, loosely bound hemicellulose and tightly bound hemicellulose fractions were extracted with 0.1 M, 1M and 6M potassium hydroxide, respectively. These fractions were further hydrolyzed with TFA and the remaining pellet (crystalline cellulose) was hydrolyzed with sulphuric acid. They were quantified by HPAEC-PAD as above.

Taken together, one sequential analysis of soluble carbohydrates, starch and either crystalline cellulose or monosaccharide composition analysis by TFA or sulphuric acid can be successfully performed with only minimum amount of an Arabidopsis leaf (40 mg), stem (70 mg) and hypocotyl (15 mg) sample from ten pooled plants. Alternatively the same sample batch from stem base is enough to be used for fractionation analysis. The above procedure combining soluble and cell wall carbohydrates analysis may be beneficial for the researchers working in this field.

3.4 Application of NMR technique for detection of cellulose crystallinity

NMR spectroscopy is a non-destructive, robust and highly informative analytical technique that can be used to determine the chemical structure of different cell wall polymers both in solid state (Maunu, 2002) and in solution (Lu and Ralph, 2003). The structural assignment is based on analysis of several spectroscopic parameters for each magnetically active nucleus (e.g. ^{1}H or ^{13}C) in the glucan. A nucleus can be identified by its resonance frequency (chemical shift), which depends on its molecular environment (Duus et al., 2000). A qualitative and quantitative global fingerprint of wood samples can be obtained by this method, from which both chemical structure of different cell wall polymers and their relative concentrations can be determined.

This technique was applied to analyze the cellulose crystallinity of mature Arabidopsis stems overexpressing *PttCel9A1* (Paper II) with the help of Dr. Mattias Hedenström, comparing the peaks originated from the crystalline interior (89 ppm) and from more amorphous regions of the fibrils (84 ppm) assigned to C4 (VanderHart and Atalla, 1984; Ha et al., 1998; Wickholm et al., 1998) with cross-polarization magic angle spinning (CPMAS) ^{13}C NMR spectrometry (Paper II). However, the peaks also contain hemicelluloses and lignin spectra. The proton spin relaxation editing (PSRE) method (Newman and Hemmingson, 1990; Newman, 1999) was further employed to remove overlapping peaks from hemicelluloses and lignin from the cellulose spectra, utilizing the fact that different spatial domains in the sample have different proton relaxation times. Incorporation of a spin-lock pulse, t_{SL} during which relaxation occur thus serves to discriminate between the slowly relaxing cellulose signals and the more rapidly decaying hemicellulose and lignin signals.

3.5 Multivariate analysis

Chemometrics is the approach of applying mathematical and statistical information to analyze chemical and biological data (Workman, 2002). The combination of NMR or FT-IR data with large number of variables and multivariate methods such as principal component analysis (PCA) (Wold, 1976), partial least squares - discriminant analysis (PLS-DA) and orthogonal projections to latent structures (OPLS) (Trygg and Wold, 2002) in classification studies results in multivariate statistical analysis with high interpretability. These methods give an overview of the variation in the data set and can visualize the spectroscopic data discriminating between sample groups (Hedenström et al., 2008). SIMCA-P version 11.0.0.0 or 11.5 (UMETRICS, Sweden) was used to do the multivariate analysis (Papers II and III).

---

[1] The experimental procedure in detail is attached as an appendix protocol 1.
[2] The experimental procedure in detail is attached as an appendix protocol 2.

4. Results and discussion

4.1 CAZyme genes in *Populus* (Papers I, II & III)

The release of genome sequence of *Populus trichocarpa* (Torr. & Gray) to public (Tuskan et al., 2006) gave us an opportunity to examine the full spectrum of CAZymes in a woody plant species for the first time. In Paper I, we identified all members of CAZyme families (1603 gene models) and closely related expansins (42 gene models), and compared their genetic diversity between *P. trichocarpa* and Arabidopsis. We further analyzed the global expression pattern of selected CAZymes in two species, focusing on sugar/starch metabolism and cell wall carbohydrate biosynthesis, using Arabidopsis microarray data available in public domain as well as *Populus* EST DB (Sterky et al., 2004). I focused on GH9 cellulases and GH10 xylanases, which are briefly described below.

4.1.1 GH9 cellulases

Twenty-six full-length and seven truncated putative GH9 genes were identified among *P. trichocarpa* gene models (Paper II, Table S1). The full-length gene models contained the amino acid residues characteristics to the consensus GH9 active site signature 1: [S/T/V]-X-[L/I/V/M/F/Y]-[S/T/V]-X-X-G-X-[N/K/R]-X-X-X-X-[P/L/I/V/M]-H-X-R and signature 2: [F/Y/W]-X-D-X-X-X-X-[F/Y/W]-X-X-X-E-X-[S/T/A]-X-X-X-N-[S/T/A] (X represents any amino acid residue) according to PROSITE (http://www.expasy.ch/prosite/) defined by Henrissat (1991). Active site residues H for the signature 1, and D and E for the signature 2 were present for all the full-length gene models (as an example for the selected gene models, see Figure 13).

Twenty-nine *PtGH9* genes that were mapped are scattered over 13 of 19 *P. trichocarpa* chromosomes, in the same way as 25 Arabidopsis *AtGH9* genes are widely distributed over the all five chromosomes. Among 26 *Populus* genes, seven pairs of genes were identified that showed over 90% identity to each other at the nucleotide (CDS) or amino acid level, which is a more frequent occurrence than that of a cellulase gene pair/trio in Arabidopsis (Table 4). Furthermore, these duplicated genes are located on different chromosomes (Paper II, Table S1). A similar observation was also made with *Populus CESA* genes (Djerbi et al., 2005). This is an indication that a chromosomal duplication (polyploidization) occurred in the *Populus* linage (Simillion et al., 2002). Polyploidization is a common phenomenon in plants and many angiosperm species have experienced at least one genome duplication event in the past (Bowers et al., 2003). Arabidopsis may have undergone three rounds of genome duplications (Simillion et al., 2002). The two copies generated after each duplication could have different fates during subsequent evolution. One of the genes may go through pseudogenization to become silent, or it may acquire a new or slightly modified function, so called neofunctionalization or subfunctionalization as long as the other copy retains its fundamental function (Prince and Pickett, 2002). For example, *PtCel9A1 (PtGH9A1)* and *PtGH9A2*, which were found to be most similar to *KOR1*, are 93.1 % and 94.0 % identical to each other at the nucleotide (CDS) and the amino acid level, respectively. However, based on the EST frequency, only *PtCel9A1* exhibits a high level of

expression. This is an indication that *PtGH9A2* may have acquired a specialized expression. The duplication mechanism is thus considered to be important for generation of new genes and adaptation to new environments in terms of evolution.

The full-length *P. trichocarpa* gene models were divided into A, B or C subclasses according to the proposed nomenclature for plant cellulases (referred to in section 1.4.2.1, Urbanowicz et al., 2007b). The proteins whose cellulase activity and substrate specificity are determined for any *Populus* species were given a trivial name "Cel", followed by the GH family number 9. Five *Pt*GH9 proteins, *Pt*Cel9A1-5, contain a single N-terminal trans membrane helix (TMH) similar to the three Arabidopsis KORs (Paper II, Figure 1a) and hence are classified into subclass A. Subclass B is composed of secreted enzymes with a predicted signal peptide (SP). Twelve *Pt*GH9 proteins were found to comprise predicted SPs. They were observed broadly distributed in the subfamilies III, V, VI, VII defined by Mølhøj et al. (2002) according to protein sequence similarity and functional studies. In subclass B, two cellulase genes from *Populus alba*, *PaPopCel1* and *PaPopCel2* have been previously reported (Nakamura and Hayashi, 1993, Ohmiya et al., 1995; Nakamura et al., 1995; Ohmiya et al., 2000; Ohmiya et al., 2003; Park et al., 2003). These cellulases were isolated in *Populus* suspension cell culture as extracellular (*Pa*PopCel1) or cell wall-bound (*Pa*PopCel2) enzymes, and have been shown to act on amorphous cellulose (Nakamura and Hayashi, 1993; Ohmiya et al., 1995). They may function to increase cell wall plasticity *in vivo* (Park et al., 2003). Similar to Arabidopsis, three gene models that encode a putative CBM 49 at the C-terminus of the protein were found in *Populus* and named *PtGH9C1-3*, in the subclass C. A CBM 49 of tomato cellulase *Sl*Cel9C1 (formerly called Tomato Cel8) was demonstrated to bind to crystalline cellulose, suggesting a new function with an activity against crystalline cellulose (Urbanowicz et al., 2007a).

The remaining gene models that could not be subclassified, due to their low probability of having a certain domain, retained CAZyme family gene IDs (Paper I, Table S1).

Table 4. The *Populus* and Arabidopsis genes that have a high identity at nucleotide or amino acid level (over 90%).

New standardized name	Amino acid identity (%)	Nucleotide (CDS) identity (%)	New standardized name	Amino acid identity (%)	Nucleotide (CDS) identity (%)
P. trichocarpa[1]			**Arabidopsis**[2]		
PtCel9A1	94.0	93,1	AtGH9B14	91.3	90.8
PtGH9A2			AtGH9B15		
PtGH9A3	87.0	90.1	AtGH9B9	91.1	93.6
PtGH9A4			AtGH9B10		
PtGH9B4	91.2	90.5	AtGH9B10	86.2	91.6
PtGH9B5			AtGH9B11		
PtGH9B6	92.1	90.4	AtGH9B9	87.0	90.9
PtGH9B7			AtGH9B11		
PtGH9B8	92.3	89.7			
PtGH9B9					
PtGH9_27	85.9	90.6			
PtGH9_28					
PtGH9C2	92.4	91.7			
PtGH9C3					

[1] Paper II; [2] Urbanowicz et al. (2007b)

4.1.2 GH10 xylanases

The *P. trichocarpa* genome contains seven *GH10* xylanase gene models denoted *PtXyn10A* to *G* (Paper I). All the gene models possess the conserved residue E located in the consensus GH10 catalytic motif [G/T/A]-X-X-[L/I/V/N]-X-[I/V/M/F]-[S/T]-E-[L/I/Y]-[D/N]-[L/I/V/M/F] (X represents any amino acid residue), (Figure 9). The active site residue E is shown to be necessary for the enzymatic activity of *Streptomyces lividans* xylanase $XlnA_{32kD}$ (Moreau et al., 1994).

In general, the *P. trichocarpa* genome contains approx. 1.6 times as many CAZyme genes as the Arabidopsis genome and genes in most families are proportionally increased, as shown in Paper I, reflecting the ancient polyploidization events during the history of the *Populus* genus (Tuskan et al., 2006). However, GH10 xylanase family is disproportionately smaller in *P. trichocarpa* than in Arabidopsis or in rice, which have 12 and 10 (or 11) members, respectively (Henrissat et al., 2001; Yokoyama et al., 2004). In the secondary cell walls of poplar, xylan, which can be the main substrate *in vivo* for xylanases, constitutes 18 - 28% of the total cell wall material and is the major hemicellulose (Figure 4, Simson and Timell, 1978 a-d; Willför et al., 2005; Davis et al., 2006). Thus, the smaller xylanase family in *P. trichocarpa* was unexpected. Perhaps *Populus GH10* genes lost the other paralogue after the duplication event while the duplicated genes in Arabidopsis or rice may have acquired new functions via neofunctionalization/subfunctionalization (Moore and Purugganan, 2005). A possible explanation for this is that maintaining two genes with the original function had disadvantages for *Populus*, for example, too strong xylanase activity could be harmful for stem longevity needed for reproduction in a tree species, by compromising the mechanical resistance of cell walls.

Only *Pt*Xyn10D is predicted to have a SP (Paper III, Figure 2; Table S1). Even though the absence of an obvious SP indicates that the other xylanase proteins should be retained in the cytoplasm, *At*Xyn1, the closest homologue to *Pt*Xyn10A in Arabidopsis, which also doesn't comprise an apparent SP, has been shown to be translocated into the cell wall (Suzuki et al., 2002). The prediction program SecretomeP 2.0 (http://www.cbs.dtu.dk/services/SecretomeP/) also suggests that *Ptt*Xyn10A protein is extracellular.

Similar to Arabidopsis, the number of CBMs predicted in each *Populus GH10* gene model varies within the GH10 family. The JGI model proposed for *Pt*Xyn10A is predicted to have four N-terminal family 22 CBMs, however, cDNA sequence of *PttXyn10A* obtained by 5'RACE-based cloning showed that *Ptt*Xyn10A would comprise only three CBMs in agreement with *At*Xyn1 sequence. *Pt*Xyn10C, D and E are predicted to have single CBMs and others to have none (Paper III, Figure 2; Table S1). CBM is a noncatalytic domain that specifically brings the linked catalytic module of the enzyme to polysaccharide substrates. The role of CBM is thought to place the enzyme on a specific substrate or even on a specific region of the substrate and facilitate the catalytic activity by concentrating the local enzyme (Bolam et al., 1998; Carrard et al., 2000). In addition, CBMs possibly disrupt the crystalline structure of the substrates thus supplying the catalytic module with more easily digestible substrates (Linder and Teeri, 1997). An enzyme possessing multiple CBMs could exhibit synergistically higher efficiency for its activity. Interestingly, *PttXyn10A* that was found to have

ESTs in wood forming tissues and was shown to be specifically upregulated during secondary cell wall biosynthesis (Aspeborg et al., 2005) contains three CBMs. However, in Paper III, we found that the mature protein found in cell walls has a lower molecular weight (MW) corresponding to the predicted deletion of two CBMs.

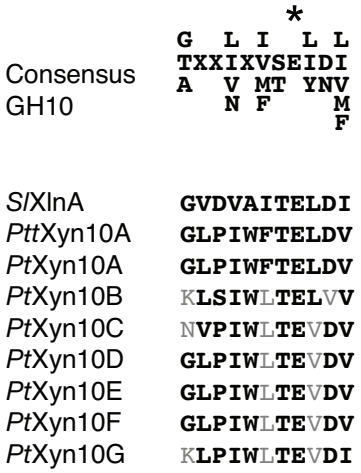

Figure 9. A comparison of the consensus amino acid sequences of the GH10 active site of *Streptomyces lividans* xylanase A $XlnA_{32kD}$ (aa 229-239) and poplar GH10 xylanases. Amino acids that are identical to the amino residues of the consensus sequences, are written in black bold. The catalytic residue E corresponding to E-236 in XlnA32kD (Moreau et al., 1994) is shown with an asterisk.

4.2 Functional genetic studies of wood-expressed cellulases *Ptt*Cel9A1 and *Ptt*GH9B3 in hybrid aspen

4.2.1 Novel role of the membrane-anchored cellulases in cellulose biosynthesis revealed by secondary growth phenotypes (Paper II)

PttCel9A1 has a predicted open reading frame made up of six exons (http://genome.jgi-psf.org/Poptr1_1/Poptr1_1.home.html) as confirmed by isolation of full-length cDNA clones. It has seven predicted N-glycosylation and 15 phosphorylation sites, a MW of 68.6 kDa and an isoelectric point (IP) of 8.86, similar to *P. tremuloides Ptr*KOR (Bhandari et al., 2006), whose encoded protein is 98.5% identical to *Ptt*Cel9A1. The sequence analysis indicates that *Ptt*Cel9A1 comprises a N-terminal cytosolic tail and a TMH, followed by an extraplasmic GH9 catalytic domain (Rudsander et al., 2003; Figure 10), which is a typical type A cellulase. A single propeptide cleavage site is predicted at aa 59 (within the cytosolic tail).

Sequence comparisons and the complementation study suggest that *Ptt*Cel9A1 is an orthologue of KOR1 (Paper II, Figures 1a & 3; section 4.2.2). The *PttCel9A1* and *KOR1* are 76% and 83% identical to each other at the nucleotide (CDS) and the amino acid level, respectively, and have the same type A modular structure. Mutations in KOR1 have been identified from a number of screens including dwarfism (Nicol et al., 1998), radial swelling of the root (Lane et al., 2001; Sato et al., 2001) and collapse of xylem vessels (Szyjanowicz et al., 2004) (Table 3). These mutations result in reduced cellulose in both primary and secondary cell walls, hence it has been suggested that KOR1 plays a central role in cellulose biosynthesis (referred to in section 1.4.2.2). The Severe dwarf phenotype of the leaky insertional mutant, *kor1-1*, and the mild allele caused by a point mutation in KOR1, *irx2-2*, have been used for the analyses in comparison to *PttCel9A1* in our study (Paper II).

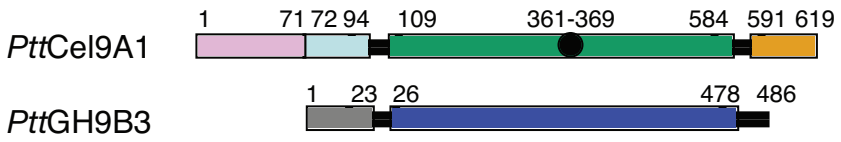

Figure 10. Schematic representation of two *Populus* cellulases, *Ptt*Cel9A1 and *Ptt*GH9B3, isolated from hybrid aspen. *Ptt*Cel9A1 domains: cytoplasmic tail (pink), transmembrane domain (TMD: light blue), GH9 catalytic domain (green), blocking loop (BL: black), proline rich domain (PRD: orange). *Ptt*GH9B3 domains: signal peptide (SP: gray), GH9 catalytic domain (blue). Numbers refer to the first or last amino acid residue of each domain.

PttCel9A1 was found to be ubiquitously expressed, but the most intense signals were observed in the secondary xylem cells in the mature stem and root (Paper II, Figure S1). In Arabidopsis, the expression of *KOR1* was higher in secondary wall-forming xylem cells and phloem sieve tubes than in cambial cells, although

relatively high levels of expression was also detected throughout the vegetative development by histochemical localization of GUS activity (Paper II, Figure 2). These expression patterns indicate *PttCel9A1* and *KOR1* are particularly important for secondary vascular developing cells, especially where the secondary cell wall is being synthesized.

Transgenic Arabidopsis lines expressing *PttCel9A1* under control of the CaMV *35S* promoter (OE lines) were generated. Elevated endo-hydrolytic activity against resorufinyl β-D-cellobioside in secondary walls was detected (section 3.2; Paper II, Figure 4), but the endogenous *KOR1* expression was not influenced by the transgene expression (data not shown). OE Arabidopsis lines exhibited defects in cell wall mechanical properties and cell elongation during primary growth, but only in the most highly expressing lines (Paper II, Figure S3). The same phenotype was observed in the severely affected *kor1-1* mutants deficient in KOR1 (personal communication with Dr. P. Ryden; Nicol et al., 1998). This suggests that *Ptt*Cel9A1/KOR1 regulates cell wall strength and primary wall plasticity, requiring a proper level of *Ptt*Cel9A1/KOR1 expression.

To investigate the role of *Ptt*Cel9A1/KOR1 in wood formation, the OE lines were examined at maturity when both stems and hypocotyls produced secondary growth. In general, *PttCel9A1* OE plants grew normally and did not exhibit any readily apparent alterations in morphology. However, excess of *Ptt*Cel9A1/KOR1 function slightly increased wall thickening and inhibited wood cell growth but wall morphology was not visibly altered, while deficiency resulted in wood cell growth defects, severe wall thinning and abnormal wall architecture (Paper II, Figure 5 & 6). In particular, fibers with sparsely distributed macrofibril-like structures were observed, suggesting a role for KOR1 in microfibril/macrofibril organization.

The effect of the overexpression of *PttCel9A1* on cellulose biosynthesis was investigated by quantifying the level of total cellulose in comparison to *irx2-2*. The *irx2-2* mutant showed no difference in amorphous cellulose content solubilized by TFA, but had a reduced level of crystalline cellulose, as reported by Szyjanowicz and co-workers (2004), whereas the OE lines exhibited an increase in amorphous cellulose, but no difference in the amount of crystalline cellulose compared to the WT (Paper II, Table 1 and Figure 7). Furthermore, we analyzed the cellulose crystallinity index by ^{13}C solid state NMR spectroscopy with the PSRE method which extracts cellulose-specific spectra (referred to in section 3.4). The crystallinity index was determined as a ratio between crystalline cellulose peak (89 ppm) and the total cellulose (sum of peak intensities at 84 and 89 ppm) (Paper II, Figure 8b). Compared to the WT, a clear reduction of the cellulose crystallinity index in OE lines and an increase in *irx2-2* were observed (Paper II, Figure 8e). Thus, the expression of *Ptt*Cel9A/KOR1 inversely correlated with cellulose crystallinity. Moreover, overexpression of *PttCel9A/KOR1* increased amorphous cellulose content.

Several hypotheses have been proposed concerning the function of KOR1 during cellulose biosynthesis (referred to in section 1.4.2.2, Figure 7). Our observation agrees with two possible hypotheses where *Ptt*Cel9A1/KOR1 plays different roles. The first hypothesis is that *Ptt*Cel9A1/KOR1 works as an editor for proper packing of cellulose microfibrils by cleaving the stalling glucan chains that are not elongating synchronously with other chains produced from rosette complexes

(Figure 7b, Mølhøj et al., 2002; Szyjanowicz et al., 2004; Somerville, 2006; Taylor, 2008). This results in an increase of amorphous cellulose due to a higher frequency of gaps and misaligned cut-ends within microfibrils.

In the second hypothesis, *Ptt*Cel9A1/KOR1 could function to hydrolyze the glucan chains bonding adjacent elementary microfibrils within the macrofibrils to produce ultimately smaller aggregates (microfibrils), based on the new model of cellulose organization proposed by Ding and Himmel (2006) (Figure 11). In this hypothesis, the defective *Ptt*Cel9A1/KOR1 in *irx2-2* would lead to accumulation of large macrofibrils, which might slow down the movement of rosettes (Paredez et al., 2008) and thus reduce the cellulose biosynthesis rate. This is in agreement with the abnormal cell wall morphology of secondary xylem elements in *kor1* mutants, which was characterized by the presence of macrofibril-like structures sparsely distributed in cell walls (Paper II, Figure 6). Conversely, excess *Ptt*Cel9A1/KOR1 would lead to extensive splitting of macrofibrils exposing microfibrils with more amorphous cellulose on the surface for association with hemicelluloses and pectin, which would lead to a less extensible wall, observed as inhibited cell growth and strength in OE lines (Paper II, Figure S3).

Thus, *Ptt*Cel9A1/KOR1 activity in cell walls could facilitate cellulose biosynthesis by either editing growing microfibrils or splitting macrofibrils for proper formation of macrofibril-microfibril network. *Ptt*Cel9A/KOR1 action might therefore be most important during the secondary wall formation where the high rate of cellulose synthesis is ongoing.

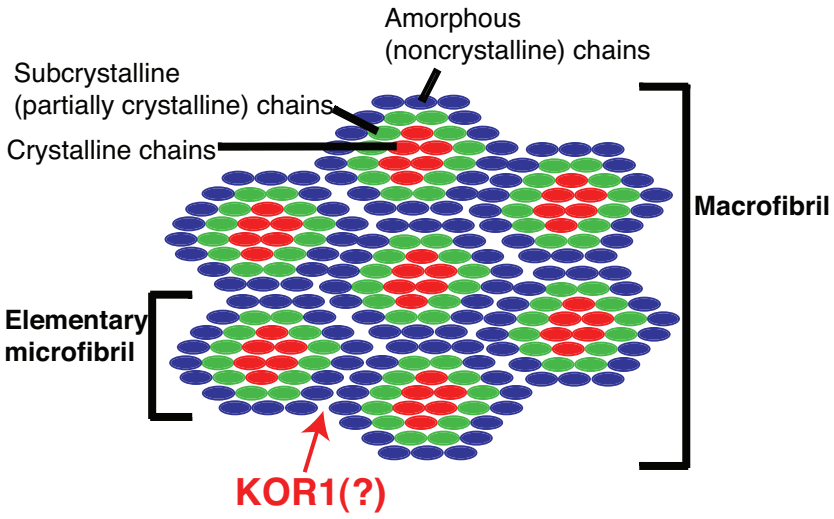

Figure 11. A structural model of cellulose fibril organization in a cross-sectional view, suggested by Ding and Himmel (2006). A cellulose synthase complex (CSC) first forms an elementary microfibril with 36 glucan chains, with crystalline cellulose (red) in the core, and amorphous cellulose (blue) in the surroundings. Seven elementary microfibrils aggregated to a macrofibril are shown. KOR1 may hydrolyze amorphous cellulose to break the aggregates into the finer fibrils seen in the cell wall.

4.2.2 Domain swapping of *Populus* cellulases (Unpublished data)

We demonstrated that full-length *Ptt*Cel9A1 could functionally substitute KOR1, while another cellulase, *Ptt*GH9B3, could not (Paper II, Figure 3). We further studied the complementation of *kor1-1* and *irx2-2* mutants with *PttCel9A1* using easily quantifiable variables serving as growth measures: the above ground biomass and the rosette leaf size. The biomass and the rosette size of *kor1-1* were enhanced by expressing *PttCel9A1*, but they were not fully restored to the WT level (Figure 12). This was also evident from the examination of plant morphology (Figure 15). The partial complementation by *PttCel9A1* could be due to the less efficient expression from the *35S* promoter as compared with the native *KOR1* promoter. Nevertheless the significant effect of *PttCel9A1* in the mutants allows us to use this complementation system to test the different modules of the protein for their function.

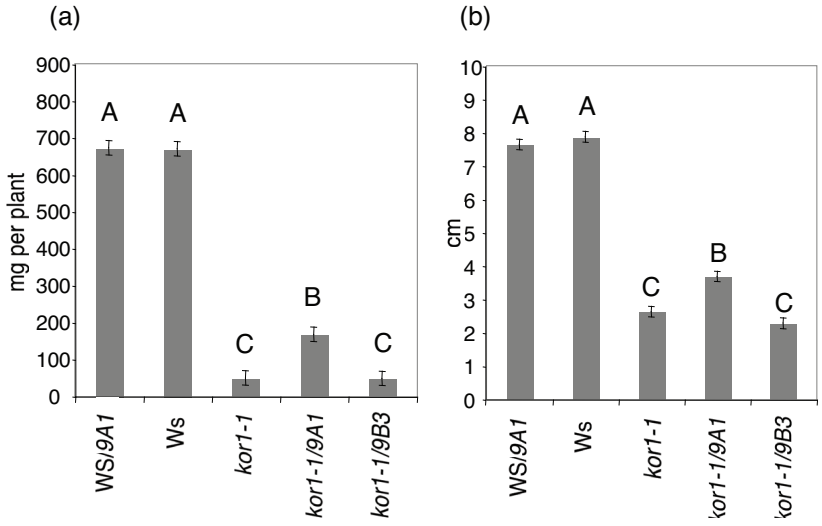

Figure 12. Complementation of the dry mass weight (a) and rosette leaf size (b) of *kor1-1* mutant by *PttCel9A1* or *PttGH9B3*. Data are from mature Arabidopsis plants. All lines carried plasmid with a hygromycin resistance gene and either *35S::PttCel9A1*, or *35S::PttGH9B3*, or no poplar gene. Seedlings of T_2 generation were grown on MS plates with hygromycin for two weeks and on soil under LD condition for 5 weeks. The full-length *PttCel9A1* driven by CaMV *35S* promoter can partially complement the *kor1-1* phenotype, while the full-length *PttGH9B3* can not. The comparison was made for all pairs using Tukey-Kramer honestly significant difference (HSD) ($P \leq 0.05$). Means ± SE; 5 transgenic lines, 6 plants each were scored. Levels not connected by the same letter are significantly different.

In order to investigate which of the *Ptt*Cel9A1 domains are important for its function *in vivo*, we created a number of constructs and introduced them into *kor1-1* and *irx2-2* mutants.

The cytoplasmic tail of *Ptt*Cel9A1 contains two putative polarized targeting signals (Figure 13a) that are present in KOR1 and are sufficient to target the protein

to the cell plate (Zuo et al., 2000). Thus, we reasoned that the cytoplasmic tail and transmembrane domain (TMD) are essential for proper targeting of the protein and the exposure of the catalytic domain to the apoplast. The question was if the catalytic domain of any type of cellulase would perform the same function. Therefore, a construct pEM10 was made in which the cytoplasmic tail and TMD were added to the catalytic domain of *Ptt*GH9B3 at the N-terminus (Figure 14). The partial complementation effect of *Ptt*Cel9A1 on the biomass and the rosette size, as well as abnormal vessel elements could not be reproduced with the pEM10 construct (Figures 15, 16 and 17) indicating that the catalytic domain of *Ptt*Cel9A1 is essential for this gene function.

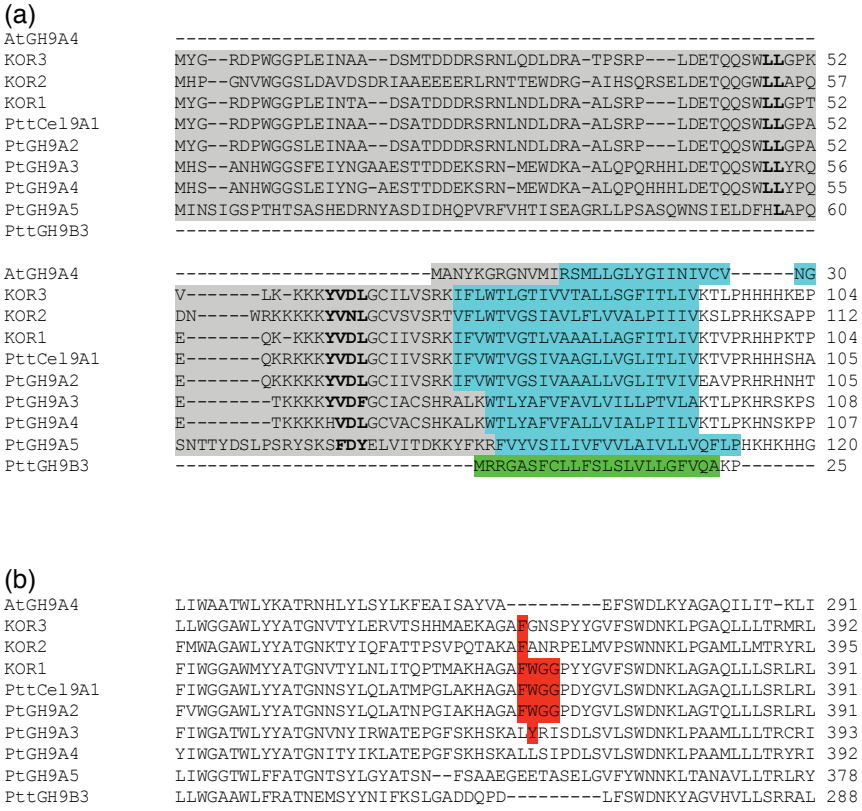

Figure 13. *Ptt*Cel9A1, *Ptt*GH9B3 and *At*KOR1 protein sequence alignments showing regions with characteristic motifs.
(a) Cytoplasmic tail (grey) and TMD (light blue; based on Nicol et al. (1998), Zuo et al. (2000) and prediction by TMHMM program at CBS). Dileucine-based and tyrosine-based cell plate targeting signals (LL and YXXΦ, with Φ referring to any hydrophobic amino acid, Zuo et al. (2000)) are in bold, SP is indicated green.
(b) Conserved BL (red) of the type A cellulase, which has four important motives (two aromatic F, W, Y residues and GG). Figure based on Rudsander (2007).

(c)

```
AtGH9A4          FLFSAYADILQKHN-QKISCGSHQFDSTHLMAFAKKQIDYILGHNPQGRSYMVGFGPNPP 403
KOR3             FLAALFSDYLEAADTPGWYCGPNFYTTEFLRNFSRSQIDYILGKNPRKMSYVVGYGQRYP 510
KOR2             FLASLFADYLNSTGVPGWYCGPTFVENHVLKDFAQSQIDYILGDNPLKMSYVVGFGKKFP 513
KOR1             FLATLYSDYLDAADTPGWYCGPNFYSTSVLRDFARSQIDYILGKNPRKMSYVVGFGTKYP 509
PttCel9A1        FLATLFSDYLEAADTPGWYCGPNFYSTDVLRDFAKTQIDYILGKNPRKMSYIVGFGNHYP 509
PtGH9A2          FLATLYSDYLEAADTPGWYCGPNFYSTDVLRDFAKTQIDYILGKNPRKMSYVVGFGNHYP 509
PtGH9A3          FLASLFVDYLNATRVPGFQCGSKFIPLDVLRSFATSQINYILGDNPMKMSYVVGYGTKFP 511
PtGH9A4          FLASLYVDYLNATRVPGLNCGPKFISLDLLRSFATSQINYILGDNPMKMSYVVGYGTKFP 510
PtGH9A5          FLGKLYSDYLELLR--------------------RSGVNYILGDNPMKMSYMVGFGNKYP 475
PttGH9B3         FLLTTYAKYMKATR-HTFNCGNLLVTPNSLLYVAKRQVDYILGENPIRMSYMVGFGPNFP 400
                    *Active site residue                              *
AtGH9A4          KQAHHRGASVPMHEAN-APLSCPLSFVKWYNKNVPNANELTGAILGGPDRQDKFQDLRWT 462
KOR3             KQVHHRGASIP---KN-MKETCTGGFK-WKKSKKNNPNAINGAMVAGPDKHDGFHDIRTN 565
KOR2             RRVHHRGATIP---NDKKRRSCREGLK-YRDTKNPNPNNITGAMVGGPNKFDEFHDLRNN 569
KOR1             RHVHHRGASIP---KNKVKYNCKGGWK-WRDSKKPNPNTIEGAMVAGPDKRDGYRDVRMN 565
PttCel9A1        KHLHHRGASIP---KNKIRYNCKGGWK-WRDTSKPNPNTLVGAMVAGPDRHDGFHDVRTN 565
PtGH9A2          KHVHHRGASIP---KNKIRYNCKGGWK-WRDTTKPNPNTLVGAMVAGPDRHDGFRDVRTN 565
PtGH9A3          RHIHHRGASIP---NDKRSYSCTGGWK-WRDSPKPNPNNITGAMVGGPDRFDRFRDVRKN 567
PtGH9A4          RHVHHRGASTP---SDKTRYSCTGGWK-WRDSSKPNPHNITGAMVGGPDRFDQFRDVRTN 566
PtGH9A5          THVHHRAASIP---WDDQHYSCPEGDR-WLYSTDPNPNILYGAMVAGPDKFDNFLDDRDK 531
PttGH9B3         KRIHHRGSSLPSLASHPQAIGCDSGFEPFFHSANPNPNILTGAIVGGPNQNDGYPDERSD 460
                    *
AtGH9A4          SVYTEPCTYINSIAVGVLAKLAAA-------------------------------- 486
KOR3             YNYTEPTLAGNAGLVAALVALSGEK-AVGGIDKNTMFSAVPPLVMATPPPPAPWTP 620
KOR2             YNASEPTLSGNAGLVAALVSLTSSG--GQQIDKNTMFNSVPPLYSPTPPPPKAWKP 623
KOR1             YNYTEPTLAGNAGLVAALVALSGEEEATGKIDKNTIFSAVPPLFPTPPPPPAPWKP 621
PttCel9A1        YNYTEPTIAGNAGLVAALVALSGDK--TTGIDKNTIFSAVPPMFPTPPPPPAPWKP 619
PtGH9A2          YNYTEPTIAGNAGLVAALVALSGDK--TTGIDKNTIFSAVPPMFPTPPPPPAPWRP 619
PtGH9A3          YNFTEPTLAGNAGLVAALSSLTSSG--GIGIDKNRMFSAVPPLYPPSPPPPPAWKP 621
PtGH9A4          YNFTEPTLAGNAGLVAALASLTSSG--GIGIDKNSIFTAVPPLYPPSPPSPPAWKP 620
PtGH9A5          PWFTEPTIASNAGLVAALIALHDPPYKSSDSNGTNLGIDLTGIFKNLQLVPPGT-- 585
PttGH9B3         YSHSEPATYINAAMVGPLAYFAATLN------------------------------ 486
```

Figure 13. (c) Conserved GH family 9 active sites signature 1 and 2 (pink). Active site residues H, D and E are indicated *. Conserved PRD at the C-terminus of type A cellulases (yellow). ^{553}Pro (in bold and large) corresponds to the mutation of *irx2-2*. Figure based on Rudsander (2007).

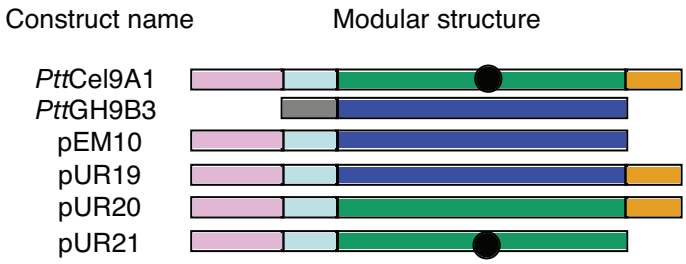

Figure 14. Schematic representation of the domain swapping constructs of poplar cellulases for complementation study with the *kor1* mutants. *Ptt*Cel9A1 domains: cytoplasmic tail (pink), TMD (light blue), catalytic domain (green), BL (black: FWGG), PRD (orange: AVPPMFPTPPPPPAPWKP). *Ptt*GH9B3 domains: SP (gray), catalytic domain (blue). Figure based on Rudsander (2007).

We then wondered which parts of the catalytic domain provide the specific functionality of KOR1/*Ptt*Cel9A1. Within the catalytic domain of type A cellulases, a conserved region called "blocking loop" (BL) has been identified (Rudsander et al., 2003; Figure 13b), whose function was speculated to limit the size of substrate that can be accommodated (Sakon et al., 1997; Russell and Wilkinson, 2005). It has been observed that microbial cellulases that do not have the BL often have broad substrate specificities (Rudsander et al., 2003), and therefore the BL may determine an enzyme's specificity towards some substrates. Another distinct motif of the *Ptt*Cel9A1 catalytic domain is the proline-rich domain (PRD) at the C-terminus (Figure 13c), which is conserved in plant type A cellulases but absent in type B cellulases (Master et al., 2004). PRDs are observed in proteins of both prokaryotes and eukaryotes (Williamson, 1994) and are important for binding to the protein-interaction domains such as Src homology 3 (SH3) and WW (two tryptophans separated by 20-22 aa) (Kay et al., 2000; Lam et al., 2001; Agrawal and Kishan, 2002).

The importance of BL and PRD domains of *Ptt*Cel9A1 was investigated with constructs pUR19, pUR20 and pUR21 (Figure 14). pUR20 was used to test the effect of deleting the BL from the active site of *Ptt*Cel9A1. In pUR19, the PRD of *Ptt*Cel9A1 was further added to a C-terminus of the hybrid construct pEM10 to test if this addition could improve the pEM10 complementation effect. In contrast, the effect of deletion of the PRD from *Ptt*Cel9A1 was tested using construct pUR21.

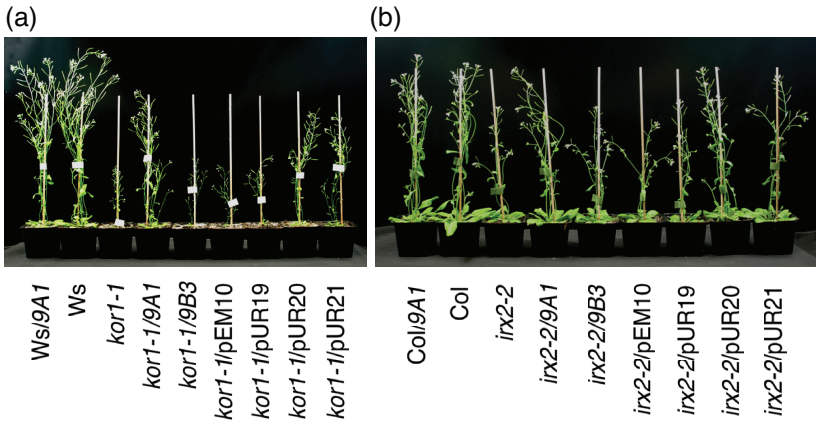

Figure 15. Morphology of the *kor1* mutants and the WT transformed with the constructs presented on Figure 14. All these constructs were fused to CaMV *35S* promoter and introduced to the homozygous *kor1-1* (a) or *irx2-2* (b) mutant lines and their respective WT plants. Empty vector was also introduced to Arabidopsis Ws or Col and to *kor1-1* or *irx2-2* mutant plants. Representative T_2 lines of several transgenic lines obtained are shown.

We observed that *PttCel9A1* deletion constructs lacking either the BL (pUR20) or the PRD (pUR21) partially restored the *kor1* mutants phenotypes such as dwarfism (height, biomass and rosette leaf size) and the collapsed vessel elements, but they were less effective than the full-length construct (Figures 15, 16 and 17). However, the addition of the PRD to the hybrid construct with the *Ptt*GH9B3 catalytic domain (pEM10) did not improve its effect. Thus, PRD presence is not enough to provide the special function of *Ptt*Cel9A1 catalytic domain. In conclusion, the BL and PRD give an additional positive effect for the full function of *Ptt*Cel9A1, however, the remaining region of the catalytic domain of *Ptt*Cel9A1 plays a decisive role for its function *in vivo*.

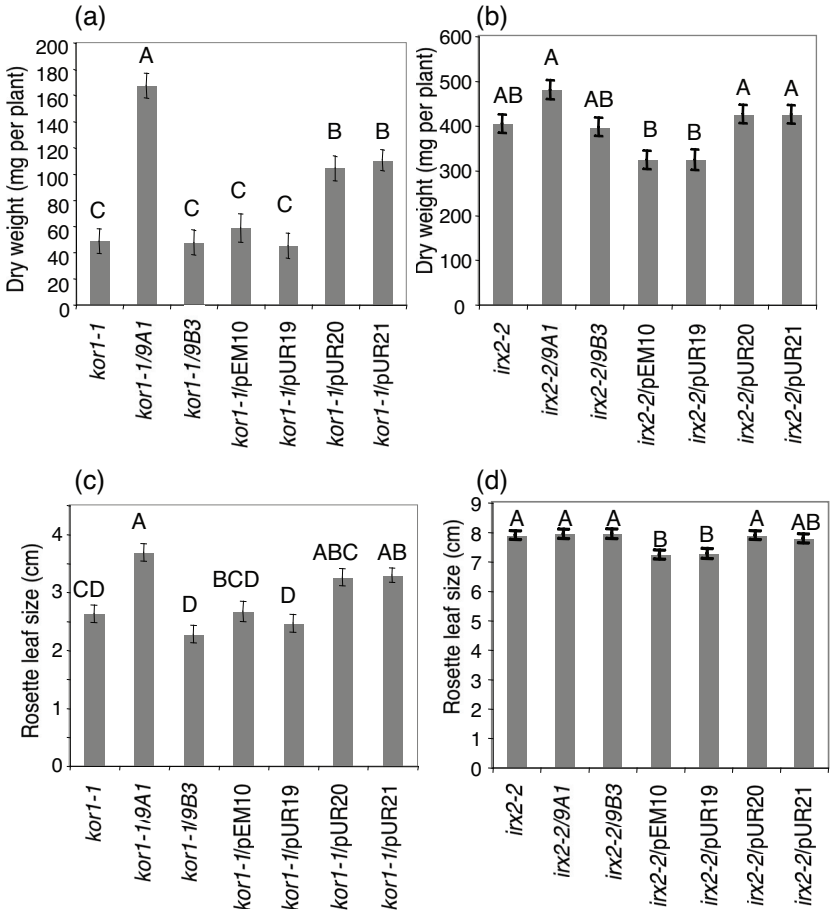

Figure 16. Dry mass weight (a & b) and rosette leaf size (c & d) of mature plants of lines transformed with the constructs shown in Figure 14, in *kor1-1* (a & c) and *irx2-2* (b & d) background. Experimental condition and statistics as in Figure 12.

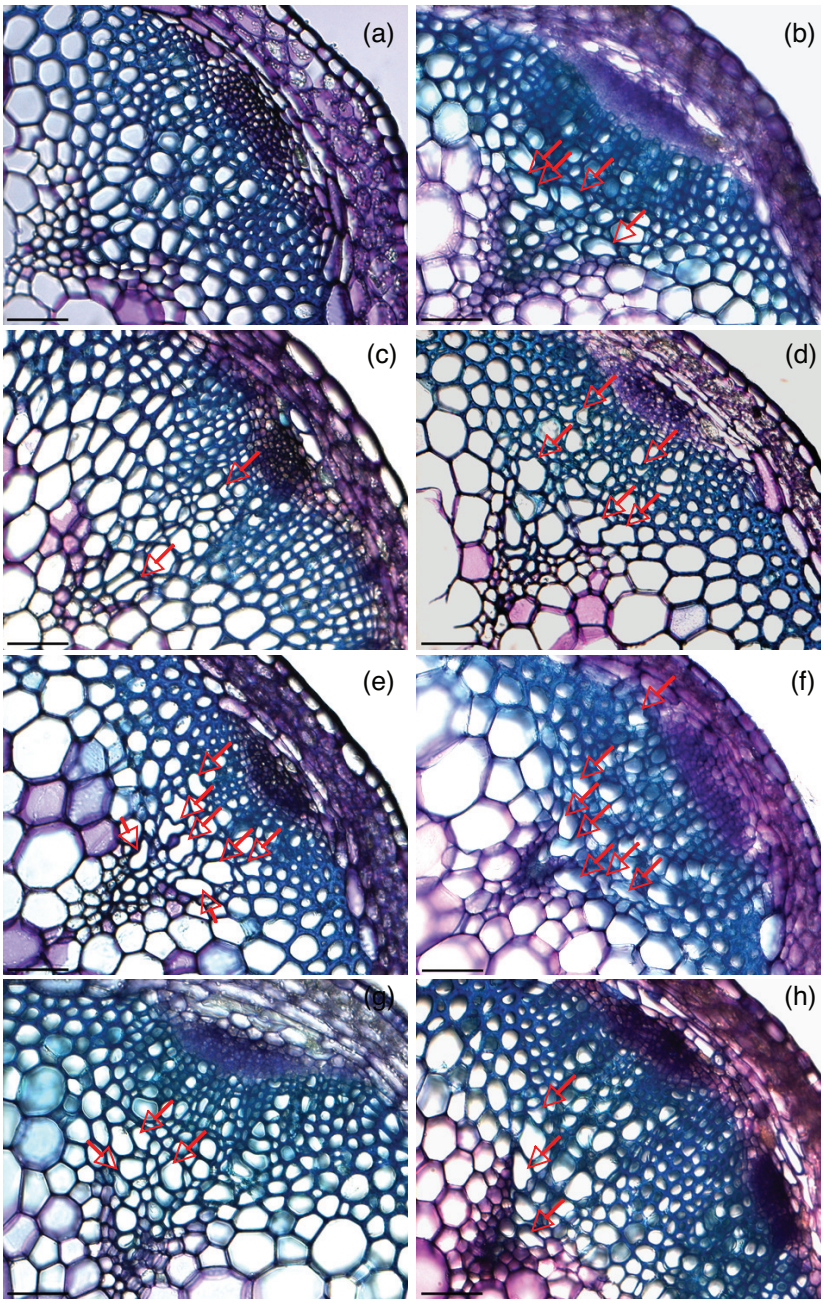

Figure 17. Complementation of irregular xylem phenotype of *irx2-2* mutant by different constructs from Figure 14. (a) Col, (b) *irx2-2*, (c) *irx2-2*/*9A1*, (d) *irx2-2*/*9B3*, (e) *irx2-2*/pEM10, (f) *irx2-2*/pUR19, (g) *irx2-2*/pUR20 (h) *irx2-2*/pUR21. Col and *irx2-2* lines carried the empty vector. Cross-sections of stem vascular bundles from the representative transgenic mature plants stained with toluidine blue are shown. Arrows indicate collapsed vessels. Scale bar=50 μm.

The importance of the BL in *Ptt*Cel9A1 action *in vivo* is difficult to understand in molecular terms. Although the BL of the *Thermobifida fusca* cellulase *Tf*Cel9A was suggested to prevent certain substrates from binding due to insuffricient room (Sakon et al., 1997), the removal of the BL from the end of the catalytic cleft (T245-L251) of *Tf*Cel9A only slightly improved the activity against filter paper, but no significant differences in the CMC, PASC or bacterial microcrystalline cellulose (BMCC) activities as well as preferential length of the substrates were found when compared to the WT enzyme (Zhou et al., 2004). We do not know if the inferior functionality of ΔBL *Ptt*Cel9A *in planta* is related to changes in enzyme activity, specificity or substrate binding.

The PRD of *Ptt*Cel9A1 contains a core motif "PXXP" (P, proline; X, any amino acid) that forms a polyproline II (PPII) helix binding SH3 domain (Feng et al., 1994; Pawson and Nash, 2003). SH3 domain is well-studied in yeast and animals, and it regulates a variety of biological activities, including signal transduction, protein and vesicle trafficking, organelle biogenesis and cytoskeletal architecture. In Arabidopsis, an SH3-containing protein, *At*SH3P1 is reported to be involved in trafficking of clathrin-coated vesicles and to be localized around the plasma membrane and its associated vesicles (Lam et al., 2001). Such a protein could be a potential candidate that interacts with the PRD of KOR1 for endosome recycling in Arabidopsis, since KOR1 has shown to be localized in intracellular compartments such as the Golgi apparatus and early endosomes (Robert et al., 2005). The colocalization and immunoprecipitation study of KOR1/*Ptt*Cel9A1 and *At*SH3P1 in comparison to the PRD-deleted protein would be interesting to show such an interaction. However, the PRD deleted construct (pUR21) could still rescue the mutant phenotype to a significant degree, suggesting that this interaction, if it exists, cannot be essential for the protein function.

When we analyzed growth of *irx2-2* plants carrying different constructs, a detrimental effect on the rosette leaf size was observed with the cytoplasmic tail-TMD-linked *Ptt*GH9B3 constructs (pEM10 and pUR19) (Figure 16d) suggesting that these constructs create a dominant-negative effect. In order to confirm this assumption, the phenotype of WT plants expressing the membrane-attached *Ptt*GH9B3 constructs should be analyzed. The hybrid protein was probably targeted to the same compartment as the native KOR1 by the polar targeting sequences of the cytoplasmic tail competing spatially for membrane localization with KOR1.

In conclusion, this work shows that the catalytic domain of *Ptt*Cel9A1, a type A cellulase, plays an essential role for its function *in vivo*. The catalytic domain of *Ptt*GH9B3, a type B cellulase, cannot fulfill this specific function. The distinctive features of the *Ptt*Cel9A1 catalytic domain, the BL and PRD, are required for the full functionality but are not essential.

4.2.3 Role of the secreted cellulases in wood formation (Unpublished data)

The structure of PttGH9B3

PttGH9B3 has a predicted open reading frame made up of six exons (http://genome.jgi-psf.org/Poptr1_1/Poptr1_1.home.html) as confirmed by isolation of full-length cDNA clones (Rudsander et al., 2003). The predicted protein has an N-terminal signal peptide (Figure 10; Paper II, Table S1). The predicted MW and the IP after cleavage, which could be an active form, is 51.3 kDa and 8.32, respectively. Sequence analysis placed *Ptt*GH9B in subfamily V, associated with extracellular cellulases (Mølhøj et al., 2002), together with Arabidopsis Cel3 and Cel5 (Paper II, Figure 1a). *Cel3* and *Cel5* are 81.9 % and 87.2 % identical to each other at the nucleotide (CDS) and amino acid level. *PttGH9B3* is 70.8 % and 76.8% identical to *Cel3* at the nucleotide (CDS) and amino acid level, respectively, and slightly less similar to *Cel5*.

The expression of PttGH9B3, Cel3 and Cel5 in the secondary growth[1]

PttGH9B3 expression was studied in different vegetative tissues of hybrid aspen by Northern blotting. It was found to be upregulated in the primary-walled developing wood cells in mature stem and root active in secondary growth (Figure 18), in agreement with the previous microarray data (Figure 8a; Hertzberg et al., 2001; Schrader et al., 2004).

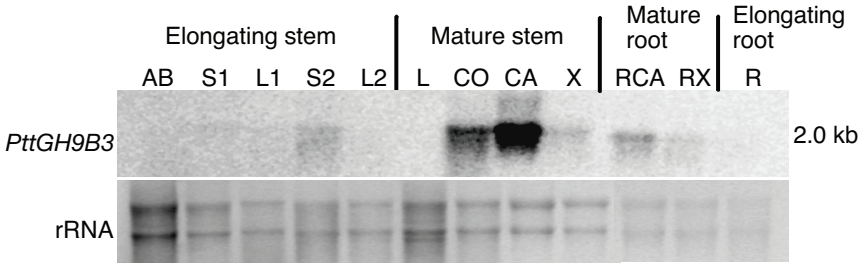

Figure 18. *PttGH9B3* expression analysis in aspen vegetative tissues by Northern blot. Ethidium bromide staining of RNA shows loadings at the bottom. 20 μg of total RNA were loaded to each lane. The tissues were collected from six-month-old hybrid aspen. AB - apical bud, S1 - stem in the primary growth, L1 - expanding leaf 1, S2 - stem in the secondary growth, L2 - expanding leaf 2, L - mature leaf, CO - cortex from mature stem, CA - cambium and phloem from mature stem, X - secondary wall forming xylem from mature stem, RCA - phloem and cambium from mature root, RX - secondary wall forming xylem from mature root, R - young root. For the experimental procedure, refer to Paper II. The *PttGH9B3* specific probe was made using PCR, which corresponds to the *PttGH9B3* nucleotide sequences 891 to 1599 (counting from the start codon) including 3'UTR.

Cel3 and *Cel5* are known to be expressed in root cap cells (del Campillo et al., 2004). The available Arabidopsis microarray data indicate that *Cel3* is expressed both in xylem and phloem in mature hypocotyl (Zhao et al., 2005), whereas *Cel5* expression is under the detectable level there. To investigate further the expression of *Cel3* and *Cel5* in vascular tissues at the cellular level, we analyzed the transformed Arabidopsis plants with the P_{Cel3}*::GUS* and P_{Cel5}*::GUS* constructs. No

expression was detected in mature stem and hypocotyls of the plants with P_{Cel5}::*GUS*, however, *Cel3* expression was observed in developing phloem and cambium in both stem and hypocotyl (Figure 19). This expression data in conjunction with the sequence analysis data suggest that *Cel3* is most likely an orthologue of *PttGH9B3*.

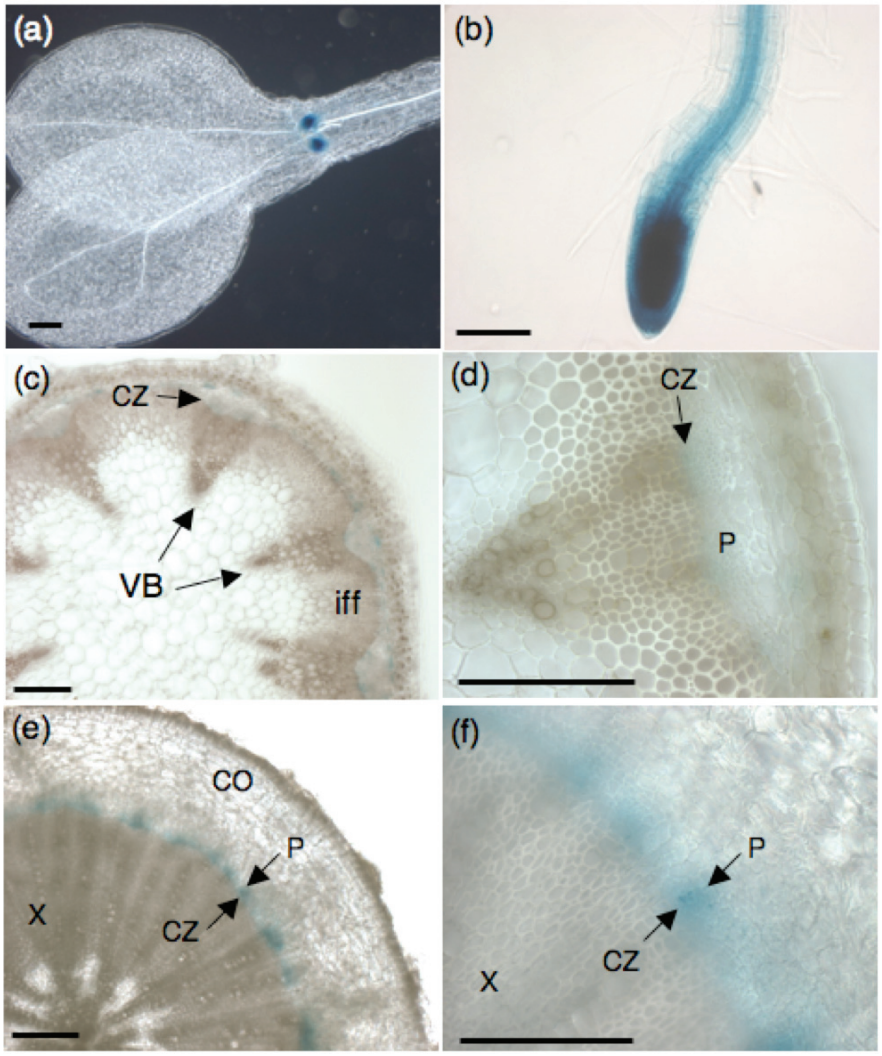

Figure 19. *AtCel3* promoter activity in Arabidopsis primary (a & b) and secondary (c-f) tissues visualized by GUS histochemistry. A shoot (a) and root (b) of ten-day-old (5 days in dark and 5 days in LD) seedling. Base of inflorescence stem (c & d) and hypocotyl (e & f) of a five-week-old plant. Five independent transgenic lines showed the same expression pattern with the strongest expression in leaf primordia, vascular bundle and elongating zone during primary growth and in cambium/phloem tissue during the secondary growth. (d & f) Close-up of the cambial region. CO - cortex; CZ - cambial zone, iff - interfascicular fibers; P - developing phloem; VB – vascular bundle; X - xylem. Scale bar=100 μm.

The phenotype of PttGH9B3 overexpressors and cel3 mutants (cel3G & cel3S)[1]

In order to study the effects of *PttGH9B3* on wood formation, transgenic Arabidopsis lines expressing *PttGH9B3* under control of the CaMV *35S* promoter were generated. Four single insert T3 homozygous lines (9B12, 13, 34 and 46) and one T2 line (9Bm14) with insertions at multiple loci were selected. The transgene expression was detected in all *PttGH9B3* OE lines (Figure 20a), while the endogenous *Cel3* expression was not different from that of the WT (data not shown). Elevated cellulase activity against CMC in the proteins extracted from the four-week-old whole plant was found in the highest overexpressing line (Figure 20b).

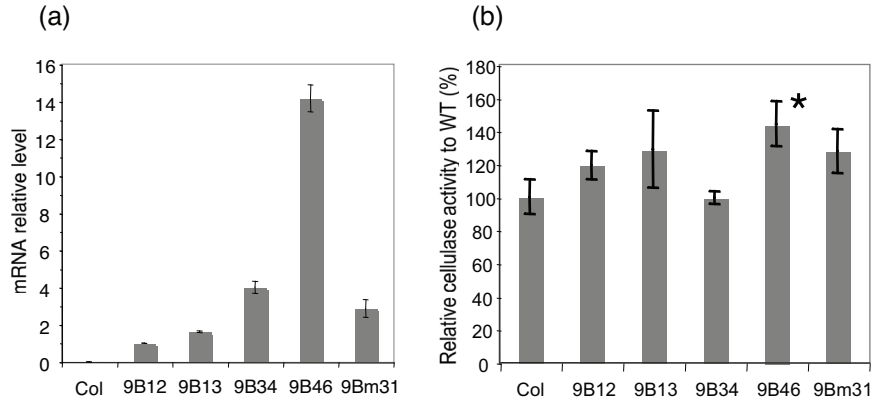

Figure 20. (a) Relative expression levels of *PttGH9B3* in four-week-old OE lines by real-time RT-PCR with the gene-specific 9B and ubiquitin (At4g36800) primer pairs as a reference gene. Averages ± SE, N = 9. For the experimental procedure, refer to Paper II. The primers used for *PttGH9B3* expression was forward (9Bfor12, 5'-CTATTGTCGGCGGTCCAAAC-3') and reverse (PttCel9BRev8, 5'-CTAATTCAAGGTAGCAGCAAAGTATGC-3').
(b) Relative cellulase activity in four-week-old OE lines in relation to the WT. Cellulase activity was tested against reaction mixtures containing 0.5% 4M-CMC, 30 mM $CaCl_2$, 50 mM sodium citrate pH 6.0 at 30º C in duplicate or triplicate for each line and incubated overnight. Three separate extractions were performed. Averages ± SE, N=9 are shown. Averages that were significantly (Duncan test, $P \leq 0.05$) different from the WT are marked with *. The gene expression of PttGH9B3 and cellulase activity had a positive correlation (r=0.65).

As a comparison to OE lines, two T-DNA insertion mutants of the *Cel3* gene, *cel3S* (SALK_057688; http://signal.salk.edu/cgi-bin/tdnaexpress) and *cel3G* (GABI_683F02; http://www.gabi-kat.de/), were obtained and the homozygous plants were subsequently selected. In the *cel3S* line, T-DNA is inserted in the last exon, 75 bp upstream from the conserved GH9 active signature 2 identified by PROSITE (Figure 21). Therefore it was expected that the interrupted transcript would consequently generate an inactive enzyme. In contrast, the *cel3G* line has T-DNA inserted in the *Cel3* promoter, 134 bp upstream from the start codon. Similarly, either completely abolished or reduced *Cel3* gene expression in the

cel3G line was expected. However, contrary to our expectation, *Cel3* gene expression was strongly induced in the *cel3G* line (Figure 22). This can be explained by either the repressor domain in the *Cel3* promoter was disturbed or the promoter of the inserted T-DNA (pAC161) for the antibiotic resistance was driving the expression of *Cel3* downstream gene resulting in a polycistronic transcript.

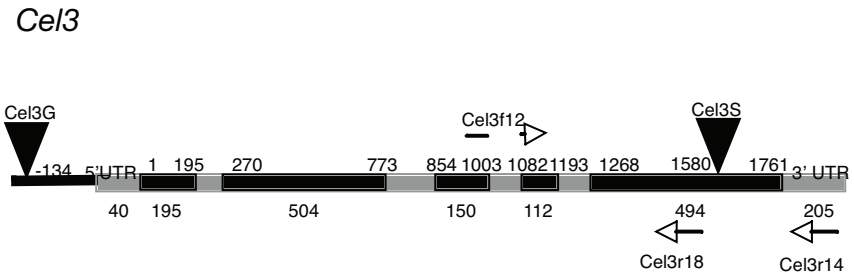

Figure 21. Diagram of SALK_057688 (*cel3S* mutant) and GABI_683F02 (*cel3G* mutant) illustrating the T-DNA insertion in the last exon and in the promoter region, respectively. Cel3f12 (5'-CTCTCACGGAGAGCATTACTT-3'), Cel3r14 (5'-CAATGGAACTACAAATCGGAGA-3') and Cel3r18 (5'-GATTGAGAACGAAGTGCGTGTGAA-3') are the gene specific primers used for semi-quantive RT-PCR, showing the annealing position and directions as indicated with arrows.

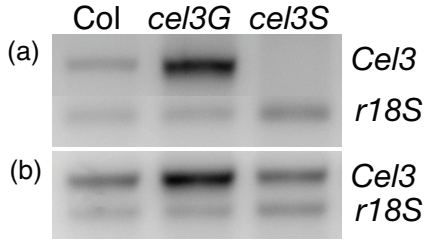

Figure 22. *AtCel3* gene expression by semi-quantitative RT-PCR from total RNA from four-week-old whole plant of WT Col (lane 1), homozygous *cel3G* mutant (lane 2) and homozygous *cel3S* mutant (lane 3). *Cel3* gene specific primers designed over the insertion of *cel3* mutant (a, primer sets: Cel3f12 & Cel3r14) and before the insertion of *cel3S* mutant (b, primer sets: Cel3f12 & Cel3r18) were used (see the Figure 21). RT-PCR was repeated three times from the RNA extraction, using ten pooled plants, and results were identical.

PttGH9B3 OE, *cel3S* and *cel3G* lines exhibited no observable alteration in terms of overall plant height, leaf size, flowering time and seed production (data not shown). The only difference in OE lines during the primary growth was that their hypocotyls (six-day-old dark grown) were shorter than those of the WT (93 % of the WT on average). There was no apparent change in the anatomy of mature hypocotyls in *cel3G* and *cel3S* mutants, however, an increased proportion of lignified xylem (xylem phase II) in *PttGH9B3* OE lines was observed (111% of the WT).

We also analyzed the morphology of libriform fibers, fiber-tracheids and vessel elements isolated from mature hypocotyls to determine if *Ptt*GH9B3/Cel3 plays a role in the growth of any of these wood cell types. The elongation of vessel elements was enhanced in OE lines (108 % of the WT on average) without any apparent alteration in the cell wall surface structure. Surprisingly, both *cel3G* and *cel3S* mutant lines also had significantly longer vessel elements (*cel3G* 113 %, *cel3S* 112% of the WT).

In order to investigate the effect of overexpression of *PttGH9B3*/*Cel3* as well as Cel3 deficiency on cell wall composition and contents during secondary growth, crystalline cellulose content was analyzed by the Updegraff method (1969) and cell wall TFA-hydrolysable monosaccharides including neutral sugars and uronic acids in the mature stem bases and mature hypocotyls were analyzed as described in section 3.3. No difference in the content of crystalline cellulose and monosaccharides was observed in any of the *PttGH9B3* OE, *cel3G* and *cel3S* lines (data not shown). In contrast to the effects seen in Arabidopsis plants with excess/deficiency of membrane-anchored cellulases, the overexpression of *PttGH9B3* did not show any influence on the crystalinity index compared to the WT, as measured by solid state NMR (Paper II, Figure 8e). Moreover, PLS-DA indicated no separation of NMR spectra of the OE lines and WT, which supports the lack of chemical alteration in secondary cell walls observed by the chemical analyses (Paper II, Figure 8d).

The possible role of PttGH9B3

When another *Populus* type B extracellular cellulase, *Pa*PopCel1, isolated from the suspension-cultured poplar (*Populus alba*) (Nakamura and Hayashi, 1993; Ohmiya et al., 2000) was overexpressed in Arabidopsis, an increased palisade and epidermis cell expansion in rosette leaves and enhanced elongation of etiolated hypocotyls were observed (Park et al., 2003). Similarly, the Arabidopsis cellulase belonging to the subclass B, *Cel1*, expressing in elongating stems (Shani et al., 1997), was overexpressed in aspen (*Populus tremula*), which resulted in significant phenotypic alterations with enhanced height growth, internode elongation, leaf expansion and stem thickening compared to the WT (Shani et al., 2004).

Both cases of overexpression of type B cellulase in heterologous systems led to enhanced leaf expansion and stem or hypocotyl elongation. In contrast, etiolated hypocotyl elongation was inhibited in our study. In addition, the overexpression of *PttGH9B3* affected neither leaf expansion nor stem elongation. The main phenotypic alteration in *PttGH9B3* OE lines was increased lignified xylem cells, which is often seen in cell wall modified plants as a compensating mechanical response (Paper II) and enhanced elongation of vessel elements. However, this was also observed in both *cel3G* and *cel3S* mutants.

The increased level of cellulase activity caused by overexpression of *PttGH9B* surely has a positive effect on vessel element elongation. On the other hand, excess/impaired Cel3 gives also the same effect. Hence, it was very difficult to deduce the true function of *PttGH9B3*.

Overexpression or downregulation of one of the genes in a multigene family can easily affect the expression of the other genes within the family especially in homologous systems (Paper IV). We did not examine the gene or protein

expression of the endogenous GH9 genes in either OE or *cel3* mutant lines whose cellulase activity has not yet been determined. The observed longer vessel elements in *cel3S* may be conversely caused by other changes in gene expression, for example, *Cel1*, *AtGH9B13* and *AtGH9B18* that are also expressed in mature hypocotyls (analyzed by AtGenExpress project, http://www.weigelworld.org/research/projects/resources/microarray/AtGenExpress/) .

*Pa*PopCel1 specifically acts on CMC and PASC, but no activity or negligible activity was found against crystalline cellulose and xyloglucan *in vitro* (Nakamura and Hayashi, 1993). Similarly, *Ptt*GH9B3 recombinant proteins hydrolyze specifically low substituted CMC, with little activity on xyloglucan or xylan, as shown by the preliminary enzymatic characterization (personal communication with Dr. U. J. Rudsander). Therefore, *Ptt*GH9B3 may function in a similar way within cell walls, for example, hydrolyzing the amorphous cellulose sites of microfibrils to loosen xyloglucan intercalation, as suggested by Park et al. (2003).

In summary, *PttGH9B3* may have a role in elongation of fusiform initials in the cambium. However, this has to be confirmed by analyzing gene/protein expression of the other type B cellulase members in the OE plant.

[1] The analyses methods (Northern blotting, promoter-GUS analysis, RT-PCR, anatomical studies, cellulose analysis by the Updegraff method or NMR, cell wall monosaccharide analysis and elongation test of seedlings) and plant growth conditions used for the study are same as those described in Paper II, except for a few differences, e.g. primers, which are mentioned in the legends of the figures.

4.3 *Ptt*Xyn10A, endo-1,4-β-xylanase is a secondary cell wall modifying enzyme in hybrid aspen (Paper III)

*Ptt*Xyn10A protein contains a GH10 catalytic module, preceded by three putative CBMs from family 22 (Paper III, Figure 1). Within the GH10 family only three enzymatic activities were reported: endo-1,4-β-xylanase (EC 3.2.1.8), endo-1,3-β-xylanase (EC 3.2.1.32) and feruolyl esterase EC 3.1.1.73). Moreover, the *Ptt*Xyn10A CBMs have the majority of the amino acid residues required for binding of xylotetraose as found in CBM22-2 from *Clostridium thermocellum* xylanase *Ct*Xyn10B (Xie et al., 2001), suggesting that *Ptt*Xyn10A is active on xylan *in vivo* (Paper III, Figure 1c).

The highest transcript levels were observed in stems and roots with secondary growth, where they were most abundant in all types of the developing xylem cells undergoing secondary cell wall synthesis (Paper III, Figures 3 & 4). The protein immunodetection studies using a polyclonal antibody (Kamisa), raised against the entire catalytic domain, localized *Ptt*Xyn10A in the cell wall-bound fraction in developing xylem tissues (Paper III, Figure 5). Curiously, a 68 kDa protein was detected instead of the predicted 101 kDa protein. The observed size corresponded well to the MW of the protein after the predicted proteolytic cleavage in CBM22_2$_{Ptt\text{Xyn10A}}$ (Paper III, Figure 1), suggesting that the mature protein undergoes proteolytic processing before accumulating in secondary walls. It has been reported that the secreted xylanases from papaya, barley and maize, *Cpa*EXY1, *Hv*Xyn-1 and *Zm*Xyn1, respectively, undergo a series of proteolytic processing steps in order to comprise only a GH10 catalytic domain before becoming active (Chen and Paull, 2003; Caspers et al., 2001; Wu et al., 2002). In contrast, the predicted processed *Ptt*Xyn10A protein still includes CBM22_3$_{Ptt\text{Xyn10A}}$, which may act to position the enzyme in the cell wall residing substrate.

When *PttXyn10A* transcripts levels were reduced by half using the antisense approach in hybrid aspen, the wood fibers were shorter and narrower than those of WT trees (Paper III, Figure 9). The wood wall chemical composition analysis indicated that there was an increased amount of xylan, mannan, and Klason and acid-soluble lignin, whereas the content of cellulose and galactan were reduced (Paper III, Table I). Further analysis by FT-IR revealed that the amount of G-lignin, and highly condensed and cross-linked lignin was increased, while the amount of cellulose and xyloglucan was reduced in the antisense lines (Paper III, Figure 7). In order to determine whether the observed phenotypes were mediated by changes of other gene transcript levels as a secondary effect, the microarray experiment was performed with the two transgenic lines against the WT. In total, transcripts of approx. 150 genes were differentially regulated in common in the two antisense lines. A striking down-regulation of several genes related to TW formation (Andersson-Gunnerås et al., 2006) including seven fasciclin-like arabinogalactan-proteins similar to Arabidopsis FLA12 was observed in the antisense lines (Paper III, Table 2). In contrast, the expression of the genes required for monolignol biosynthesis was unchanged (Paper III, Table 2).

The phenotypic data are consistent with *Ptt*Xyn10A having a hydrolytic activity as xylanase, which is also supported by the conservation of xylan-binding residues in

the *Ptt*Xyn10A CBMs (Paper III) and by the observed xylanase activity of its homologous xylanase genes, *HvXyn-1*, *ZmXyn1* and *AtXyn1* from barley, maize and Arabidopsis, respectively (Caspers et al., 2001; Wu et al., 2002; Suzuki et al., 2002). However, the amount of mannose was increased even more in the antisense lines without a detectable upregulation of the mannan biosynthetic genes (Paper III). Hence, we cannot exclude a possibility that *Ptt*Xyn10A also has a hydrolytic activity towards mannan. In order to elucidate what substrates *Ptt*Xyn10A prefers, biochemical assays should be performed with a purified protein. In any case, it appears to be a secreted hydrolytic enzyme acting on hemicelluloses in secondary walls.

Considering the expression pattern of *PttXyn10A* and its homologue *AtXyn1*, together with the effects of *PttXyn10A* downregulation on the fiber cell size, *PttXyn10A* might act to facilitate fiber growth during the final stages of cell expansion and the initial phase of secondary cell wall formation. In agreement with this, we observed altered morphology only in fiber cells, but not in vessel elements that complete the differentiation earlier (referred to in section 1.1.1). The hydrolysis of xylan by *Ptt*Xyn10A might be required to reduce the tight xylan-lignin interaction to allow the fibers to grow and adjust the cell shape to fill-in the available space.

Impaired *Ptt*Xyn10A apparently influenced overall secondary cell wall architecture, affecting in turn several aspects of physiological functions such as TW response indicated by the global transcriptome analysis. The link between *PttXyn10A* expression and TW reaction might be that the enzyme could regulate wall porosity for the transport of signaling molecules through secondary walls. This aspect warrants further study.

4.4 The possible role of XETs in wood formation (Paper IV)

Among the 41 XTH genes (Paper I) at least 17 genes are expressed in the mature stem with specific distribution of transcripts across different stem tissues (Paper IV). *PttXET16-34* is specifically expressed in the cambium zone and it also appears to be an important transcript in wood-forming tissues as indicated by the EST frequency (Paper I; Paper IV, Table 1). A gene-specific macroarray, however, detected *PttXET16-35* as the most abundant XTH transcript in the developing wood tissues. Nevertheless, by overexpression of *PttXET16-34* it was possible to increase the XET activity extracted from the wood forming tissues, both at the primary- and the secondary-walled stage of development (Paper IV, Figure 3).

XET is considered to be a prime enzyme required for cell expansion, because it extends the xyloglucan chains by grafting the newly synthesized xyloglucan oligosaccharides into the existing xyloglucan. However, it is also considered as a wall-strengthening enzyme, as it introduces newly formed oligoxyloglucans to the cut ends of existing xyloglucan that could make additional cross-links between cellulose microfibrils. In the experiments with split pea segments (Takeda et al., 2002), endogenous XET activity resulted in either growth promotion or inhibition depending on whether a short- or a long-chain xyloglucan was applied. Whether a similar mechanism might operate *in vivo* is not known. Overexpressing XET in aspen resulted in stem height growth inhibition, suggesting a wall-strengthening role (Paper IV, Figure S2). However, the effects on fibers and vessel elements differed: fiber cell elongation and radial expansion were inhibited compared to the WT, while radial expansion of vessel elements was induced (Paper IV, Figure 4). Similarly, opposite effects of XET expression were observed in transgenic plants; cell growth inhibition in leaves was reported in Arabidopsis leaves when a hot pepper *CaXTH3* was overexpressed (Cho et al., 2006), whereas cell growth promotion was observed in case of *AtXTH18* and *AtXTH21* in Arabidopsis roots (Osato et al., 2006; Liu et al., 2007).

Considering the results with split pea segments, it seems that the action of XET should always be considered in relation to the biosynthesis of xyloglucan. In the hemicellulose fraction extracted by 24 % KOH, the higher amounts of xyloglucan in primary-walled tissues were obtained in the OE lines and its average MW was reduced compared with that of the WT (Paper IV, Table 2 & Figure 5). My contribution to this project was to estimate the content of xyloglucans in different wood developmental stages, cell types and genotypes by TEM. The increased amount of CCRC-M1-detectable fucosylated xyloglucan in the cambium and in the radial expansion zone was consistently observed in the OE lines compared to the WT by TEM analysis (Paper IV, Figures 6 & 7). The increased CCRC-M1 signal in OE lines was observed both in fibers and vessel elements, though fibers were significantly more labeled than vessel elements in both genotypes.

These data suggest that XET activity in the cambium and the radial expansion zone has a role in the incorporation of small xyloglucan molecules into cell walls of fusiform cells that would become fibers by transglycosylation activity. The deposition of xyloglucan into cell walls during secondary cell wall formation is limited by XET and this must be especially important for reinforcing connections between primary and secondary cell wall layers, which could eventually influence the strength of plant body. In contrast, XET enhances enlargement of vessel elements that are more rapidly growing than fibers in the radial expansion phase,

most probably by extending xyloglucan chains. These distinct reactions of XET in different cell types would be dependent on availability or/and length of free xyloglucans within the cell walls.

5. Conclusions and future perspectives

Genes highly expressed in wood forming tissues are noble candidates for regulating essential parameters of wood property. Intensive research has been performed to elucidate functions of the wood specific CAZymes, which could directly influence cell wall constituents and structure (Bourquin et al., 2002, Djerbi et al., 2004, Nishikubo et al., 2007, Siedlecka et al., 2008). In this thesis, four *Populus* hydrolase genes that are highly expressed either in the cambium and early radial expansion stage, or secondary wall forming stage during wood formation were selected for elucidating their functions through the reverse genetic approach.

The gene encoding for a XET, *PttXET16-34* and a secreted cellulase, *PttGH9B3* are strongly expressed during the meristematic stage in developing wood. *Ptt*XET16-34 at this phase plays a critical role in retaining strength within the cell walls of expanding fiber cells, while it plays a role in weakening vessel cell walls for rapid cell expansion. *Ptt*GH9B3 may be involved in elongation of fusiform initials. The secondary cell wall expressed xylanase, *Ptt*Xyn10A, is important for hydrolysis of xylans cross-linked to lignin for the remaining cell expansion during the initial phase of secondary cell wall formation. Manipulation of these genes can be useful for modifying fiber length to meet not only constant paper-industrial demands, but also rapidly growing interests for using natural wood fibers as a new isolation material for nature-friendly houses where shorter fibers are preferred (personal communication with A. Eriksson, Glommershus AB).

We revealed that the membrane-anchored cellulase *Ptt*Cel9A1/KOR1 is necessary for the formation of normal architecture of both fibers and vessel elements by way of facilitating the proper cellulose microfibril formation – either by severing the stalling glucan chains or by splitting macrofibrils. Based on the phenotype of *kor1* mutants, enhanced mechanical strength, crystalline cellulose production and biomass from overexpression of *PttCel9A1* was anticipated as an application to biotechnological aspects. However, the phenotype of the *PttCel9A1* OE lines was similar to that of the WT or *kor1* mutants, indicating that an optimal level of *Ptt*Cel9A1/KOR1 required for proper formation of wood, which is well-coordinated in nature. Plants must have evolved to acquire a suitable level of gene expression for the best equilibrium with their environment, e.g. maintaining the strongest wall property against physical mechanical stress. Furthermore, the limiting factors for cellulose biosynthesis are other enzymes or substrate availability rather than *Ptt*Cel9A1/KOR1. However, overexpression of *PttCel9A1* induces production of amorphous cellulose that can be useful for production of biofuels such as bioethanol as a new sustainable bioenergy. Still today, large quantities of production of bioethanol are dependent on non-crystalline forms of raw materials such as sugar cane and cereals like corn or grain (Jørgensen et al., 2007). Although challenges of using cellulosic biomass instead are currently being made, the initial conversion of cellulosic material into fermentable sugars is a key bottleneck (Lynd et al., 2008). *PttCel9A1* OE plants represent a new possibility to turn lignocellulosic woody plants into more efficiently utilizable materials for biofuel production.

In our study, the catalytic domain of *Ptt*Cel9A1 was shown to be essential for restoring growth of cellulose deficient *kor1* mutants by the domain swapping experiment. This is the first observation that a type B cellulase catalytic domain does not function for cellulose synthesis even if it is targeted to the membrane. However, we do not know whether the localization of type A cellulase, *Ptt*Cel9A1,

in the plasma membrane is necessary or not. The examination of the *kor1* phenotype by introducing the construct only with the *Ptt*Cel9A1 catalytic domain or the one conjugated to SP could be very interesting. In addition, complementation analysis with point mutation constructs of the remaining *Ptt*Cel9A1 catalytic domain is the next step in finding the key residues involved in cellulose biosynthesis.

In conclusion, xylogenesis is such a dynamic process involving many different genes at a specific phase of the development. The expression of the genes responsible for each process seems to be tightly regulated within plants, as we saw that the manipulation of a gene belonging to a multi-gene family accompanied the alteration of the other gene expressions within the family in order to maintain their natural forms or that loss/gain of function mutants showed same phenotype. This thesis presented interesting features of four carbohydrate-active hydrolases that have distinct functions during wood development to determine its final property and which could eventually influence our quality of life.

6. List of abbreviations

aa or AA	amino acid(s)
AGP	arabino galactan protein
AIR	alcohol insoluble residue
Ara	arabinose
At	*Arabidopsis thaliana*
BAC	bacterial artificial chromosome
BL	blocking loop
BMCC	bacterial microcrystalline cellulose
bp	base pair(s)
Ca	*Capsicum annuum*
CaMV	cauliflower mosaic virus
CAZyme	carbohydrate-active enzyme
CBD	cellulose-binding domain
CBH	cellobiohydrolase
CBM	carbohydrate-binding module
cDNA	complementary DNA
CDS	coding sequence
CE	carbohydrate esterase
CESA	cellulose synthase
Cel	cellulase, endo-1,4-β-glucanase
CLSM	confocal laser scanning microscopy
CMC	carboxymethyl cellulose
Col	Columbia ecotype
Cpa	*Carica papaya*
CPMAS	cross-polarization magic angle spinning
CSC	cellulose synthase complex
Csl	cellulose synthase-like
CT	cellotriose
Ct	*Clostridium thermocellum*
Da	Dalton
DB	database
DNA	deoxyribonucleic acid
DP	degree of polymerization
dsRNA	double-stranded RNA
DW	dry weight
EMS	ethyl methanesulfonate
ER	endoplasmic reticulum
EST	expressed sequence tag
EtOH	ethanol
FT-IR	Fourier transform infrared spectroscopy
Fuc	fucose
FW	fresh weight
G or Glc	glucose
Gal	galactose
GalUA	galacturonic acid
GFP	green fluorescent protein
GH9	glycoside hydrolase family 9

G-layer	gelatinous layer
Glc-Res	resorufinyl β-D-glucopyranoside
Glc_2-Res	resorufinyl β-D-cellobioside
GlcUA	glucuronic acid
G lignin	guaiacyl lignin
GPI	glycosylphosphatidyl inositol
GT	glycosyl transferase
GUS	beta-glucuronidase
HEC	hydroxyethylcellulose
Hepes	4-(2-hydroxyethyl)-1-piperazineethanesulfonic acid
HPAEC-PAD	high-performance anion exchange chromatography with pulsed amperometric detection
HPLC	high performance liquid chromatography
Hv	*Hordeum vulgare*
IP	isoelectric point
irx	irregular xylem
KOR	KORRIGAN
LD	long day
Man	mannose
MES	2-(*N*-morpholino)ethanesulfonic acid
miRNA	microRNA
mRNA	messenger RNA
MW	molecular weight
NMR	nuclear magnetic resonance
OE	overexpressing or overexpressor
O/N	over night
OPLS	orthogonal projections to latent structures
Pa	*Populus alba*
PASC	phosphoric acid swollen cellulose
PCA	principal component analysis
PCD	programmed cell death
PCR	polymerase chain reaction
PL	polysaccharide lyase
PLS-DA	partial least squares discriminant analysis
PM	plasma membrane
PPII	polyproline II
PRD	proline-rich domain
PSRE	proton spin relaxation editing
Pt	*Populus trichocarpa*
Ptr	*Populus tremuloides*
Ptt	*Populus tremula x tremuloides*
qRT-PCR	quantitative reverse transcription PCR
RACE	rapid amplification of cDNA ends
RG	rhamnogalacturonan
Rha	rhamnose
RISC	RNA-induced silencing complex
RNA	ribonucleic acid
RNAi	RNA interference
S1	Secondary cell wall layer 1

SCD	sitosterol-cellodextrin
SDS-PAGE	sodium dodecyl sulfate polyacrylamide gel electrophoresis
SEC	size exclusion chromatography
SG	sitosterol-β-glucoside
SH3	Src homology 3
siRNA	small interfering RNA
S lignin	syringal lignin
SP	signal peptide
Src	*Rous sarcoma* virus transforming protein
SSR	simple sequence repeats
T_1	transformed generation 1
TC	terminal complex
T-DNA	transferred DNA
TEM	transmission electron microscopy
Tf	*Thermobifida fusca*
TFA	trifluoroacetic acid
TM	transmembrane
TMD	transmembrane domain
TMH	Transmembrane helix
TW	tension wood
UDP	uridine 5' – diphosphate
UDP-Glc	UDP-glucose
UTR	untranslated region
Ws	Wassilewskija ecotype
WT	wild type
WW	two tryptophans
XEH	xyloglucan endohydrolase
XET	xyloglucan endotransglycosylase
XG	xyloglucan
XGO	xyloglucan origosaccharide
XTH	xyloglucan endotransglycosylase/hydrolase
Xyn	endo-1,4-β-xylanase
Xyl	xylose
YFP	yellow fluorescent protein
Zm	*Zea mays*

7. Acknowledgements

During these years in Umeå, I have had the opportunity to meet so many people both in my work and private time. I would like to thank all of you coming from all over the world for enriching my life throughout the PhD time. Before coming to Umeå, who could imagine that there is really no border between people? I am especially grateful to UPSC for being such an inspiring place to work!

My main supervisor **Assoc. Prof. Ewa Mellerowicz** for leading the projects, for the many discussions and especially for the great support in the final stage of completing the thesis. It would never have been possible to reach this goal without you. …Just sometimes I was scared with how large our collaborations could become... and whether the names of all authors would fit on one page...

My co-supervisor **Prof. Björn Sundberg** for analytical comments on experimental setups and manuscripts. Making me realize that science has to be always criticized.

Prof. Thomas Moritz for your warm support when I had a difficult time. I could concentrate on the work without worrying much about the situation during the last months.

Reference group members: **Prof. Leszek Kleczkowski** and **Assoc. Prof. Catherine Bellini** for bringing new thoughts into my projects concerning Arabidopsis genetics and protein works.

Prof. Geoffery Daniel and **Dr. Errin Johnson** are greatly acknowledged for giving valuable input concerning linguistic corrections. Generous last-aid postdoc researchers: **Dr. Maribel Garcia**, **Dr. Takahide Ishida** and **Dr**. **Mélanie Mauriat** for worthy contributions to the thesis before printing.

The collaborations with **Prof. Tuula Teeri**'s group at KTH, Stockholm have been very innovative. **Dr. Ulla Rudsander** is especially acknowledged for running the poplar cellulase projects together over many years. **Dr. Emma Master**, **Dr. Åsa Kallas** and **Anders Winzéll** were also great co-workers for the poplar cellulase/xylanase projects. The initiation of *in situ* cellulase activity test was performed by **Dr. Harry Brumer** and **Dr. Farid M. Ibatullin** at KTH.

For the P_{Kor1}*::GUS* and P_{Cel5}*::GUS* lines as well as homozygous *cel5* T-DNA mutant lines, **Assoc. Prof. Elena del Campillo** at University of Maryland, USA is greatly acknowledged.

It would never have been possible to understand the structure of cellulose without the NMR analysis by **Dr. Mattias Hedenström** and **Dr. Susanne Wiklund** at Umeå University. I learned the technique of cell wall chemical analysis at the lab of **Prof. Henrik Vibe Scheller** at KVL, Copenhagen, Denmark with the help of **Dr. Jesper Harholt**. Great efforts by the FT-IR expert **András Gorzsás**, and analytical chemists **Dr. Peter Immerzeel** and **Lorenz Gerber** at UPSC for the analysis of wall chemicals here (still ongoing). It has been interesting to discuss Arabidospsis hypocotyl mechanical property with **Dr. Peter Ryden** at Institute of Food Research, Norwich, UK.

In addition, I am grateful to all other **co-authors** involved in the projects for the great work.

Former and present E.M and B.S group members, especially late **Dr. Anna Siedlecka** (**Ania!**) and **Dr. Sara Andersson-Gunnerås** for introducing me to the real scientific world. **Christine Ratke** for cheering me up here and there! **Kjell Olofsson** for not only anatomical assistance but also taking me to the fascinating mushroom world! The Japanese postdocs, **Dr. Nobuyuki Nishikubo** for his extraordinary kindness in the lab and making me realize what a PhD really means, **Dr. Tatsuya Awano** for skillful TEM techniques and philosophical discussions and **Dr. Satoshi Endo** for never ending critical comments – "Are you really doing such a thing?"

Besides, **former and present Japanese postdocs** at UPSC are greatly thanked for answering my naive questions and explaining well in Japanese. お世話になりました。

Polish guest researchers: **Dr. Marta Derba-Maceluch** & **Dr. Alicja Banasiak** for skilled anatomical assistance, valuable discussions and being a good company during a fascinating journey through Poland.

Two memorable students: **Kumar Appari**, without your help it would never have been possible to handle the E.M. scaled projects alone, and **Nicolas Amelot** for being such a great measure-man (please update your certificate).

Prof. Torgny Näsholm and **Margareta Zetherström** for access to soluble sugar analysis and **UPSC technicians** and **secretaries** for the technical and administrative assistance.

The baby-boom office: **Jenny**, **Henrik S.**, **Åsa**, **Sandra**, **Takahide** and **Totte**. It has been great to share the room with you all. The lab neighbors – **Maria I.N.**, **Henrik B.** and **Mathieu** for letting me use your pens and scissors.

Maribel for being such a nice friend especially for exchanging exciting semi-internal information at our confidential lunch meetings.

IKSU Spa committee: **Aurora** and **Sandra** for exchanging yet more exciting internal information.

Meng for our fantastic days in Copenhagen! I learned a lot about kinship of royal families.

Renuka for really good Indian dinners.

Two unforgettable French girls: **Charleen** & **Nadia**. You gave me so much strength!

Professional Boletus hunters: **GaiMath** for sharing the joys of being a parent.

Catrin för att lära mig smålandska genom att spela Risk.

Det har varit bara så kul att umgås med er, **Aiko** & **Johan**.

Ludvigsson familj i Lund för att visa mig ett idealt kvinnligt ledarskap!

Anders och **familjen Eriksson** i Glommersträsk för att hälpa mig att hitta förbindelser mellan min forskning och den stora svenska skogsindustrin.

Marianne for sharing the passion for biology.

Yoshiko, your occasional email encouraged me to go forward.

UPSC activity teams: film committee, innebandy, bonsai (**Eva** & **Ken**) and 2006 Maharaja pumpkin group. Umeå film festival (that has temporary (?) vanished), Folketsbio Japanese animation festival committee (**Ramona** & **Elmira**), Camerata Umensis (**Lars Gunnar**, **Kjell**, **Agnieszka**, **Aleksandra** and **Magda**), Kyrkokören and Japanese (kids) society in Umeå.

Reina for supporting me from a distance, as also being a PhD student.

I am grateful to my **TakahaSchmidt family**. **Takahashi family**, for letting me be here for many years without much asking what I was actually doing in Sweden. ありがとう。**Schmidt family**, for thousands of humorous conversations. Ganz spezieller Dank an **Mutti**, for enormous help at home during the last months. Thanks to you, my sleepless days became **not so** sleepless!

My life supporter, **Florian**. Ever since I met you, my life started having real meaning. **Elias Ryo** for opening my eyes to the fact that there is much much much more to discover. You are a real antidepressant!

…Och äntligen vill jag tacka **Sverige** för att vara så.

This work was supported by the fundings from Formas, Swedish Research Council (VR), European project EDEN (QLK5-CT-2001-00443), Wood Ultrastructure Research Centre and Scandinavia-Japan Sasakawa Foundation.

8. References

Abe, H., Funada, R., Ohtani, J. and Fukazawa, K. (1997) Changes in the arrangement of cellulose microfibrils associated with the cessation of cell expansion in tracheids. *Trees*, **11**, 328-332.

Agrawal, V. and Kishan, K.V.R. (2002) Promiscuous binding nature of SH3 domains to their target proteins. *Protein Pept. Lett.,* **9,** 185-193.

Altamura, M.M., Possenti, M., Matteucci, A., Baima, S., Ruberti, I. and Morelli, G. (2001) The development of the vascular system in the *Arabidopsis* floral stem. *New Phytol.,* **151**, 381-389.

Andersson-Gunneråas, S., Mellerowicz, E.J., Love, J., Segerman, B., Ohmiya, Y., Coutinho, P.M., Nilsson, P., Henrissat, B., Moritz, T. and Sundberg, B. (2006) Biosynthesis of cellulose enriched tension wood in *Populus*: global analysis of transcripts and metabolites identifies biochemical and developmental regulators in secondary wall biosynthesis. *Plant J.,* **45**, 144-165.

Andersson, S.I. and Samuelson, O. (1983) Structure of the reducing end-groups in spruce xylan. *Carbohydr. Res*., **111**, 283-288.

The Arabidopsis Initiative. (2000) Analysis of the genome sequence of the flowering plant *Arabidopsis thaliana*. *Nature,* **408**, 796-815.

Araki, R., Ali, M.K., Sakka, M., Kimura, T., Sakka, K. and Ohmiya, K. (2004) Essential role of the family-22 carbohydrate-binding modules for beta-1,3-1,4-glucanase activity of *Clostridium stercorarium* Xyn10B. *FEBS Lett.,* **561**, 155-158.

Arrowsmith, D.A. and de Silva, J. (1995) Characterization of 2 tomato fruit-expressed cDNAs encoding xyloglucan endo-transglycosylase. *Plant Mol. Biol.,* **28**, 391-403.

Aspeborg, H., Schrader, J., Coutinho, P.M., Stam, M., Kallas, Å., Djerbi, S., Nilsson, P., Denman, S., Amini, B., Sterky, F., Master, E., Sandberg, G., Mellerowicz, E., Sundberg, B., Henrissat, B. and Teeri, T.T. (2005) Carbohydrate-Active enzymes involved in the secondary cell wall biogenesis in hybrid aspen. *Plant Physiol.,* **137**, 983-997.

Baima, S., Possenti, M., Matteucci, A., Wisman, E., Altamura, M.M., Ruberti, L. and Morelli, G. (2001) The Arabidopsis ATHB-8 HD-Zip protein acts as a differentiation-promoting transcription factor of the vascular meristems. *Plant Physiol.,* **126**, 643-655.

Banik, M., Garrett, T.P.J. and Fincher, G.B. (1996) Molecular cloning of cDNAs encoding (1,4)-β-xylan endohydrolases from the aleurone layer of germinated barley (*Hordeum vulgare*). *Plant Mol. Biol.,* **31**, 1163–1172.

Banik, M., Li, C.D., Langridge, P. and Fincher, G.B. (1997) Structure, hormonal regulation, and chromosomal location of genes encoding barley (1-->4)-beta-xylan endohydrolases. *Mol. Gen. Genet.,* **253**, 599-608.

Barka, E.A., Kalantari, S., Makhlouf, J. and Arul, J. (2000) Impact of UV-C irradiation on the cell wall-degrading enzymes during ripening of tomato (*Lycopersicon esculentum* L.) fruit. *J. Agric. Food Chem.,* **48**, 667 -671.

Barnett, J.R. (1981) Secondary xylem cell development. In *Xylem cell development*. (Barnett, J.R. ed.), Castle House Publications, Tunbridge Wells. pp. 47-95.

Bauer, S., Vasu, P., Persson, S., Mort, A.J. and Somerville, C.R. (2006) Development and application of a suite of polysaccharide degrading enzymes for analyzing plant cell walls. *Proc. Natl. Acad. Sci. USA*, **103**, 11417-11422.

Beg, Q.K., Kapoor, M., Mahajan, L. and Hoondal, G.S. (2001) Microbial xylanases and their industrial applications: a review. *Appl. Microbiol. Biotechnol.,* **56**, 326-338.

Benjavongkulchai, E. and Spencer, M.S. (1986) Purification and characterization of barley-aleurone xylanase. *Planta,* **169**, 415-419.

Bhalerao, R., Nilsson, O. and Sandberg, G. (2003) Out of the woods: forest biotechnology enters the genomic era. *Curr. Opin. Biotechnol.*, **14**, 206-213.

Bhandari, S., Fujino, T., Thammanagowda, S., Zhang, D., Xu, F. and Joshi, C.P. (2006) Xylem-specific and tension stress-responsive coexpression of KORRIGAN endoglucanase and three secondary wall-associated cellulose synthase genes in aspen trees. *Planta,* **224**, 828-837.

Bih, F.Y., Wu, S.S.H., Ratnayake, C., Walling, L.L., Nothnagel, E.A. and Huang, A.H.C. (1999) The predominant protein on the surface of maize pollen is an endoxylanase synthesized by a tapetum mRNA with a long 5 ' leader. *J. Biol. Chem.,* **274**, 22884-22894.

Boerjan, W., Ralph, J. and Baucher, M. (2003) Lignin biosynthesis. *Annu. Rev. Plant Biol.,* **54**, 519-546.

Bolam, D.N., Ciruela, A., McQueen-Mason, S., Simpson, P., Williamson, M.P., Rixon, J.E., Boraston, A., Hazlewood, G.P. and Gilbert, H.J. (1998) Pseudomonas cellulosebinding domains mediate their effects by increasing enzyme substrate proximity. *Biochem. J.,* **331**, 775-781.

Boraston, A.B., Bolam, D.N., Gilbert, H.J. and Davies, G.J. (2004) Carbohydrate-binding modules: fine-tuning polysaccharide recognition. *Biochem. J.*, **382**, 769-781.

Bourquin, V., Nishikubo, N., Abe, H., Brumer, H., Denman, S., Eklund, M., Christiernin, M., Teeri, T.T., Sundberg, B. and Mellerowicz, E.J. (2002) Xyloglucan endotransglycosylases have a function during the formation of secondary cell walls of vascular tissues. *Plant Cell*, **14**, 3073–3088.

Bowers, J.E., Chapman, B.A., Rong, J. and Paterson, A.H. (2003) Unravelling angiosperm genome evolution by phylogenetic analysis of chromosomal duplication events. *Nature,* **422**, 433-438.

Bradshaw, H.D., Ceulemans, R., Davis, J. and Stettler, R. (2000) Emerging model systems in plant biology, Poplar (*Populus*) as a model forest tree. *J. Plant Growth Regul.,* **19**, 306-313.

Brown, D.M., Zeef, L.A.H., Ellis, J., Goodacre, R. and Turner, S.R. (2005) Identification of novel genes in Arabidopsis involved in secondary cell wall formation using expression profiling and reverse genetics. *Plant Cell*, **17**, 2281-2295.

Brown, D.M., Goubet, F., Wong, V.W., Goodacre, R., Stephens, E., Dupree, P. and Turner, S.R. (2007) Comparison of five xylan synthesis mutants reveals new insight into the mechanisms of xylan synthesis. *Plant J.,* **52**, 1154-1168.

Brummell, D.A., Catala, C., Lashbrook, C.C. and Bennett, A.B. (1997) A membrane-anchored E-type endo-1,4-beta-glucanase is localized on Golgi and plasma membranes of higher plants. *Proc. Natl. Acad. Sci. USA,* **94**, 4794-4799.

Brunner, A.M., Busov, V.B. and Strauss, S.H. (2004) Poplar genome sequence: functional genomics in an ecologically dominant plant species. *Trends Plant Sci.*, **9**, 49-56.

Burstin, J. (2000) Differential expression of two barley XET-related genes during coleoptile growth. *J. Exp. Bot.,* **51,** 847-852.

Campbell, P. and Braam, J. (1999) Xyloglucan endotransglycosylases: diversity of genes, enzymes and potential wall-modifying functions. *Trends Plant Sci.,* **4**, 361-366.

Carpita, N.C. and Gibeaut, D.M. (1993) Structural models of primary-cell walls in flowering plants – consistency of molecular structures with the physical properties of the wall during growth. *Plant J.,* **3**, 1-30.

Carpita, N.C. (1996) Structure and biogenesis of the cell walls of grasses. *Ann. Rev. Plant Physiol. Plant Mol. Biol.,* **47**, 445-476.

Carrard, G., Koivula, A., Soderlund, H. and Beguin, P. (2000) Cellulose-binding domains promote hydrolysis of different sites on crystalline cellulose. *Proc. Natl. Acad. Sci. USA,* **97**, 10342-10347.

Caspers, M.P.M., Lok, F., Sinjorgo, K.M.C., van Zeijl, M.J., Nielsen, K.A. and Cameron-Mills, V. (2001) Synthesis, processing and export of cytoplasmic *endo*-beta-1,4-xylanase from barley aleurone during germination. *Plant J.,* **26**, 191-204.

Chaffey, N., Cholewa, E., Regan, S. and Sundberg, B. (2002) Secondary xylem development in *Arabidopsis*: a model for wood formation. *Physiol. Plant.*, **114**, 594-600.

Charnock, S.J., Bolam, D.N., Turkenburg, J.P., Gilbert, H.J., Ferreira, L.M., Davies, G.J. and Fontes, C.M. (2000) The X6 "thermostabilizing" domains of xylanases are carbohydrate-binding modules: structure and biochemistry of the *Clostridium thermocellum* X6b domain. *Biochemistry,* **39**, 5013-5021.

Chen, N.J. and Paull, R.E. (2003) Endoxylanase expressed during papaya fruit ripening: purification, cloning and characterization. *Funct. Plant Biol.,* **30**, 433 – 441.

Cho, S.K., Kim, J.E., Park, J.A., Eom, T.J. and Kim, W.T. (2006) Constitutive expression of abiotic stress-inducible hot pepper *CaXTH3*, which encodes a xyloglucan endotransglucosylase/hydrolase homolog, improves drought and salt tolerance in transgenic *Arabidopsis* plants. *FEBS Lett.*, **580**, 3136-3144.

Cleemput, G., Hessing, M., Van Oort, M., Deconynck, M. and Delcour, J.A. (1997a) Purification and characterization of a [beta]-D-xylosidase and an endo-xylanase from wheat flour. *Plant Physiol.,* **113**, 377-386.

Cleemput, G., Van Laere, K., Hessing, M., Van Leuven, F., Torrekens, S. and Delcour, J.A. (1997b) Identification and characterization of a novel arabinoxylanase from wheat flour. *Plant Physiol.,* **115**, 1619-1627.

Collins, T., Gerday, C. and Feller, G. (2005) Xylanases, xylanase families and extremophilic xylanases. *FEMS Microbiol. Rev.,* **29**, 3-23.

Cosgrove, D.J. (2005) Growth of the plant cell wall. *Nat. Rev. Mol. Cell Biol.*, **6**, 850-861.

Courtois-Moreau, C. (2008) Programmed cell death in xylem development. *PhD thesis*. UPSC, Department of Plant Physiology, Umeå Univertsity.

Coutinho, P.M. and Henrissat, B. (1999) Carbohydrate-active enzymes, an integrated database approach. In *Recent advances in carbohydrate bioengineering*. (Gibert, H.J., Davies, G., Henrissat, B. and Svensson, B. eds.), The Royal Society of Chemistry, Cambridge. pp. 3-12.

Darley, C.P., Forrester, A.M. and McQueen-Mason, S.J. (2001) The molecular basis of plant cell wall extension. *Plant Mol. Biol.,* **47**, 179-195.

Davies, G. and Henrissat, B. (1995) Structures and mechanisms of glycosyl hydrolases. *Structure,* **3**, 853-859.

Davis, M.F., Tuskan, G.A., Payne, P., Tschaplinski, T.J. and Meilan, R. (2006) Assessment of *Populus* wood chemistry following the introduction of a Bt toxin gene. *Tree Physiol.,* **26**, 557–564.

del Campillo, E. (1999) Multiple endo-1,4-*β*-D-glucanase (cellulase) genes in *Arabidopsis*. *Curr. Top. Dev. Biol.,* **46**, 39-61.

del Campillo, E., Abdel-Aziz, A., Crawford, D. and Patterson, S.E. (2004) Root cap specific expression of an endo-β-1,4-D-glucanase (cellulase): a new marker to study root development in Arabidopsis. *Plant Mol. Biol*., **56**, 309-323.

Delmer, D.P. (1999) Cellulose biosynthesis: Exciting times for a difficult field of study. *Annu. Rev. Plant Physiol. Plant Mol. Biol.,* **50**, 245-276.

Demura, T. and Fukuda, H. (2007) Transcriptional regulation in wood formation. *Trends Plant Sci.*, **12**, 64-70.

Desprez, T., Juraniec, M., Crowell, E.F., Jouy, H., Pochylova, Z., Parcy, F., Höfte, H., Gonneau, M. and Vernhettes, S. (2007) Organization of cellulose synthase complexes involved in primary cell wall synthesis in *Arabidopsis thaliana*. *Proc. Natl. Acad. Sci. USA*, **104**, 15572-15577.

Devillard, E., Bera-Maillet, C., Flint, H.J., Scott, K.P., Newbold, C.J., Wallace, R.J., Jouany, J.P. and Forano, E. (2003) Characterization of XYN10B, a modular xylanase from the ruminal protozoan *Polyplastron multivesiculatum*, with a family 22 carbohydrate-binding module that binds to cellulose. *Biochem. J.*, **373**, 495-503.

Ding, S.Y. and Himmel, M.E. (2006) The maize primary cell wall microfibril: A new model derived from direct visualization. *J. Agric. Food Chem.,* **54**, 597-606.

Djerbi, S., Aspeborg, H., Nilsson, P., Sundberg, B., Mellerowicz, E., Blomqvist, K. and Teeri, T.T. (2004) Identification and expression analysis of genes encoding putative cellulose synthases (CesA) in the hybrid aspen, *Populus tremula* (L.) x *P. tremuloides* (Michx.). *Cellulose,* **11**, 301-312.

Djerbi, S., Lindskog, M., Arvestad, L., Sterky, F. and Teeri, T.T. (2005) The genome sequence of black cottonwood (*Populus trichocarpa*) reveals 18 conserved cellulose synthase (CesA) genes. *Planta,* **221**, 739-746.

Doblin, M.S., Kurek, I., Jacob-Wilk, D. and Delmer, D.P. (2002) Cellulose biosynthesis in plants: from genes to rosettes. *Plant Cell Physiol.,* **43**, 1407-1420.

Dolan, L., Janmaat, K., Willemsen, V., Linstead, P., Poethig, S., Roberts, K. and Scheres, B. (1993) Cellular organization of the *Arabidopsis thaliana* root. *Development*, **119**, 71–84.

Dolan, L. and Roberts, K. (1995) Secondary thickening in roots of *Arabidopsis thaliana*: anatomy and cell surface changes. *New Phytol.*, **131,** 121–128.

Donaldson, L. (2007) Cellulose microfibril aggregates and their size variation with cell wall type. *Wood Sci. Technol.,* **41**, 443-460.

Donaldson, L., Hague, J. and Snell, R. (2001) Lignin distribution in coppice poplar, linseed and wheat straw. *Holzforshung,* **55**, 379-385.

Duus, J., Gotfredsen, C. H. and Bock, K. (2000) Carbohydrate structural determination by NMR Spectroscopy: Modern methods and limitations. *Chem. Rev.*, **100**, 4589 – 4614.

Ebringerová, A. and Heinze, T. (2000) Xylan and xylan derivatives –biopolymers with valuable properties. 1. Naturally occuring xylans structures, isolation procedures and properties. *Macromo. Rapid Commun.*, **21**, 542-556.

Edashige, Y. and Ishii, T. (1999) Extracellular polysaccharides from suspension-cultures of *Populus alba* L.. *Holzforschung,* **53**, 137–141.

Fanutti, C., Gidley, M.J. and Reid, J.S. (1993) Action of a pure xyloglucan endotransglycosylase (formerly called xyloglucan-specific endo-(1-->4)-beta-D-glucanase) from the cotyledons of germinated nasturtium seeds. *Plant J.,* **3**, 691-700.

Feng, S., Chen, J.K., Yu, H., Simon, J.A. and Schreiber, S.A. (1994) Two binding orientation for peptides to the Src SH3 domain: Development of a general model for SH3-ligand interactions. *Science*, **266,** 1241–1247.

Fire, A., Xu, S., Montgomery, M., Kostas, S., Driver, S. and Mello, C. (1998) Potent and specific genetic interference by double-stranded RNA in *Caenorhabditis elegans*. *Nature,* **391**, 806–811.

Forsum, Å., Dahlman, L., Näsholm, T. and Nordin, A. (2006) Nitrogen utilization by *Hylocomium splendens* in a boreal forest fertilization experiment. *Funct. Ecol.*, **20**, 421-426.

Franz, G. and Blaschek, W. (1990) Cellulose. In *Methods in Plant Biochemistry vol 2, Carbohydrates.* (Dey, P.M. and Harborn, J.B. eds.), Academic Press, New York. pp.

291-322.

Freshour, G., Clay, R.P., Fuller, M.S., Albersheim, P., Darvill, A.G. and Hahn, M.G. (1996) Developmental and tissue-specific structural alterations of the cell-wall polysaccharides of *Arabidopsis thaliana* Roots. *Plant Physiol.,* **110**, 1413-1429.

Fry, S.C. (1988) The growing plant cell wall: chemical and metabolic analysis. Longman Scientific and Technical, Essex, UK.

Fry, S.C. (1989) The structure and functions of xyloglucan. *J. Exp. Bot.*, **40,** 1-11.

Fry, S.C., Smith, R.C., Renwick, K.F., Martin, D.J., Hodge, S.K. and Matthews, K.J. (1992) Xyloglucan endotransglycosylase, a new wall-loosening enzyme activity from plants. *Biochem. J.,* **282**, 821-828.

Fukuda, H. (1996) Xylogenesis: initiation, progression, and cell death. *Annu. Rev. Plant Physiol. Plant Mol. Biol.,* **47**, 299-325.

Fukuda, H. (2000) Programmed cell death of tracheary elements as a paradigm in plants. *Plant Mol. Biol.,* **44**, 245-253.

Fukuda, H. (2004) Signals that control plant vascular cell differentiation. *Nat. Rev. Mol. Cell Biol.,* **5**, 379–391.

Gebler, J., Gilkes, N.R., Claeyssens, M., Wilson, D.B., Beguin, P., Wakarchuk, W.W., Kilburn, D.G, Miller Jr, R.C., Warren, R.A. and Withers, S.G. (1992) Stereoselective hydrolysis catalyzed by related beta-1,4-glucanases and beta-1,4-xylanases *J. Biol. Chem*., **267**, 12559-12561.

Gendreau, E., Traas, J., Desnos, T., Grandjean, O., Caboche, M. and Höfte, H. (1997) Cellular basis of hypocotyls growth in *Arabidopsis thaliana. Plant Physiol.*, **114**, 295-305.

Gilkes, N.R., Warren, R.A., Miller, R.C.J. and Kilburn, D.G. (1988) Precise excision of the cellulose binding domains from two *Cellulomonas fimi* cellulases by a homologous protease and the effect on catalysis. *J. Biol. Chem.,* **263**, 10401-10407.

Goué, N., Lesage-Descauses, M-C., Mellerowicz, E.J., Magel, E., Label, P. and Sundberg, B. (2008) Microgenomic analysis reveals cell type-specific gene expression patterns between ray and fusiform initials within the cambial meristem of *Populus*. *New Phytol.,* **180**, 45-56.

Guo, S. and Kemphues, K. (1995) *par-1*, a gene required for establishing polarity in C. elegans embryos, encodes a putative Ser/Thr kinase that is asymmetrically distributed. *Cell,* **81**, 611–620.

Ha, M.A., Apperley, D.C., Evans, B.W., Huxham, M., Jardine, W.G., Vietor, R.J., Reis, D., Vian, B. and Jarvis, M.C. (1998) Fine structure in cellulose microfibrils: NMR evidence from onion and quince. *Plant J.*, **16**, 183-190.

Harada, H. and Côté, W.A. (1985) Biosynthesis and biodegradation of wood components. (Higuchi, T. ed.), Academic Press, Orlando. pp.1-42.

Harholt, J., Jensen, J.K., Sørensen, S.O., Orfila, C., Pauly, M. and Scheller, H.V. (2006) ARABINAN DEFICIENT 1 is a putative arabinosyltransferase involved in biosynthesis of pectic arabinan in *Arabidopsis*. *Plant Physiol.*, **140**, 49-58.

Hatfield, R. and Nevins, D.J. (1986) Characterization of the hydrolytic activity of avocado cellulase. *Plant Cell Physiol.,* **27**, 541-552.

Hayashi, T. (1989) Xyloglucans in the primary cell wall. *Annu. Rev. Plant Physiol. Plant Mol. Biol.,* **40**, 139-168.

Hayashi, T., Yoshida, K., Park, Y.W., Konishi, T. and Baba, K. (2005) Cellulose metabolism in plants. *Int. Rev. Cytol.,* **247**, 1-34.

Hedenström, M., Öman, T., Wiklund, S., Sundberg, B., Edlund, U. and Ralph, J. (2008) NMR spectroscopy: A tool for chemical characterization and classification of poplar wood. *Funcfiber International Symposium on the Biology and Biotechnology of wood, Abstract,* pp. 15.

Henrissat, B. (1991) A classification of glycosyl hydrolases based on amino acid sequence similarities. *Biochem. J.,* **280**, 309-316.

Henrissat, B. and Bairoch, A. (1996) Updating the sequence-based classification of glycosyl hydrolases. *Biochem. J.,* **316**, 695–696.

Henrissat, B. and Davies, G. (1997) Structural and sequence-based classification of glycoside hydrolases. *Curr. Opin. Struct. Biol.*, **7**, 637-644.

Henrissat, B. and Davies, G.J. (2000) Glycoside hydrolases and glycosyltransferases. Families, modules, and implications for genomics. *Plant Physiol,* **124**, 1515-1519.

Henrissat, B., Coutinho, P.M. and Davies, G.J. (2001) A census of carbohydrate-active enzymes in the genome of *Arabidopsis thaliana*. *Plant Mol Biol,* **47**, 55-72.

Hertzberg, M., Aspeborg, H., Schrader, J., Andersson, A., Erlandsson, R., Blomqvist, K., Bhalerao, R., Uhlen, M., Teeri, T.T., Lundeberg, J., Sundberg, B., Nilsson, P. and Sandberg, G. (2001) A transcriptional road map to wood formation. *Proc. Natl. Acad. Sci. USA*, **98**, 14732-14737.

Hildén, L. and Johansson, G. (2004) Recent developments on cellulases and carbohydrate-binding modules with cellulose affinity. *Biotechnol. Lett.,* **26,** 1683-1693.

His, I., Driouich, A., Nicol, F., Jauneau, A. and Höfte, H. (2001) Altered pectin composition in primary cell walls of *korrigan*, a dwarf mutant of *Arabidopsis* deficient in a membrane-bound endo-1,4-β-glucanase. *Planta*, **212**, 348-358.

Imamura, T., Watanabe, T., Kuwahara, M. and Koshijima, T. (1994) Ester linkages between lignin and glucuronic-acid in lignin-carbohydrate complexes from *Fagus crenata*. *Phytochem.,* **37**, 1165-1173.

Jansson, S., and Douglas, C.J. (2007) *Populus*: a model system for plant biology. *Annu. Rev. Plant. Biol.*, **58**, 435-458.

Johansson, M.H. and Samuelson, O. (1977) Reducing end groups in birch xylan and

their alkaline degradation. *Wood Sci. Technol.*, **11**, 251–263.

Jørgensen, H., Kristensen, J.B. and Felby, C. (2007) Enzymatic conversion of lignocellulose into fermentable sugars: Challenges and opportunities. *Biofuels Bioprod. Bioref.,* **1**, 119-134.

Joshi, C.P., Bhandari, S., Ranjan, P., Kalluri, U.C., Liang, X., Fujino, T. and Samuga, A. (2004) Genomics of cellulose biosynthesis in poplars. *New Phytol.*, **164,** 53-61.

Joshi, C. P. and Mansfield, S. D. (2007) The cellulose paradox – simple molecule, complex biosynthesis. *Curr. Opin. Plant Biol.*, **10,** 220-226.

Kallas, Å.M. Piens, K., Denman, S.E., Henriksson, H., Fäldt, J., Johansson, P., Brumer, III H. and Teeri, T.T. (2005) Enzymatic properties of native and deglycosylated hybrid aspen (*Populus tremula x tremuloides*) xyloglucan endotransglycosylase 16A (PttXET16A) expressed in *Pichia pastoris. Biochem. J.,* **390**, 105-113.

Kay, B. K., Williamson, M. P. and Sudol, M. (2000) The importance of being proline: The interaction of proline-rich motifs in signaling proteins with their cognate domains. *FASEB J.,* **14**, 231-241.

Keegstra, K. and Walton, J. (2006) β-Glucans--brewer's bane, dietician's delight. *Science*, **311**, 1872 – 1873.

Kennedy, C.J., Cameron, G.J., Šturcová, A., Apperley, D.C., Altaner, C., Wess, T.J. and Jarvis, M.C. (2007) Microfibril diameter in celery collenchyma cellulose: X-ray scattering and NMR evidence. *Cellulose,* **14**, 235-246.

Kimura, S., Laosinchai, W., Itoh, T., Cui, X., Linder, C.R. and Brown, M.R. (1999) Immunogold labeling of rosette terminal cellulose-synthesizing complexes in the vascular plant *Vigna angularis*. *Plant Cell*, **11**, 2075-2085.

Krishnamurthy, K. V. (1999) Methods in cell wall cytochemistry. CRC Press LLC, Florida.

Klahre, U., Noguchi, T., Fujioka, S., Takatsuto, S., Yokota, T., Nomura, T., Yoshida, S. and Chua, N.H. (1998) The Arabidopsis *DIMINUTO/DWARF1* gene encodes a protein involved in steroid synthesis. *Plant Cell*, **10**, 1677-1690.

Ko, J.H. and Han, K.H. (2004) Arabidopsis whole-transcriptome profiling defines the features of coordinated regulations that occur during secondary growth. *Plant Mol. Biol.*, **55**, 433–453.

Ko, J.H., Han, K.H., Park, S. and Yang, J. (2004) Plant body weight-induced secondary growth in Arabidopsis and its transcription phenotype revealed by whole transcriptome profiling. *Plant Physiol.*, **135**, 1069–1083.

Koshland, D.E. (1953) Stereochemistry and the mechanism of enzymatic reactions. *Biol.Rev.,* **28**, 416-436.

Koyama, M., Helbert, W., Imai, T., Sugiyama, J. and Henrissat, B. (1997) Parallel-up structure evidences the molecular directionality during biosynthesis of bacterial cellulose. *Proc. Natl. Acad. Sci. USA,* **94**, 9091–9095.

Lam, B.C.H., Sage, T.L., Bianchi, F. and Blumwald, E. (2001) Role of SH3 domain-containing proteins in clathrin-mediated vesicle trafficking in Arabidopsis. *Plant Cell*, **13**, 2499-2512.

Lane, D.R., Wiedemeier, A., Peng, L.C., Höfte, H., Vernhettes, S., Desprez, T., Hocart, C.H., Birch, R.J., Baskin, T.I., Burn, J.E., Arioli, T., Betzner, A.S. and Williamson, R.E. (2001) Temperature-sensitive alleles of *RSW2* link the KORRIGAN endo-1,4-β-glucanase to cellulose synthesis and cytokinesis in Arabidopsis. *Plant Physiol.,* **126**, 278-288.

Larson, P. R. (1994) The vascular cambium. Springer Verlag, Berlin.

Leitch, I.J., Hanson, L., Winfield, M., Parker, J. and Bennett, M.D. (2001) Nuclear DNA C-values complete familia representation in gymnosperms. *Ann. Bot.,* **88,** 843-849.

Lerouxel, O., Cavalier, D.M., Liepman, A.H. and Keegstra, K. (2006) Biosynthesis of plant cell wall polysaccharides - A complex process. *Curr. Opin. Plant Biol.*, **9,** 621–630.

Lev-Yadun, S. (1994) Induction of sclereid differentiation in the pith of *Arabidopsis thaliana* (L.) Heynh. *J. Exp. Bot.*, **45,** 1845–1849.

Levy, S., Maclachlan, G. and Staehelin, L.A. (1997) Xyloglucan sidechains modulate binding to cellulose during in vitro binding assays as predicted by conformational dynamics simulations. *Plant J.,* **11**, 373-386.

Li, X.L., Spániková, S., de Vries, R.P. and Biely, P. (2007) Identification of genes encoding microbial glucuronoyl esterases. *FEBS Lett.,* **581**, 4029-4035.

Libertini, E., Li, Y. and McQueen-Mason, S.J. (2004) Phylogenetic analysis of the plant endo-β-1,4-glucanase gene family. *J. Mol. Evol.,* **58**, 506-515.

Liese, W. and Ammer, U. (1958) Investigation on the length of wood fibers in poplars. *Holzforschung,* **11**, 69-174.

Linder, M. and Teeri, T. T. (1997) The roles and function of cellulose-binding domains. *J. Biotechnol.*, **57**, 15-28.

Liu, Y-B., Lu, S-M., Zhang, J-F., Liu, S. and Lu, Y-T. (2007) A xyloglucan endotransglucosylase/hydrolase involves in growth of primary root and alters the deposition of cellulose in *Arabidopsis*. *Planta,* **226**, 1547–1560.

Lu, F. and Ralph, J. (2003) Non-degradative dissolution and acetylation of ball-milled plant cell walls: high-resolution solution-state NMR. *Plant J.,* **35**, 535-544.

Lynd, L.R., Laser, M.S., Bransby, D., Dale, B.E., Davison, B., Hamilton, R., Himmel, M., Keller, M., McMillan, J.D., Sheehan, J. and Wyman, C.E. (2008) How biotech can transform biofuels. *Nat. biotechnol.*, **22**, 169 – 172.

Lynd, L.R., Weimer, P.J., van Zyl, W.H. and Pretorius, I.S. (2002) Microbial cellulose utilization: Fundamentals and biotechnology. *Microbiol. Mol. Biol. Rev.*, **66**, 506-577.

Malinowski, R., Filipecki, M., Tagashira, N., Wisniewska, A., Gaj, P., Plader, W. and

Malepszy, S. (2004) Xyloglucan endotransglucosylase/hydrolase genes in cucumber (*Cucumis sativus*) - differential expression during somatic embryogenesis. *Physiol. Plant.,* **120**, 678-685.

Master, E.R., Rudsander, U.J., Zhou, W., Henriksson, H., Divne, C., Denman, S., Wilson, D.B. and Teeri, T.T. (2004) Recombinant expression and enzymatic characterization of PttCel9A, a KOR homologue from *Populus tremula* x *tremuloides*. *Biochemistry*, **43**, 10080-10089.

Matthysse, A. G., White, S., and Lightfoot, R. (1995) Genes required for cellulose synthesis in *Agrobacterium-tumefaciens*. *J. Bacteriol.,* **177**, 1069-1075.

Maunu, S.L. (2002) NMR studies of wood and wood products. *Prog. NMR spectrosc.*, **40**, 151-174.

McCann, M.C., Wells, B. and Roberts, K. (1990) Direct visualization of cross-links in the primary plant cell wall. *J. Cell Sci.*, **96**, 323-334.

Meissner, K., Wassenberg, D. and Liebl, W. (2000) The thermostabilizing domain of the modular xylanase XynA of *Thermotoga maritima* represents a novel type of binding domain with affinity for soluble xylan and mixed-linkage beta-1,3/beta-1,4-glucan. *Mol. Microbiol.,* **36**, 898-912.

Mellerowicz, E.J., Baucher, M., Sundberg, B. and Boerjan, W. (2001) Unravelling cell wall formation in the woody dicot stem. *Plant Mol. Biol.*, **47**, 239–274.

Mellerowicz, E.J. (2006) Xylem cell expansion – Lessons from poplar. In *The science and lore of the plant cell wall*. (Hayashi, T., ed.), Boca Raton, FL, Universal Publishers Brown Walker Press. pp. 267- 275.

Mellerowicz, E.J., Immerzeel, P. and Hayashi, T. (2008) Xyloglucan: The molecular muscle of trees. *Ann. Bot*., Published online, doi:10.1093/aob/mcn170.

Mellerowicz, E.J. and Sundberg, B. (2008) Wood cell walls: biosynthesis, developmental dynamics and their implications for wood properties**.** *Curr. Opin. Plant Biol.,* **11**, 293-300.

Mølhøj, M., Ulvskov, P. and Dal Degan, F. (2001) Characterization of a functional soluble form of a *Brassica napus* membrane-anchored endo-1,4-β-glucanase heterologously expressed in *Pichia pastoris*. *Plant Physiol.,* **127**, 674-684.

Mølhøj, M., Pagant, S. and Höfte, H. (2002) Towards understanding the role of membrane-bound endo-β-1,4-glucanases in cellulose biosynthesis. *Plant Cell Physiol.,* **43**, 1399-1406.

Moore, R.C. and Purugganan, M.D. (2005) The evolutionary dynamics of plant duplicate genes. *Curr. Opin. Plant Biol.*, **8**, 122–128.

Moreau, A., Roberge, M., Manin, C., Shareck, F., Kluepfel, D. and Morosoli, R. (1994) Identification of two acidic residues involved in the catalysis of xylanase A from *Streptomyces lividans*. *Biochem. J.,* **302**, 291-295.

Moreau, C., Aksenov, N., Garcia-Lorenzo, M., Segerman, B., Funk, C., Nilsson, P., Jansson, S. and Tuominen, H. (2005) A genomic approach to investigate developmental cell death in woody tissues of *Populus* trees. *Genome Biol.,* **6,** R34.

Motose, H., Sugiyama, M. and Fukuda, H., (2004) A proteoglycan mediates inductive interaction during plant vascular development. *Nature*, **429**, 873-878.

Müller, M., Burghammer, M. and Sugiyama, J. (2006) Direct investigation of the structural properties of tension wood cellulose microfibrils using microbeam X-ray fibre diffraction. *Holzforschung*, **60**, 474-479.

Mutwil, M., Debolt, S. and Persson, S. (2008) Cellulose synthesis: a complex complex. *Curr. Opin. Plant Biol.*, **11**, 252-257.

Nakamura, S. and Hayashi, T. (1993) Purification and properties of an extracellular endo-1,4-β-glucanase from suspension-cultured poplar cells. *Plant Cell Physiol.*, **34**, 1009-1013.

Nakamura, S., Mori, H., Sakai, F. and Hayashi, T. (1995) Cloning and sequencing of a cDNA for poplar endo-1,4-β-glucanase. *Plant Cell Physiol.*, **36**, 1229-1235.

Nakashima, K., Yamada, L., Satou, Y., Azuma, J. and Satoh, N. (2004) The evolutionary origin of animal cellulose synthase. *Dev. Genes Evol.*, **214**, 81-88.

Newman, R.H. and Hemmingson, J.A. (1990) Determination of the degree of cellulose crystallinity in wood by C-13 Nuclear-Magnetic-Resonance spectroscopy. *Holzforschung*, **44**, 351-355.

Newman, R.H. (1999) Estimation of the lateral dimensions of cellulose crystallites using C-13 NMR signal strengths. *Solid State NMR,* **15**, 21-29.

Nicol, F., His, I., Jauneau, A., Vernhettes, S., Canut, H. and Höfte, H. (1998) A plasma membrane-bound putative endo-1,4-β-D-glucanase is required for normal wall assembly and cell elongation in *Arabidopsis. EMBO J.*, **17**, 5563-5576.

Nieminen, K.M., Kauppinen, L. and Helariutta, Y. (2004) A weed for wood? Arabidopsis as a genetic model for xylem development. *Plant Physiol.,* **135**, 653-659.

Nishikubo, N., Awano, T., Banasiak, A., Bourquin, V., Ibatullin, F., Funada, R., Brumer, H., Teeri, T.T., Hayashi, T., Sundberg, B. and Mellerowicz, E.J. (2007) Xyloglucan Endo-transglycosylase (XET) functions in gelatinous layers of tension wood fibers in Poplar - A glimpse into the mechanism of the balancing act of trees. *Plant Cell Physiol.*, **48**, 843-855.

Nishitani, **K.** (1997) The role of endoxyloglucan transferase in the organization of plant cell walls. *Int. Rev. Cytol.* **173**, 157–206.

Nishitani, **K.** (1998) Construction and restructuring of the cellulose-xyloglucan framework in the apoplast as mediated by the xyloglucan-related protein family—A hypothetical scheme. *J. Plant Res.,* **111**, 159–166.

Nishitani, K. and Tominaga, R. (1992) Endo-xyloglucan transferase, a novel class of glycosyltransferase that catalyzes transfer of a segment of xyloglucan molecule to another xyloglucan molecule. *J. Biol. Chem.,* **267**, 21058-21064.

Øbro, J., Harholt, J., Scheller, H.V. and Orfila, C. (2004) Rhamnogalacturonan I in *Solanum tuberosum* tubers contains complex arabinogalactan structures. *Phytochemistry*, **65**, 1429-1438.

Oh, S., Park, S. and Han, K.H. (2003) Transcriptional regulation of secondary growth in *Arabidopsis thaliana*. *J. Exp. Bot.*, **54**, 2709–2722.

Ohmiya, Y., Takeda, T., Nakamura, S., Sakai, F. and Hayashi, T. (1995) Purification and properties of a wall-bound endo-1,4-β-glucanase from suspension-cultured poplar cells. *Plant Cell Physiol.*, **36**, 607-614.

Ohmiya, Y., Samejima, M., Shiroishi, M., Amano, Y., Kanda, T., Sakai, F. and Hayashi, T. (2000) Evidence that endo-1,4-β-glucanases act on cellulose in suspension-cultured poplar cells. *Plant J.,* **24**, 147-158.

Ohmiya, Y., Nakai, T., Park, Y.W., Aoyama, T., Oka, A., Sakai, F. and Hayashi, T. (2003) The role of PopCel1 and PopCel2 in poplar leaf growth and cellulose biosynthesis. *Plant J.*, **33**, 1087-1097.

O'Neill, M.A. and York, W.S. (2003) The composition and structure of plant primary cell walls. In *Plant cell wall*. (Rose, J.K.C. ed.), CRC Press, Oxford.

Osato, Y., Yokoyama, R. and Nishitani, K. (2006) A principal role for AtXTH18 in *Arabidopsis thaliana* root growth: a functional analysis using RNAi plants. *J. Plant Res.,* **119**, 153–62.

Paredez, A.R., Somerville, C.R. and Ehrhardt, D.W. (2006) Visualization of cellulose synthase demonstrates functional association with microtubules. *Science*, **312**, 1491-1495.

Paredez, A.R., Persson, S., Ehrhardt, D.W. and Somerville, C.R. (2008) Genetic evidence that cellulose synthase activity influences microtubule cortical array organization. *Plant Physiol.,* **147**, 1723-1734.

Park, Y.W., Tominaga, R., Sugiyama, J., Furuta, Y., Tanimoto, E., Samejima, M., Sakai, F. and Hayashi, T. (2003) Enhancement of growth by expression of poplar cellulase in *Arabidopsis thaliana*. *Plant J.*, **33**, 1099-1106.

Paull, R.E. and Chen, N.J. (1983) Postharvest variation in cell wall-degrading enzymes of papaya (*Carica papaya* L.) during fruit ripening. *Plant Physiol.,* **72**, 382–385.

Pauly, M., Albersheim, P., Darvill, A. and York, W.S. (1999) Molecular domains of the cellulose/xyloglucan network in the cell walls of higher plants. *Plant J.*, **20**, 629-639.

Pawson, T. and Nash, P. (2003) Assembly of cell regulatory systems through protein interaction domains. *Science,* **300**, 445-452.

Peña, M.J., Zhong, R., Zhou, G.K., Richardson, E.A., O'Neill, M.A., Darvill, A.G., York, W.S. and Ye, Z.H. (2007) Arabidopsis irregular xylem8 and irregular xylem9: implications for the complexity of glucuronoxylan biosynthesis. *Plant Cell*, **19**, 549–563.

Peng, L., Kawagoe, Y., Hogan, H. and Delmer, D. (2002) Sitosterol-β-glucoside as primer for cellulose synthesis in plants. *Science*, **295**, 147-150.

Persson, S., Wei, H., Milne, J., Page, G.P. and Somerville, C.R. (2005) Identification of genes required for cellulose synthesis by regression analysis of public microarray data sets. *Proc. Natl. Acad. Sci. USA*, **102**, 8633-8638.

Persson, S., Caffall, K.H., Freshour, G., Hilley, M.T., Bauer, S., Poindexter, P., Hahn, M.G., Mohnen, D. and Somerville, C. (2007a) The Arabidopsis *irregular xylem 8* mutant is deficient in glucuronoxylan and homogalacturonan, which are essential for secondary cell wall integrity. *Plant Cell*, **19**, 237–255.

Persson, S., Paredez, A., Carroll, A., Palsdottir, H., Doblin, M., Poindexter, P., Khitrov, N., Auer, M. and Somerville, C.R. (2007b) Genetic evidence for three unique components in primary cell-wall cellulose synthase complexes in Arabidopsis. *Proc. Natl. Acad. Sci. USA*, **104**, 15566-15571.

Pilate, G., Déjardin, A., Laurans, F. and Leplé, J-C. (2004) Tension wood as a model for functional genomics of wood formation. *New Phytol.,* **164**, 63–72.

Plomion, C., Leprovost, G. and Stokes, A. (2001) Wood formation in trees. *Plant Physiol.*, **127**, 1513-1523.

Prince, V.E. and Pickett, F.B. (2002) Splitting pairs: the diverging fates of duplicated genes. *Nat. Rev. Genet.*, **3**, 827-837.

Raven, P.H., Evert, R.F. and Eichhorn, S.E. (1999) Biology of plants, 6th edition. W.H. Freeman and Company, New York, USA.

Reid, J.S.G. (1997) Carbohydrate metabolism: structural carbohydrates. In *Plant Biochemistry.* (Dey, P. M. and Harborne, J. B., eds.), Academic Press, London. pp. 205-236.

Reidy, B., Nosberger, J. and Fleming, A. (2001) Differential expression of XET-related genes in the leaf elongation zone of *F. pratensis*. *J. Exp. Bot.,* **52**, 1847-1856.

Reiter, W.D. Chapple, C.C.S. and Somerville, C.R. (1993) Altered growth and cell walls in a fucose deficient mutant of Arabidopsis. *Science*, **261**, 1032-1035.

Reiter W.D. (2002) Biosynthesis and properties of the plant cell wall. *Curr. Opin. Plant Biol.,* **5**, 536-542.

Richmond, T. and Somerville, C. (2001) Integrative approaches to determining Csl function. *Plant Mol. Biol.*, **47**, 131-143.

Robert, S., Mouille, G. and Hofte, H. (2004) The mechanism and regulation of cellulose synthesis in primary walls: lessons from cellulose-deficient Arabidopsis mutants. *Cellulose* **11**, 351-364.

Robert, S., Bichet, A., Grandjean, O., Kierzkowski, D., Satiat-Jeunemaitre, B., Pelletier, S., Hauser, M.T., Höfte, H. and Vernhettes, S. (2005) An *Arabidopsis* endo-1,4-β-D-glucanase involved in cellulose synthesis undergoes regulated intracellular cycling. *Plant Cell*, **17**, 3378-3389.

Ronen, R., Zauberman, G., Akerman, M., Weksler, A., Rot, I. and Fuchs, Y. (1991) Xylanase and xylosidase activities in avocado fruit. *Plant Physiol.*, **95**, 961-964.

Rose, J.K., Brummell, D.A. and Bennett, A.B. (1996) Two divergent xyloglucan endotransglycosylases exhibit mutually exclusive patterns of expression in nasturtium. *Plant Physiol.,* **110**, 493-499.

Rose, J.K.C. and Bennett, A.B. (1999) Cooperative disassembly of the cellulose-xyloglucan network of plant cell walls: Parallels between cell expansion and fruit ripening. *Trends Plant Sci.,* **4**, 176-183.

Rose, J.K., Braam, J., Fry, S.C. and Nishitani, K. (2002) The XTH family of enzymes involved in xyloglucan endotransglucosylation and endohydrolysis: current perspectives and a new unifying nomenclature. *Plant Cell Physiol.,* **43**, 1421-1435.

Rudsander, U., Denman, S., Raza, S. and Teeri, T.T. (2003) Molecular features of family GH9 cellulases in hybrid aspen and the filamentous fungus *Phanerochaete chrysosporium*. *J. Appl. Glycobiol.,* **50**, 253-256.

Rudsander, U.J. (2007) Functional studies of a membrane-anchored cellulase from poplar. *PhD thesis*. KTH.

Rudsander, U.J., Sandstrom, C., Piens, K., Master, E.R., Wilson, D.B., Brumer, H.III, Kenne, L. and Teeri, T.T. (2008) Comparative NMR analysis of cello-oligosaccharide hydrolysis by GH9 bacterial and plant endo-1,4-β-glucanases. *Biochemistry,* **47**, 5235–5241.

Russell, N. S. and Wilkinson, K. D. (2005) The deubiquitinating enzymes. In *Protein Degradation: Ubiquitin and the Chemistry of Life*. (Mayer, R.J., Ciechanover, A.J. and Rechsteiner, M. eds.), WILEY-VCH Verlag GmbH & Co. KGaA, Weinheim. pp.194-219.

Sakon, J., Irwin, D., Wilson, D.B. and Karplus, P.A. (1997) Structure and mechanism of endo/exocellulase E4 from *Thermomonospora fusca*. *Nat. Struct. Biol.,* **4**, 810-818.

Salmén, L. (2004) Micromechanical understanding of the cell-wall structure. *C.R. Biologies*, **327**, 873-880.

Sato, S., Kato, T., Kakegawa, K., Ishii, T., Liu, Y.G., Awano, T., Takabe, K., Nishiyama, Y., Kuga, S., Sato, S., Nakamura, Y., Tabata, S. and Shibata, D. (2001) Role of the putative membrane-bound endo-1,4-β-glucanase KORRIGAN in cell elongation and cellulose synthesis in *Arabidopsis thaliana*. *Plant Cell Physiol.,* **42**, 251-263.

Saxena, I.M. and Brown, R.M. (2005) Cellulose biosynthesis: Current views and evolving concepts. *Ann. Bot.* **96**, 9-21.

Scheible, W.R. and Pauly, M. (2004) Glycosyltransferases and cell wall biosynthesis, novel players and insights. *Curr. Opin. Plant Biol.,* **7**, 285-295.

Schrader, J. (2003) Developmental biology of wood formation – Finding regulatory factors through functional genomics. *PhD thesis*. UPSC, Department of Forest Genetics and Plant Physiology, SLU.

Schrader, J., Nilsson, J., Mellerowicz, E., Berglund, A., Nilsson, P., Hertzberg, M. and Sandberg, G. (2004) A high-resolution transcript profile across the wood-forming meristem of poplar identifies potential regulators of cambial stem cell identity. *Plant Cell*, **16**, 2278-2292.

Schrick, K., Mayer, U., Horrichs, A., Kuhnt, C., Bellini, C., Dangl, J., Schmidt, J., and Jurgens, G. (2000) FACKEL is a sterol C-14 reductase required for organized cell division and expansion in Arabidopsis embryogenesis. *Gene Dev.,* **14**, 1471-1484.

Schrick, K., Mayer, U., Martin, G., Bellini, C., Kuhnt, C., Schmidt, J., and Jurgens, G. (2002) Interactions between sterol biosynthesis genes in embryonic development of Arabidopsis. *Plant J.,* **31**, 61-73.

Schrick, K. Fujioka, S., Takatsuto, S., Stierhof, Y-D, Stransky H., Yoshida, S. and Jurgens, G. (2004) A link between sterol biosynthesis, the cell wall, and cellulose in Arabidopsis. *Plant J.,* **38**, 227-243.

Schröder, R., Wegrzyn, T.F., Bolitho, K.M. and Redgwell, R.J. (2004) Mannan transglycosylase: a novel enzyme activity in cell walls of higher plants. *Planta,* **219**, 590-600.

Scott, A.S. and Melvin, E.H. (1953) Determination of dextran with anthrone. *Anal. Chem*., **25**, 1656-1661.

Sederoff, R., Kirst, M., Johnson, A., Retzel, E., Whetten, R., Vasques-Kool, J. and O'Malley, D. (2002) Homology of expressed genes in loblolly pine (*Pinus taeda* L.) with *Arabidopsis thaliana*. *Abstract, The 10th IAPTC&B Congress, Orlando FL.* pp. 23-28.

Shani, Z., Dekel, M., Tsabary, G. and Shoseyov, O. (1997) Cloning and characterization of elongation specific endo-1,4-beta-glucanase (cel1) from *Arabidopsis thaliana*. *Plant Mol. Biol.*, **34**, 837-842.

Shani, Z., Dekel, M., Tsabary, G., Goren, R. and Shoseyov, O. (2004) Growth enhancement of transgenic poplar plants by overexpression of *Arabidopsis thaliana* endo-1,4–β-glucanase (*cel*1). *Mol. Breed.*, **14**, 321-330.

Shin, E.S., Yang, M.J., Jung, K.H., Kwon, E.J., Jung, J.S., Park, S.K., Kim, J., Yun, H.D. and Kim, H. (2002) Influence of the transposition of the thermostabilizing domain of *Clostridium thermocellum* xylanase (XynX) on xylan binding and thermostabilization. *Appl. Environ. Microbiol*., **68**, 3496-3501.

Siedlecka, A., Wiklund, S., Péronne, M.A., Micheli, F., Lesniewska, J., Sethson. I,, Edlund, U., Richard, L., Sundberg, B. and Mellerowicz, E.J. (2008) Pectin methyl esterase inhibits intrusive and symplastic cell growth in developing wood cells of *Populus*. *Plant Physiol.*, **146**, 554-565.

Simillion, C., Vandepoele, K., Van Montagu, M.C., Zabeau, M. and Van de Peer, Y. (2002) The hidden duplication past of *Arabidopsis thaliana*. *Proc. Natl. Acad. Sci. USA*, **99**, 13627–13632.

Simpson, D.J., Fincher, G.B., Huang, A.H.C. and Cameron-Mills, V. (2003) Structure and function of cereal and related higher plant (1 → 4)-beta-xylan endohydrolases. *J. Cereal Sci.,* **37,** 111-127.

Simson, B.W. and Timell, T.E. (1978a) Polysaccharides in cambial tissues of *Populus tremuloides* and *Tilia americana*. I. Isolation, fractionation, and chemical composition of the cambial tissues. *Cell Chem. Technol.*, **12**, 39–50.

Simson, B.W. and Timell, T.E. (1978b) Polysaccharides in cambial tissues of *Populus tremuloides* and *Tilia americana*. II. Isolation and structure of a xyloglucan. *Cell Chem. Technol.*, **12**, 51–62.

Simson, B.W. and Timell, T.E. (1978c) Polysaccharides in cambial tissues of *Populus tremuloides* and *Tilia americana*. IV. 4-*O*-methylglucuronoxylan and pectin. *Cell Chem. Technol.,* **12**,79–84.

Simson, B.W. and Timell, T.E. (1978d) Polysaccharides in cambial tissues of *Populus tremuloides* and *Tilia americana*. V. Cellulose. *Cell Chem. Technol.*, **12**, 137–141.

Slade, A.M., Hoj, P.B., Morrice, N.A. and Fincher, G.B. (1989) Purification and characterization of three (1,4)-beta-D-xylan endohydrolases from germinated barley. *Eur. J. Biochem.,* **185**, 533-539.

Smriti and Sanwal, G.G. (1999) Purification and characterization of a cellulase from *Catharanthus roseus* stems. *Phytochemistry,* **52**, 7-13.

Somerville, C., Bauer, S., Brininstool, G., Facette, M., Hamann, T., Milne, J., Osborne, E., Paredez, A., Persson, S., Raab, T., Vorwerk, S. and Youngs, H. (2004) Toward a systems approach to understanding plant cell walls. *Science,* **306**, 2206-2211.

Somerville, C. (2006) Cellulose synthesis in higher plants. *Annu. Rev. Cell Dev. Bi.*, **22**, 53-78.

Spániková, S. and Biely, P. (2006) Glucuronoyl esterase – novel carbohydrate esterase produced by Schizophyllum commune. *FEBS Lett.,* **580**, 4597-4601.

Spániková, S., Polakova, M., Joniak, D., Hirsch, J. and Biely, P. (2007) Synthetic esters recognized by glucuronoyl esterase from Schizophyllum commune. *Arch. Microbiol*. **188**, 185-189.

Steele, N.M. and Fry, S.C. (2000) Differences in catalytic properties between native isoenzymes of xyloglucan endotransglycosylase (XET). *Phytochem.,* **54**, 667-680.

Sterky, F., Regan, S., Karlsson, J., Hertzberg, M., Rohde, A., Holmberg, A., Amini, B., Bhalerao, R., Larsson, M., Villarroel, R, Van Montagu, M., Sandberg, G., Olsson, O., Teeri, T.T., Boerjan, W., Gustafsson, P., Uhlen, M., Sundberg, B. and Lundeberg, J. (1998) Gene discovery in the wood-forming tissues of poplar, Analysis of 5,692 expressed sequence tags. *Proc. Natl. Acad. Sci. USA*, **95**, 13330-13335.

Sterky, F., Bhalerao, R.R., Unneberg, P., Segerman, B., Nilsson, P., Brunner, A.M., Campaa, L., Jonsson, L.J., Tandre, K., Strauss, S.H., Sundberg, B., Gustafsson, P., Uhlen, M., Bhalerao, R.P., Nilsson, O., Sandberg, G., Karlsson, J., Lundeberg, J. and Jansson, S. (2004) A *Populus* EST resource for plant functional genomics. *Proc. Natl. Acad. Sci. USA*, **101**, 13951-13956.

Sunna, A. and Antranikian, G. (1997) Xylanolytic enzymes from fungi and bacteria. *Crit. Rev. Biotechnol.,* **17**, 39-67.

Suzuki, M., Kato, A., Nagata, N. and Komeda, Y. (2002) A xylanase, AtXyn1, is predominantly expressed in vascular bundles, and four putative xylanase genes were identified in the *Arabidopsis thaliana* genome. *Plant Cell Physiol.,* **43**, 759 - 767.

Szyjanowicz, P.M.J., McKinnon, I., Taylor, N.G., Gardiner, J., Jarvis, M.C. and Turner, S.R. (2004) The *irregular xylem 2* mutant is an allele of *korrigan* that affects the secondary cell wall of *Arabidopsis thaliana. Plant J.,* **37**, 730-740.

Tabuchi, A., Mori, H., Kamisaka, S. and Hoson, T. (2001) A new type of endo-xyloglucan transferase devoted to xyloglucan hydrolysis in the cell wall of azuki bean epicotyls. *Plant Cell Physiol.,* **42**, 154-161.

Takabe, K., Miyauchi, S., Tsunoda, R. and Fukazawa, K. (1992) Distribution of guaiacyl and syringyl lignins in Japanese beech (*Fagus crenata*), variation within an annual ring. *IAWA Bull,* **13**, 105-112.

Takayama, K.M. and Inouye M. (1990) Antisense RNA. *Crit. Rev. Biochem. Mol. Biol.*, **25**, 155–184.

Takeda, T., Furuta, Y., Awano, T., Mizuno, K., Mitsuishi, Y. and Hayashi, T. (2002) Suppression and acceleration of cell elongation by integration of xyloglucans in pea stem segments. *Proc. Natl. Acad. Sci. USA*, **99**, 9055-9060.

Taylor, G. (2002) *Populus*: Arabidopsis for forestry. Do we need a model tree? *Ann. Bot.,* **90**, 681-689.

Taylor, N.G., Howells, R.M., Huttly, A.K., Vickers, K. and Turner, S.R. (2003) Interactions among three distinct CesA proteins essential for cellulose synthesis. *Proc. Natl. Acad. Sci. USA,* **100**, 1450-1455.

Taylor, N.G. (2008) Cellulose biosynthesis and deposition in higher plants. *New Phytol.,* **178**, 239-252.

Teeri, T.T. (1997) Crystalline cellulose degradation: new insight into the function of cellobiohydrolases. *Trends Biotechnol.,* **15**, 160-167.

Timell, T.E. (1967) Recent progress in the chemistry of wood hemicelluloses. *Wood Sci.Techn.,* **1**, 45-70.

Timell, T.E. (1986) Compression wood in gymnosperms, vol 2. Springer-Verlag, Heidelberg.

Tomme, P., Van Tilbeurgh, H., Pettersson, G., Van Damme, J., Vandekerckhove, J., Knowles, J., Teeri, T. and Claeyssens, M. (1988) Studies of the cellulolytic system of *Trichoderma reesei* QM 9414. Analysis of domain function in two cellobiohydrolases by limited proteolysis. *Eur. J. Biochem.,* **170**, 575-581.

Tomme, P., Warren, R.A.J., Miller, R.C., Kilburn, D.G. and Gilkes, N.R. (1995) Cellulose-binding domains: Classification and properties. In *Enzymatic degradation of insoluble carbohydrates*. Washington, Amer Chemical Soc.. pp. 142-163.

Trygg, J. and Wold, S. (2002) Orthogonal projections to latent structures (O-PLS). *J. Chemom.,* **16**, 119-128.

Turner, S.R. and Somerville, C.R. (1997) Collapsed xylem phenotype of Arabidopsis identifies mutants deficient in cellulose deposition in the secondary cell wall. *Plant Cell*, **9**, 689-701.

Turner, S., Gallois, P. and Brown, D. (2007) Tracheary element differentiation. *Annu. Rev. Plant. Biol.,* **58**, 407-433.

Tuskan, G.A., DiFazio, S., Jansson, S., Bohlmann, J., Grigoriev, I., Hellsten, U., Putnam, N., Ralph, S., Rombauts, S., Salamov, A., Schein, J., Sterck, L., Aerts, A., Bhalerao, R.R., Bhalerao, R.P., Blaudez, D., Boerjan, W., Brun, A., Brunner, A., Busov, V., Campbell, M., Carlson, J., Chalot, M., Chapman, J., Chen, G.L., Cooper, D., Coutinho, P.M., Couturier, J., Covert, S., Cronk, Q., Cunningham, R., Davis, J., Degroeve, S., Dejardin, A., Depamphilis, C., Detter, J., Dirks, B., Dubchak, I., Duplessis, S., Ehlting, J., Ellis, B., Gendler, K., Goodstein, D., Gribskov, M., Grimwood, J., Groover, A., Gunter, L., Hamberger, B., Heinze, B., Helariutta, Y., Henrissat, B., Holligan, D., Holt, R., Huang, W., Islam-Faridi, N., Jones, S., Jones-Rhoades, M., Jorgensen, R., Joshi, C., Kangasjarvi, J., Karlsson, J., Kelleher, C., Kirkpatrick, R., Kirst, M., Kohler, A., Kalluri, U., Larimer, F., Leebens-Mack, J., Leple, J.C., Locascio, P., Lou, Y., Lucas, S., Martin, F., Montanini, B., Napoli, C., Nelson, D.R., Nelson, C., Nieminen, K., Nilsson, O., Pereda, V., Peter, G., Philippe, R., Pilate, G., Poliakov, A., Razumovskaya, J., Richardson, P., Rinaldi, C., Ritland, K., Rouze, P., Ryaboy, D., Schmutz, J., Schrader, J., Segerman, B., Shin, H., Siddiqui, A., Sterky, F., Terry, A., Tsai, C.J., Uberbacher, E., Unneberg, P., Vahala, J., Wall, K., Wessler, S., Yang, G., Yin, T., Douglas, C., Marra, M., Sandberg, G., de Peer, Y.V. and Rokhsar, D. (2006) The genome of black cottonwood, *Populus trichocarpa* (Torr. & Gray). *Science,* **313**, 1596-1604.

Updegraff, D.M. (1969) Semi-micro determination of cellulose in biological materials. *Anal. Biochem.,* **32**, 420-424.

Urbanowicz, B.R., Catalá, C., Irwin, D., Wilson, D.B., Ripoll, D.R. and Rose, J.K.C. (2007a) A tomato endo-β-1,4-glucanase, SlCel9C1, represents a distinct subclass with a new family of carbohydrate binding modules (CBM49). *J. Biol. Chem.*, **282**, 12066-12074.

Urbanowicz, B.R., Bennett, A.B., del Campillo, E., Catalá, C., Hayashi, T., Henrissat, B., Höfte, H., McQueen-Mason, S.J., Patterson, S.E., Shoseyov, O., Teeri, T.T. and Rose, J.K.C. (2007b) Structural organization and a standardized nomenclature for plant endo-1,4-β-glucanases (cellulases) of glycosyl hydrolase family 9. *Plant Physiol.,* **144**, 1693-1696.

VanderHart, D.L. and Atalla, R.H. (1984) Studies of microstructure in native celluloses using solid-state ^{13}C NMR. *Macromolecules*, **17**, 1465-1472.

Vierhuis, E., York, W.S., Kolli, V.S.K., Vincken, J.P., Schols, H.A., Van Alebeek, G.J.W.M. and Voragen, A.G.J. (2001) Structural analyses of two arabinose containing oligosaccharides derived from olive fruit xyloglucan: XXSG and XLSG. *Carbohydr. Res.,* **332**, 285-297.

Vincken, J.P., York, W.S., Beldman, G. and Voragen, A.G.J. (1997) Two general branching patterns of xyloglucan, XXXG and XXGG. *Plant Physiol.,* **114,** 9-13.

Vissenberg, K., Oyama, M., Osato, Y., Yokoyama, R., Verbelen, J.P. and Nishitani, K.

(2005) Differential expression of AtXTH17, AtXTH18, AtXTH19 and AtXTH20 genes in Arabidopsis roots. Physiological roles in specification in cell wall construction. *Plant Cell Physiol.,* **46**, 192-200.

Vorwerk, S., Somerville, S. and Somerville, C. (2004) The role of plant cell wall polysaccharide composition in disease resistance. *Trends Plant Sci.,* **9**, 203-209.

Wenham, M.W. and Cusick, F. (1975) The growth of secondary wood fibres. *New Phytol.,* **74**, 247-261.

Whetten, R., Sun, Y.H., Zhang, Y. and Sederoff, R. (2001) Functional genomics and cell wall biosynthesis in loblolly pine. *Plant Mol. Biol.*, **47**, 275-291.

Wickholm, K., Larsson, P.T. and Iversen, T. (1998) Assignment of non-crystalline forms in cellulose I by CP/MAS C-13 NMR spectroscopy. *Carb. Res.,* **312**, 123-129.

Willför, S., Sundberg, A., Pranovich, A. and Holmbom, B. (2005) Polysaccharides in some industry important hardwood species. *Wood Sci. Technol.*, **39**, 601-617.

Williamson, M. P. (1994) The structure and function of prolinerich regions in proteins, *Biochem. J.,* **297**, 249-260.

Williamson, R.E., Burn, J.E. and Hocart, C.H. (2002) Towards the mechanism of cellulose synthesis. *Trends Plant Sci.*, **7**, 461-467.

Wilson, D.B. and Irwin, D.C. (1999) Genetics and properties of cellulases. In *Advances in biochemical engineering/biotechnology*. Springer Berlin / Heidelberg. pp. 1-21.

Wold, S. (1976) Pattern recognition by means of disjoint principalcomponents models. *Pattern Recogn.,* **8**, *127-139*.

Wong, Y.S., Fincher, G.B. and Maclachlan, G.A. (1977a) Cellulases can enhance β-glucan synthesis. *Science*, **195**, 679 - 681.

Wong, Y.S., Fincher, G.B. and Maclachlan, G.A. (1977b) Kinetic properties and substrate specificities of two cellulases from auxin-treated pea epicotyls. *J. Biol. Chem.,* **252**, 1402-1407.

Woolley, L.C., James, D.J. and Manning, K. (2001) Purification and properties of an endo-beta-1,4-glucanase from strawberry and down-regulation of the corresponding gene, *cel1*. *Planta*, **214**, 11-21.

Workman, J. (2002) The state of multivariate thinking for scientists in industry: 1980-2000. *Chemometr. Intell. Lab.,* **60**, 13-23.

Wu, S.S.H., Suen, D.F., Chang, H.C. and Huang, A.H.C. (2002) Maize tapetum xylanase is synthesized as a precursor, processed and activated by a serine protease, and deposited on the pollen. *J. Biol. Chem.,* **277**, 49055-49064.

Wullschleger, S.D., Jansson, S. and Taylor, G. (2002) Genomics and forest biotechnology: *Populus* emerges as the perennial favorite. *Plant Cell,* **14**, 2651-2655.

Xie, H.F., Gilbert, H.J., Charnock, S.J., Davies, G.J., Williamson, M.P., Simpson, P.J.,

Raghothama, S., Fontes, C.M.G.A., Dias, F.M.V., Ferreira, L.M.A. and Bolam, D.N. (2001) *Clostridium thermocellum* Xyn10B carbohydrate-binding module 22-2: The role of conserved amino acids in ligand binding. *Biochemistry,* **40**, 9167-9176.

Yamaki, S. and Kakiuchi, N. (1979) Changes in hemicellulose-degrading enzymes during development and ripening of Japanese pear fruit. *Plant Cell Physiol.*, **20**, 301-309.

Ye, Z.H., Freshour, G., Hahn, M.G., Burk, D.H. and Zhong, R. (2002) Vascular development in Arabidopsis. *Intern. Rev. Cyt.*, **220**, 225-256.

Yokoyama, R. and Nishitani, K. (2000) Functional diversity of xyloglucan-related proteins and its implications in the cell wall dynamics in plants. *Plant Biol.* **2**, 598-604.

Yokoyama, R. and Nishitani, K. (2001) A comprehensive expression analysis of all members of a gene family encoding cell-wall enzymes allowed us to predict cis-regulatory regions involved in cell-wall construction in specific organs of Arabidopsis. *Plant Cell Physiol.,* **42**, 1025-1033.

Yokoyama, R., Rose, J.K. and Nishitani, K. (2004) A surprising diversity and abundance of xyloglucan endotransglucosylase/hydrolases in rice. Classification and expression analysis. *Plant Physiol.*, **134**, 1088-1099.

York, W.S. and O'Neill, M.A. (2008) Biochemical control of xylan biosynthesis - which end is up? *Curr. Opin. Plant Biol.,* **11**, 258-265.

Yoshida, K. and Komae, K. (2006) A rice family 9 glycoside hydrolase isozyme with broad substrate specificity for hemicelluloses in type II cell walls. *Plant Cell Physiol.,* **47**, 1541-1554.

Zablackis, E., Huang, J., Muller, B., Darvill, A.G. and Albersheim, P. (1995) Characterization of the cell-wall polysaccharides of *Arabidopsis thaliana* leaves. *Plant Physiol.*, **107**, 1129-1138.

Zhao, C., Johnson, B.J., Kositsup, B. and Beers, E.P. (2000) Exploiting secondary growth in Arabidopsis. Construction of xylem and bark cDNA libraries and cloning of three xylem endopeptidases. *Plant Physiol.,* **123**, 1185-1196.

Zhao, C., Craig, J.C., Petzold, H.E., Dickerman, A.W. and Beers, E.P. (2005) The xylem and phloem transcriptomes from secondary tissues of the *Arabidopsis* root-hypocotyl. *Plant Physiol.*, **138**, 803-818.

Zhong, R.Q., Pena, M.J., Zhou, G.K., Nairn, C.J., Wood-Jones, A., Richardson, E.A., Morrison, W.H., Darvill, A.G., York, W.S. and Ye, Z.H. (2005) Arabidopsis fragile fiber8, which encodes a putative glucuronyltransferase, is essential for normal secondary wall synthesis. *Plant Cell*, **17**, 3390–3408.

Zhou, G.K., Zhong, R.Q., Richardson, E.A., Morrison, W.H., Nairn, C.J., Wood-Jones, A. and Ye, Z.H. (2006) The poplar glycosyltransferase GT47C is functionally conserved with Arabidopsis fragile fiber8. *Plant Cell Physiol.*, **47**, 1229-1240.

Zhou, G.K., Zhong, R.Q., Himmelsbach, D.S., McPhail, B.T. and Ye, Z.H. (2007) Molecular characterization of PoGT8D and PoGT43B, two secondary wall-associated

glycosyltransferases in poplar. *Plant Cell Physiol.*, **48**, 689-699.

Zhou, W.L., Irwin, D.C., Escovar-Kousen, J. and Wilson, D.B. (2004) Kinetic studies of *Thermobifida fusca* Cel9A active site mutant enzymes. *Biochemistry,* **43**, 9655-9663.

Zuo, J.R., Niu, Q.W., Nishizawa, N., Wu, Y., Kost, B. and Chua, N.H. (2000) KORRIGAN, an Arabidopsis endo-1,4-β-glucanase, localizes to the cell plate by polarized targeting and is essential for cytokinesis. *Plant Cell*, **12**, 1137-1152.

9. Appendix: Protocols of the discussed experimental procedures

1. Cellulase activity *in situ* (referred to in section 3.2)

This method was tested with hypocotyls and the bottom of inflorescence stems of five to eight-week-old Arabidopsis.

Solutions:

100 mM MES (2-(*N*-morpholino)ethanesulfonic acid) buffer, pH 6.0, with sterilization by filtration. (100 mM acetate buffer, pH 6.0 could also work but was not tested)

Substrate solution:

For detection of cellulase and β-glucosidase:
Resorufinyl β-D-cellobioside (Glc_2-Res), *M* 537 g/mol

For detection of β-glucosidase as a control:
Resorufinyl β-D-glucopyranoside (Glc-Res), *M* 375 g/mol

0.25 mg/ml (0.4655 $x10^{-3}$ mol/l) Glc_2-Res and 0.175 mg/ml (0.4655 $x10^{-3}$ mol/l) Glc-Res was dissolved in 100 mM MES pH 6.0 as a concentrated stock solution. The substrate stock solution was diluted five times (0.05 mg/ml) as a working solution for the analysis. It takes some time to dissolve the substrates (especially Glc-Res) completely. Making a stock solution at least a day before could be practical. The compound seems stable in solution at least two weeks in the dark at ambient temperature. Precipitation could occur when stored at 4°C.

Method:

1, Make fresh sections (200 μm thickness) and immerse into 100 mM MES buffer or acetate buffer.

2, Place sections on slides. Remove excess buffer and add 40 μl of substrate or control mix. Seal edges of a coverslip with glycerol or nail polish. Start observation immediately. Optimize the right timing compared to the control with Glc-Res. The sections I observed started giving a signal after 1.5 min of incubation. The activity is detected using an excitation wavelength of 567 nm (green) and a detection wavelength of 580 nm and above (red) by CLSM.

Additional controls:

1, Heat denatured sections – heat 30 min at 100°C in 100 mM MES or acetate buffer.
2, Autofluorescence – incubate in 100 mM MES or acetate buffer instead of reaction mix.

2. Carbohydrate analysis (referred to in section 3.3)

N.B. 1. Contains strong acids – use eye/face protection, handle acids in the fume hood.
N.B. 2. If starch quantification is not necessary, deplete starch by placing plants in darkness at least for 24 hours before harvesting.

(a) **Soluble sugar extraction** (Reiter et al., 1993 and Forsum et al., 2006)

1) Freeze-dry the material O/N, considering the sample amounts described in the "Methodological overview".
2) Grind up material by beads-milling.
3) Weigh tissue. Weigh screw-cap tubes, in case you can't quantify only AIR later. Use the same amount of tissues to have equal extraction efficiency (20 mg - leaf or stem, 15 mg - hypocotyl).
4) Place in labelled screw-cap tubes (label sides and top as it is easily removed) with 0.5 ml 80% EtOH containing 4 mM Hepes (4-(2-hydroxyethyl)-1-piperazineethanesulfonic acid) pH 7.5.
5) Incubate at 80°C for at least 30 min (mix by inversion occasionally).
6) Centrifuge at 14000 rpm for 15 min. Save the supernatant (0.5 ml), which contains soluble sugars (starch is in pellet).
7) Repeat steps 4-6 once more with 80% EtOH containing 4 mM Hepes pH 7.5 and two times with 50 % EtOH containing 4 mM Hepes pH 7.5 (mix very well when adding new EtOH). Save and combine the supernatants from four repeated extractions (total 2 ml). Can be stored at -20°C until analysis.
8) Sugars can be analyzed by ion chromatography (e.g. Metrohm, Switzerland). The column metrosep Carb-250 was run isocratic with the eluent 0.1 mM NaOH (0.98 ml min-1) for my samples.

(b) **Starch extraction**

1) The pellets contain starch and cell wall materials. For starch quantification, add 0.5 ml water. Vortex very well, take 50 µl of homogeneous suspension using cut-end tips. (Since taking homogeneous samples from this is difficult, make at least three replicates.) Keep the remaining pellet for crystalline cellulose analysis.
2) Mix the 50 µl suspension with 450 µl 50 mM sodium acetate buffer pH 4.8 containing 6.3 units amyloglucosidase (from *Aspergillus niger*, Fluka chemie GmbH, Cat nr. 10115, 73.8 U/mg).
3) Incubate for 16 h at 40°C.
4) Centrifuge for 15 min at 14000 rpm.
5) Transfer supernatant 500 µl (glucose solution) to a new tube. This can be stored at -20°C.
6) For quantification, take 50 µl from (5), dry with Speedvac, dilute with water to a sufficient volume for the chromatograph as mentioned above in step 8 of (a).

(c) **Crude wall preparation** (Zablackis et al., 1995)

1) Add 1 ml of acetone to the remaining pellet not used for starch extraction, mix very well, let the tubes stand for at least 2 min. centrifuge 14000 rpm for 5 min.
2) Remove acetone and allow to air dry.
3) Dry completely under vacuum (about 3 min).
4) Amylase treatment – digest cell wall with alpha-amylase (Sigma A-6255). Use 50 units of alpha-amylase (=1.6 µl)/10 mg cell wall material/mL of 0.1M KPO_4.
5) Incubate for up to 24 hours at 30°C in a shaking water bath. (This step may be repeated once more to ensure removal of all starch.) For non-starch depleted leaves (20 mg DW) requires 2 O/N amylase treatments. Stem (20 mg DW) requires at least 1 O/N. Hypocotyl (15 mg DW) contains much less starch than stem, 1 O/N is enough. The remaining starch can be traced by ion chromatography described in soluble sugar extraction protocol above (a8). Centrifuge 8000*g* for 20 min.
6) Wash pellet with 1 ml 0.1M KPO_4, followed by centrifuge 8000*g* 20 min. Wash with water and centrifuge again.
7) Dry completely again with 1 ml acetone. Centrifuge 8000*g* for 20 min. Remove and Speedvac for 30-50 min.
8) Weigh the pellet (AIR) (if weighing a pellet itself is not possible, weigh including an eppendorf tube) and transfer the AIR to 10 ml screw cap borosilicate glass tubes. More than 6 mg AIR is ideal to proceed to crystalline cellulose analysis (d), 3 mg AIR for monosaccharide composition analysis by trifluoroacetic acid (TFA) (f) or sulphuric acid (g) hydrolysis. 15 mg AIR is ideal for fractionation analysis (h).

(d) **<u>Crystalline cellulose determination</u>** (Updegraff, 1969)

1) Carefully add 3 ml of acetic-nitric reagent (Acetic acid : Nitric acid : Water, 8:1:2, made by adding 15 ml of conc. nitric acid to 150 ml of 80 % acetic acid) to the AIR wall material. It is convenient to use filter paper (10 mg) as a control. Cap the tubes, use only PTFE seals (not rubber – they will disintegrate).
2) Place in a boiling water bath for 30 min. Allow to cool on bench.
3) Spin the samples at 2500*g* for 5 min in a bench top centrifuge.
4) Remove and discard the supernatant.
5) Add 8 ml of water, mix by inverting the tubes. Spin as above if necessary. Remove the supernatant and discard.
6) Repeat step 5 using 4 ml of acetone. At this point, don't shake or invert the tubes. Cellulose should stay at the bottom and all should be digested in 1ml sulphuric acid.
7) Air dry pellet, then dry completely under vacuum (15 min). The extracted cellulose can be stored at this point.
8) Add 1 ml of 67% sulphuric acid. Make sure all the material is covered by the acid. Shake for 5-6 h at room temperature until digested completely. If you incubate too long, they become dark, which may disturb absorption of colouration at 620 nm.

9) Assay cellulose content by the anthrone (Sigma 10740) method. 10 µl is usually enough from a stem or hypocotyl sample, 25 µl from a leaf sample and 1 µl for a paper standard.

(e) **<u>Anthrone method for determination of glucose content</u>** (Scott and Melvin, 1953)

1) Place sample (1-100 µl) in a screw cap 2 ml eppendorf or other appropriate heat resistant tube. Make volume up to 500 µl with water and carefully layer on 1 ml of 0.3% anthrone in conc. sulphuric acid. Mix thoroughly by inversion (take care as the tubes will get hot).
2) Place in a boiling water bath for 5 min. Cool on ice.
3) Measure $OD_{620,}$ using disposable cuvettes. Include a set of standards that contain 5-50 µg of glucose in 500 µl of water. Filter paper should give around 80% cellulose.

(f) **<u>Monosaccharide composition analysis by TFA hydrolysis</u>** (Øbro et al., 2004 and Harholt et al., 2006)

1) Add 850 µl water to 3 mg AIR.
2) Afterwards add 150 µl TFA. This should be done under the hood. Close the lid thoroughly and vortex.
3) Incubate at 120°C in a heatblock for 1 h.
4) Let the sample cool down to room temperature. The samples look brown at this point.
5) Dry the sample in Speedvac O/N to remove the TFA.
6) When the samples are dry, you can additionally add 200 µl water to eliminate excess TFA, which should be dried in Speedvac.
7) Resuspend in 1 ml water. Vortex thoroughly, wait for 30 min and vortex again until the pellet is dissolved.

(g) **<u>Monosaccharide composition analysis by sulphuric acid hydrolysis</u>** (Øbro et al., 2004 and Harholt et al., 2006)

1) Suspend 3 mg AIR in 125 µl 72% sulphuric acid.
2) Shake until dissolved, about for 1 h.
3) Add 1.275 ml water.
4) Heat for 120°C for 1 h in heating block.
5) Cool and transfer to 15 ml falcon tubes.
6) Wash screw-cap tubes with 0.5 ml water, add to falcon tubes.
7) Add 2 drops (5 µl) of 1% bromphenol blue.
8) Slowly add 5.5 ml 0.18 M barium hydroxide with vigorous stirring.
9) The solution should not be blue at this point.
10) Add approx 0.5 g of barium carbonate or until the indicator goes blue. The reaction is rather slow so don't add too much barium carbonate in one go.
11) Centrifuge for 10 min at 4000-5000*g* and collect supernatant and transfer to a new tube.
12) Freeze and thaw the supernatant a few times and centrifuge.

13) Take 100 µl supernatant to a new eppendorf tube. Dilute if necessary.

(h) <u>Fractionation</u>

1) Add 5 ml 0.1 M potassium hydroxide to 15 mg AIR, vortex and shake for 1 h.
2) Centrifuge at 5000*g* for 10 min, collect supernatant.
3) Add 5 ml 1 M potassium hydroxide to pellet and vortex and shake for 1h.
4) Centrifuge at 5000*g* for 10 min, collect supernatant.
5) Add 5 ml 6 M potassium hydroxide to pellet and vortex and shake for 1h.
6) Centrifuge at 5000*g* for 10 min, collect supernatant.
7) Neutralize all potassium hydroxide samples with glacial acetic acid, you can use bromphenol blue as an indicator and this is done in fume hood. Note the amount of acetic acid used.
8) All potassium hydroxide extracted samples are TFA hydrolyzed, so add 150 µl TFA to 850 µl of a sample. Proceed as above in the TFA hydrolysis protocol.
9) The pellet is hydrolyzed using the sulphuric acid method due to the presence of cellulose. Add 1 ml sulphuric acid (72%) and dissolve the cellulose in the pellet. Take 125 µl of the dissolved pellet and add to 1.275 ml water. Then proceed as for protocol g4.

(i) Preparation of samples for the DIONEX (HPAEC-PAD) (Øbro et al., 2004 and Harholt et al., 2006)

1) The sample (e.g. take only the upper 200 µl of the TFA-hydrolyzed samples to avoid the unclear solution) is filtrated through a 0.2 µl spinfilter. Spin at 2000*g* for 1 min.
2) Dilute the samples 5-25 times.
3) 130-150 µl sample is loaded onto DIONEX inlet as well as together with 9 standards 0.001-0.006 mg/ml.